Performance of Ultra-Wideband Communication Systems using DS-SS PPM with BCH Coding

by

Hanfeng Chen
B.Eng, Shanghai Jiao Tong University, 1994

A Thesis Submitted in Partial Fulfillment of the Requirements
for the Degree of

MASTER OF APPLIED SCIENCE

in the Department of Electrical and Computer Engineering

Performance of Ultra-Wideband Communication Systems using DS-SS PPM with BCH Coding

by

Hanfeng Chen

B.Eng, Shanghai Jiao Tong University, 1994

Supervisory Committee

Dr. T. Aaron Gulliver, Co-Supervisor (Dept. of Electrical and Computer Engineering)

Dr. Wei Li, Co-Supervisor (Dept. of Electrical and Computer Engineering)

Dr. Jens Bornemann, Member (Dept. of Electrical and Computer Engineering)

Supervisory Committee

Dr. T. Aaron Gulliver, Co-Supervisor (Dept. of Electrical and Computer Engineering)

Dr. Wei Li, Co-Supervisor (Dept. of Electrical and Computer Engineering)

Dr. Jens Bornemann, Member (Dept. of Electrical and Computer Engineering)

ABSTRACT

Ultra-Wideband (UWB) technologies have recently drawn great attention for short-range wireless communication due to their many attractive advantages such as high data rates, robustness to multipath fading and coexistence with narrowband wireless systems.

In wireless digital communication, to improve the system performance error correcting codes are very efficient and widely used. In this thesis, we employ Bose-Chaudhuri-Hochquenghem (BCH) codes in a UWB communication system. We consider UWB direct sequence spread spectrum pulse position modulation (DS-SS PPM) system with BCH coding for both additive white Gaussian noise (AWGN) and UWB fading channels, multi-access and single-user performance results are given for errors-only and errors-and-erasures decoding. The simulation results show the effectiveness of the system in improving performance.

Table of Contents

List of Tables

List of Figures

List of Abbreviations

AWGN	additive white Gaussian noise
BCH code	Bose-Chaudhuri-Hochquenghem code
BER	bit error probability
BPSK	binary phase shift keying
CDMA	code-division multiple access
DC	direct current
DS	direct sequence
EIRP	equivalent isotropically radiated power
FCC	Federal Communications Commission
FH	frequency hopping
Gbps	gigabits per second
GF	Galois field
GPS	global positioning system
IEEE	Institute of Electrical and Electronics Engineers
LCM	least common multiple polynomial
LFSR	linear feedback shift register
MAC	medium access control
Mbps	megabits per second
PAM	pulse amplitude modulation
PN	pseudo-random noise
PPM	pulse position modulation
PSD	power spectral density
RF	radio frequency

SNR	signal noise ratio
SS	spread spectrum
STDL	stochastic tapped delay-line
TH	time hopping
UWB	Ultra-Wideband
WLAN	wireless local area network
WPAN	wireless personal area network

Acknowledgement

I would like to express my deep appreciation for the invaluable advice, continuous support and adequate patience I have received from my supervisor, Dr. T. Aaron Gulliver. This research could have never been completed without his precious advice and encouragement he has given to me.

I would like to give my special thanks for Dr. Wei Li for his great support and suggestions in my difficuties.

I would like to offer my gratitude to Dr. Jens Bornemann and Dr. Sudhakar Ganti for their participation on my committee.

I would further like to acknowledge the varied support of my colleagues in the Communication Research Group, namely: Ahmed Abubaker, Yousry Abdel-Hamid, Caner Budakoglu, Neil Carson, Omar Farooq, Massoud Ghassemi, Behzad Bahr Hosseini, Li Jing, Carlos Quiroz Perez, Shiva Jumar Planjery, Yongsheng Shi, Yue Wang, Le Yang, Dr. Hao Zhang, Rongrong Zhang,Yihai Zhang. Thank you for being such good friends. I appreciate the experiences and time that you have shared with me.

Most importantly, researching and fulfilling this thesis would not have been possible without the love, sacrifice and understanding of my family especially my wife and my lovely daughter.

Dedication

For my wife and daughter

Chapter 1

Introduction

Ultra-Wideband (UWB) radio is an emerging technology with uniquely attractive features which invite major advances in wireless communications. In the past two decades, UWB has been used for radar, remote sensing and military communications. In 2002, the Federal Communications Commission (FCC) in the United States issued a ruling that UWB could be used for data communications as well as for radar and safety applications. In addition, significant bandwidth (3.1-10.6 GHz) was allocated so that UWB radios overlaying coexistent RF systems can operate using low-power ultra-short information bearing pulses [1]. This enormous bandwidth is the largest allocation to any commercial terrestrial system, and so has the potential to offer data rates on the order of gigabits per second (Gbps). Thus there is a great motivation to bring UWB systems to market.

When the FCC proposed the UWB allocation, they received almost 1000 submissions opposing the proposal because of the concern from many groups having existing systems which overlap with the UWB bandwidth [2]. Fortunately, the UWB allocation was approved with the restriction that the power levels be very low (below -41.3 dBm/MHz) [1]. This allows UWB technology to overlay already available services such as the global positioning system (GPS) and IEEE 802.11 a/b/g wireless local area networks (WLANs) that lie in the 3.1-10.6 GHz band [1]. This effectively limits UWB systems to indoor, short-range communications for high data rates, or very low data rates for substantial link distances [2]. Applications such as wireless UWB and personal area networks have been proposed, from

hundreds of Mbps to several Gbps and distances of 1 to 10 meters. For 20 meters or more, the achievable data rates are very low compared with existing WLANs [2].

1.1 UWB Basics

According to the FCC UWB regulations, the prevailing definition of a UWB radio system is as follows: A system is classified as a UWB system if the instantaneous bandwidth is in excess of 500 MHz or if it has a fractional bandwidth greater than 0.20. The fractional bandwidth is defined as B_f/f_C, where $B_f = f_H - f_L$ denotes the -10 dB bandwidth of the system, $f_C = (f_H + f_L)/2$ denotes the center frequency with f_H the upper frequency corresponding to the -10 dB emission point, and f_L the lower frequency corresponding to the -10 dB emission point [3]. The 'short-pulse' or 'carrierless' UWB systems typically transmit a train of ultra-short impulse waveforms (nanosecond scale) resulting in an ultra-wide spectrum [4]. The energy of the baseband signal is spread from a low frequency to several GHz [5]. Owing to its low transmission power levels, the UWB signal is very hard to be detected and intercepted by others. Furthermore, the extremely low power spectral density of a UWB signal allows it to coexist with existing narrow-band radio systems [2].

UWB has a number of advantages that motivate research and development activities for consumer communications applications [2, 4]. Specifically, they include:

- High data rate — UWB systems can provide very high data rates (from several hundred Mbps to several Gbps) in short-range wireless communications.
- Potentially low complexity and low cost — First, due to the baseband nature of UWB signals, there is no need for an additional RF (radio frequency) mixing stage. UWB systems also do not need additional up-conversion, amplification or down-conversion at the receiver. This also means the elimination of the associated complex delay and a local oscillator at the receiver. Secondly, developments in silicon technologies make commercial low-cost UWB systems possible.

- Immunity to severe multipath propagation and less path loss — UWB channels exhibit extreme frequency-selective fading characteristics and every received signal contains a large number of resolvable multipath components [6, 7]. In addition, UWB signals have fairly low material penetration losses.
- Very good time domain resolution — Very high multipath resolution can be achieved due to the large bandwidth. The very narrow time domain impulses also allow fine timing precision which is much better than GPS (global positioning system) [2]. In the spatial domain, UWB signals distinguish reflecting objects as small as a few centimeters. Thus UWB can be used in short range radar applications such as rescue and anti-crime operations, surveying, and in the mining industry [2].
- Low transmission power levels — According to the FCC UWB regulations, UWB signal power levels should be below -41.3 dBm/MHz which is much less than 802.11 WLANs, as illustrated in Figure 1.1 [1]. Thus UWB signals are difficult to detect [2].
- Low interference with existing narrow-band radio systems in the same spectrum — The low transmission power together with the ultra-wide bandwidth makes the power spectral density of UWB signals extremely low. This allows UWB systems to coexist with narrowband radio systems operating in the same spectrum without causing undue interference.

Figure 1.1 shows that the power spectral density (PSD) of UWB signals is much lower than other wireless systems such as IEEE 802.11 WLAN, BlueTooth and GPS.

1.1.1 UWB History and Regulatory Issues

More than a century ago, Guglielmo Marconi utilized a very large bandwidth to convey information using a spark-gap transmitter. In the late 1960s, the pioneers in UWB communications, Ross and Robbins at Sperry Rand Corporation, Harmuth at Catholic University of America and Paul van Etten at the USAF Rome Air Development Center, independently

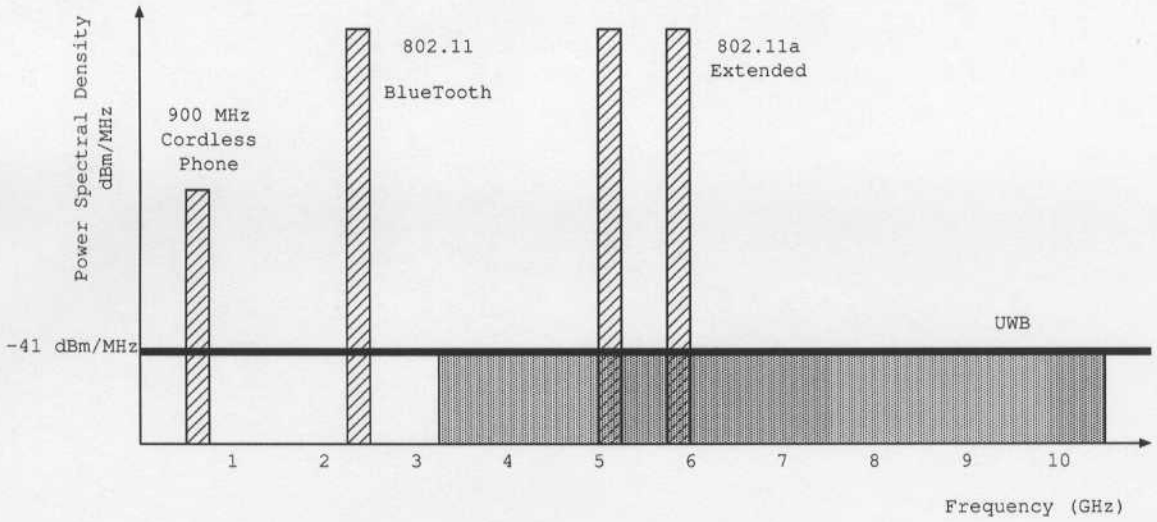

Figure 1.1. *Comparison of the PSD and bandwidth for UWB and other wireless technologies.*

started their work on UWB system design, testing and implementation [8]. Concurrently, the development of pulse transmitters, receivers, antennas and sampling oscilloscopes unintentionally motivated the introduction of UWB radar systems [8]. Much research work was done on pulse generation techniques during the 1970s and 1980s. In 1989, the U.S. Department of Defense coined the term "ultra wideband" for a signal that occupies more than 1.5 GHz, or a -20 dB fractional bandwidth beyond 25% [9].

The FCC began UWB deliberations in 1998. In February 2002, the first FCC UWB Report and Order was released with four different categories: imaging systems, communication systems, measurement systems, and vehicular radar systems. Spectral masks were also defined for each category [3]. The FCC radiation limits are given in Table 1.1 for indoor and outdoor data communication applications.

Besides the United States, regulatory efforts are also ongoing in Europe, China, Japan and Singapore. Because of its leading position in the regulation process, FCC decisions

Table 1.1. *FCC Spectral Masks for Indoor and Outdoor UWB Communications – EIRP (Equivalent Isotropically Radiated Power)*

Frequency[MHz]	Indoor EIRP(dBm)	Outdoor EIRP(dBm)
960-1610	-75.3	-75.3
1610-1990	-53.3	-63.3
1990-3100	-51.3	-61.3
3100-10600	-41.3	-41.3
$\geq$ 10600	-51.3	-61.3

will heavily influence UWB regulations in other countries [2]. Furthermore, due to the fact that UWB technology is still at an early stage for many commercial applications, the development of other signal processing applications will probably have considerable impact on UWB system designs [1]. For instance, the IEEE 802.15 wireless personal area network (WPAN) groups are working on physical layer and medium access control (MAC) layer concepts for short-range, high-data-rate ad hoc in-home networks. Their intention is to develop high-quality real-time video and multimedia links for cable replacement. For the IEEE 802.15.4 standard, UWB technology is a promising physical layer candidate [1]. Other applications include sensor networks where high data-rate wireless communications is required for real-time sensory data exchange with low power and low cost; and imaging systems where UWB systems are able to provide more sensitivity to scattering objects than conventional radar signals [1].

1.1.2 UWB Modulation

There are many UWB impulse generation techniques that meet FCC regulations. Typically, a transmitted UWB signal is an impulse based waveform. An impulse is referred to as a monocycle. From communication theory, the narrower the signal is in the time domain, the wider the signal is in the frequency domain. Thus, the very narrow UWB impulses in the

time domain correspond to a very wide spectrum in the frequency domain. Consequently, a UWB signal can span from DC to several GHz. To follow the FCC spectral mask requirements for UWB transmission, the majority of the impulse energy must lie in the 3.1-10.6 GHz frequency range. The amplitude and/or position of the impulse is used to carry the information.

Impulse Waveforms

In recent research, rectangular, Rayleigh, Gaussian and Gaussian doublet waveforms have been considered. A rectangular waveform is the simplest UWB impulse waveform. This waveform has width T_w and unity energy, and can be represented as

$$W_R(t) = (1/T_w)^{1/2} N_{T_w}(t), \tag{1.1}$$

where $N_{T_w}(t)$ denotes the unit function with width T_w. Due to its simplicity, the rectangular waveform is widely used in research. However, the large DC component makes it unsuitable for UWB applications.

The remaining three waveforms are more complex. A Rayleigh impulse waveform is the first derivative of a Gaussian pulse, and is given by

$$W_{Rl}(t) = G_{Rl} \left(\frac{t-\mu}{\sigma^2} \right) \exp \left[-\frac{(t-\mu)^2}{2\sigma^2} \right], \tag{1.2}$$

where G_{Rl} is a constant, μ denotes the center of the Rayleigh waveform and σ determines the waveform width. Within the time duration $T = 7\sigma$ with center $\mu = 3.5\sigma$, 99.99% of the total waveform energy is included [4].

A Gaussian impulse waveform is the second derivative of a Gaussian pulse, and is given by [10]

$$W_G(t) = G_G \left[1 - \left(\frac{t-\mu}{\sigma} \right)^2 \right] \exp \left[-\frac{(t-\mu)^2}{2\sigma^2} \right], \tag{1.3}$$

where G_G is a constant, μ denotes the center of the waveform and σ determines the waveform width. For the time duration of $T = 7\sigma$ and center $\mu = 3.5\mu$, 99.99% of the total waveform energy is included [4]. This is the same as for the Rayleigh waveform.

A Gaussian doublet impulse waveform is a bipolar signal consisting of two amplitude reversed Gaussian pulses with a time gap between the pulses. The expression for the waveform is

$$W_{Gd}(t) = G_{Gd}\left\{\exp\left[-\frac{(t-\mu)^2}{2\sigma^2}\right] - \exp\left[-\frac{(t-\mu-T_a)^2}{2\sigma^2}\right]\right\}, \tag{1.4}$$

where G_{Gd} is a constant, μ is the center of the first Gaussian pulse, $(\mu + T_a)$ is the center of the second Gaussian pulse, σ is the width of the Gaussian pulses and T_a is the time gap between the centers of the pulses. For the Gaussian pulses, the time width $T = 7\sigma$ centered at $t = \mu$ and $t = \mu + T_a$ contains 99.99% of the total pulse energy.

In Figure 1.2, all four impulse waveforms are shown. The corresponding power spectral densities (PSDs) are given in Figure 1.3. Note that the Gaussian waveform and the Rayleigh waveform have smaller out-of-band side lobes than the Gaussian Doublet waveform and the Rectangular waveform.

Modulation Techniques

In communication systems, spread spectrum (SS) techniques are widely used to combat multiple access interference and alleviate the effects of multipath interference. A spread-spectrum signal occupies a bandwidth much greater than the minimum bandwidth necessary with the spreading achieved by an independent code sequence [11]. In UWB systems, the two most common SS models are time hopping spread spectrum (TH-SS) and direct sequence spread spectrum (DS-SS).

TH-SS is based on the transmission of several very short impulse waveforms having

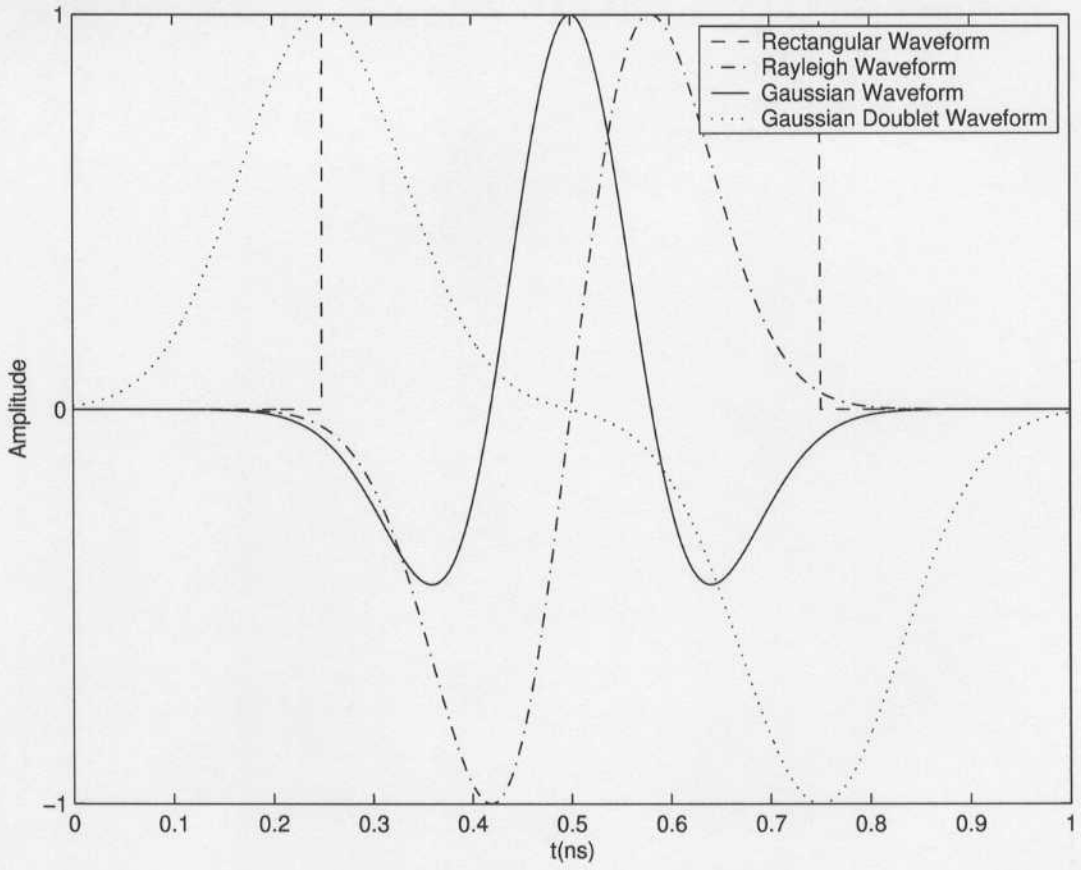

Figure 1.2. *Typical UWB impulse waveforms.*

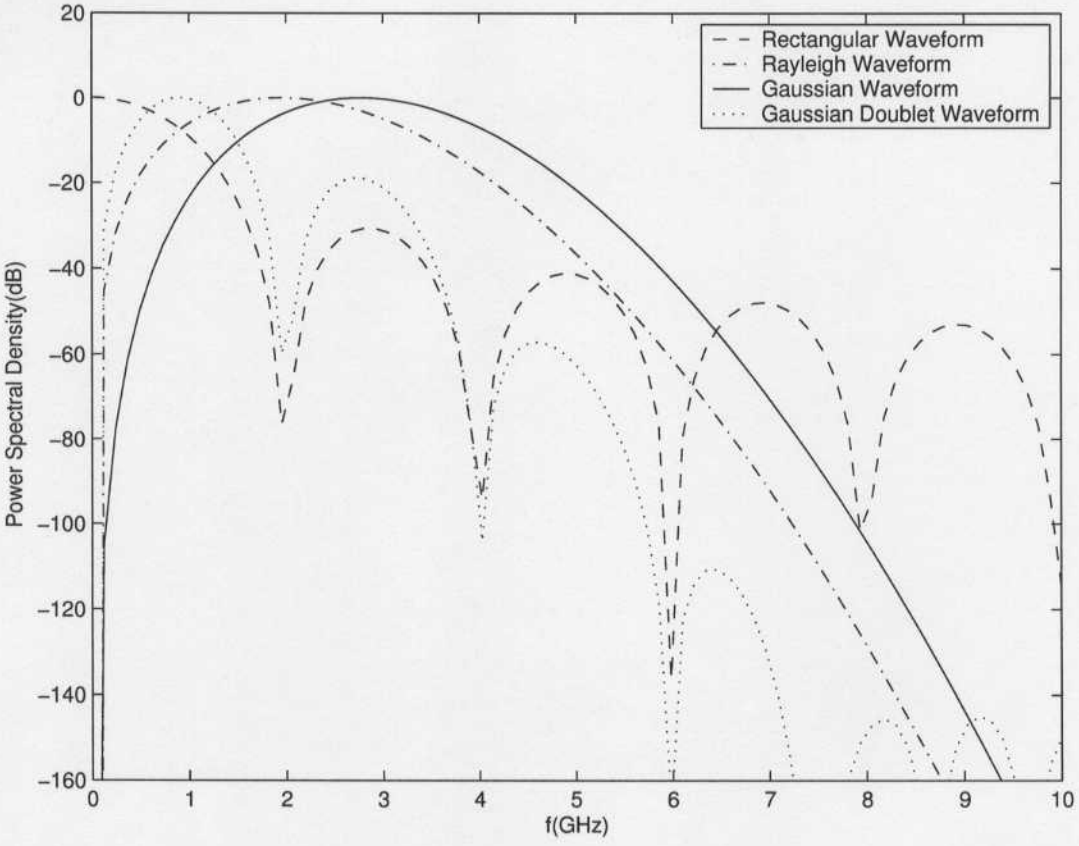

Figure 1.3. *Power spectral densities of the UWB impulse waveforms given in Fig. 1.2.*

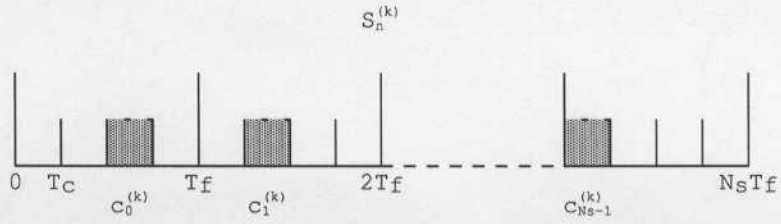

Figure 1.4. *An example of the time slots used by a TH-SS PPM data bit for* $\delta = 0$.

a pseudorandom shift pattern. One data bit consists of a fixed number of waveforms. A typical TH-SS PPM (pulse position modulation) signal is given by

$$S^{(k)}(t) = \sum_{n=1}^{\infty} \sum_{m=0}^{N_s-1} w(t - nT_d - mT_f - c_m^{(k)} T_c - \delta_{d_n^{(k)}}) \tag{1.5}$$

where $w(t)$ denotes the impulse waveform, k is the user number, n denotes the nth transmitted data bit, N_s is the number of waveforms modulated by each data bit, T_f is the waveform repetition interval, m is the interval number, T_d is the data bit interval, T_c is the minimum chip interval, δ is the waveform delay corresponding to the symbol ("0" or "1"), and $\{c_m^{(k)}\}$ is the periodic pseudorandom time hopping code for user k. Figure 1.4 illustrates the TH-SS PPM structure for one bit.

To avoid catastrophic collisions in multiple access systems, a distinct pulse shift pattern $\{c_m^{(k)}\}$ is assigned to each user (indexed by k) [5]. These periodic pseudorandom time hopping code sequences have the same length N and very low cross-correlation (sequences should be near orthogonal). In the code sequences $\{c_m^{(k)}\}$, each code element is a nonnegative integer in the range

$$0 \leq c_m^{(k)} \leq N_{TH} < T_f/T_c \tag{1.6}$$

where N_{TH} is the maximum value of $\{c_m^{(k)}\}$. A sufficiently large value for N_{TH} is required to avoid catastrophic collisions. In this case, the multiple-access interference can be modeled as a Gaussian random process for a sufficient number of users [5].

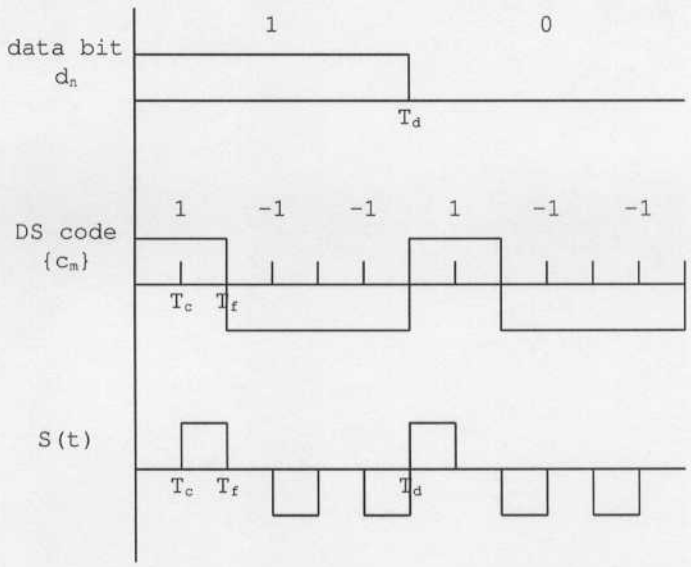

Figure 1.5. *A DS-SS PPM signal with 3-chip PN sequence, $\delta_1 = T_c$ and $\delta_0 = 0$.*

DS-SS is based on the transmission of several very short impulse waveforms having a pseudorandom pattern in waveform amplitudes. A typical DS-SS signal is given by

$$S^{(k)}(t) = \sum_{n=1}^{\infty} \sum_{m=0}^{N_s-1} c_m^{(k)} w(t - nT_d - mT_f - \delta_{d_n^{(k)}}), \tag{1.7}$$

where $w(t)$ denotes the impulse waveform, k denotes the user number, n denotes the nth transmitted data bit, N_s is the number of waveforms modulated by each data bit, T_f is the waveform repetition interval, m is the interval, T_d is the data bit interval, δ is the delay of waveforms for symbol "0" or "1" corresponding to the subscript index, $\{c_m^{(k)}\}$ is a periodic pseudorandom spreading sequence for user k. Typically, $c_m \in \{-1, +1\}$ where "-1" corresponds to symbol "0" and "+1" corresponds to symbol "1" in the spreading sequences.

Figure 1.5 depicts the generation of a DS-SS PPM signal. In this figure, $\{c_m\}$is a 3-chip sequence $\{+1, -1, -1\}$. Data bit "1" introduces an extra time delay T_c and data bit "0" has no extra delay (PPM modulation).

In UWB systems, applying spread spectrum techniques has two distinct advantages.

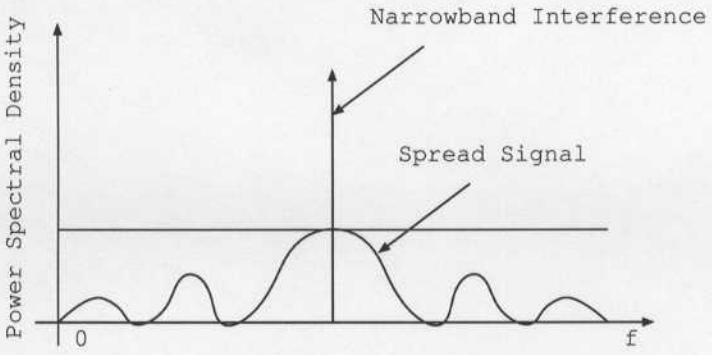

(a) PSD of Spread Signal and Narrowband Interference

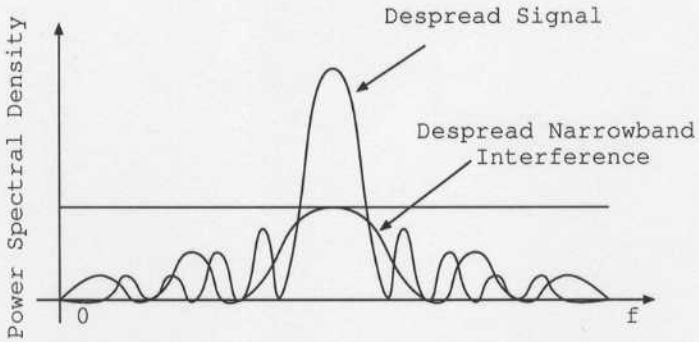

(b) PSD of Despread Signal and Narrowband Interference

Figure 1.6. *The effect of DS-SS on a UWB signal with narrowband interference.*

First, the UWB signal will have greater immunity against narrowband interference if proper pseudorandom sequences are employed [12]. Figure 1.6 shows the effect of DS-SS on a UWB signal interfered by a narrowband signal. It shows that after being despread (multipled by the identical direct sequence), the narrowband interference is greatly suppressed. Secondly, the UWB signal power emission level is decreased as required by the FCC regulations.

Furthermore, a distinct spreading sequence having very good auto-correlation and cross-correlation characteristics for each user is necessary to provide high quality multi-access UWB communications.

In UWB transmission, TH-SS and DS-SS are the most popular modulation techniques. The data modulation is typically PPM and/or pulse amplitude modulation (PAM).

PPM is a modulation scheme in which the information is encoded in the time delay between pulses. As described in (1.5) and (1.7), δ determines the phase shift in each impulse repetition interval. Considering binary modulation, δ has two values corresponding to symbol "0" and symbol "1".

PAM is a signal modulation scheme in which the message information is encoded in the amplitude of a series of signal pulses. In UWB systems, combined with TH-SS and DS-SS, there are TH-SS PAM and DS-SS PAM modulations. The transmitted signal using TH-SS PAM is given by

$$S^{(k)}(t) = \sum_{n=1}^{\infty} \sum_{m=0}^{N_s-1} w(t - nT_d - mT_f - c_m^{(k)} T_c) d_n^{(k)}, \tag{1.8}$$

where the definitions are the same as those in (1.5). The difference is that in TH-SS PAM, the data modulated part is the amplitude of the waveform instead of the time shift.

The transmitted signal using DS-SS PAM is expressed as

$$S^{(k)}(t) = \sum_{n=1}^{\infty} \sum_{m=0}^{N_s-1} c_m^{(k)} w(t - nT_d - mT_f) d_n^{(k)}, \tag{1.9}$$

where the definitions are the same as those in (1.7). The difference is that in DS-SS PAM, the modulated part is the amplitude of the waveforms instead of the time shift.

In these four modulation techniques, DS-SS PAM can have a 100% duty cycle, which is defined as the ratio of the time that a waveform is present to the waveform repetition interval. The definition can be presented as T_w/T_f (T_w is the width of the waveform). It is higher than what is possible with the other three techniques. With a high duty cycle, DS-SS

PAM can provide higher data rates with the same impulse waveform pulse width than the other three techniques.

The disadvantage with DS-SS PAM is that the gap between adjacent spectrum lines in the frequency domain is proportional to $1/T_f$. This is because the impulse waveforms are distributed with constant frequency $1/T_f$. These spectrum lines may result in excessive interference to other existing wireless communication systems operating in the same bandwidth.

DS-SS PPM modulation is a type of hybrid DS-TH with a constant TH code sequence [13]. It is similar to DS-FH (direct-sequence and frequency-hopping) SS. Its duty cycle is higher than TH-SS PPM and TH-PAM with the same impulse waveform width. Furthermore, as the waveforms appear randomly due to the time shift from δ in (1.7), the interference to other existing wireless communications at kT_f (k is an integer) will be less than that of DS-SS PAM. This makes DS-SS PPM a more desirable waveform.

1.2 Error Correcting Codes

Error correcting codes are also called channel codes. They are widely used in digital communication systems to increase signal immunity to noise and interference. Error protection is achieved by adding specified redundant bits to the information bits. This process is called encoding. The redundancy is used at the receiver to determine the most likely sequence of bits transmitted. BCH codes belong to the class of block codes and are one of the most popular classes of error correcting codes [14]. They were independently discovered by A. Hocquenghem in 1959 and Bose and Ray-Chaudhuri in 1960 [14]. Since then, they have been widely used in digital communication systems because they can provide significant performance improvements. In this thesis, we employ BCH codes in a UWB DS-SS PPM system and consider errors-only and errors-and-erasures decoding schemes.

1.3 Thesis Outline

This chapter presented an introduction to UWB systems, modulation techniques and error correcting codes. Four typical UWB system impulse waveforms were presented in the time domain and frequency domain. Then DS-SS PPM, DS-SS PAM, TH-SS PPM and TH-SS PAM systems were explained and compared. In Chapter 2, the fundamentals of BCH codes and the decoding algorithms developed are given. This includes errors-only decoding and errors-and-erasures decoding. Chapter 3 presents the system model which employs DS-SS PPM UWB and BCH coding over an additive white Gaussian noise (AWGN) channel. Simulation results are presented and summarized. Chapter 4 presents the performance over a fading channel. Chapter 5 concludes the thesis and suggests some directions for future work.

Chapter 2

BCH Codes and Decoding

In digital communications, the performance of a communication system is heavily influenced by noise, fading and path loss. To improve system performance, error correcting codes have been developed and widely used since Richard Hamming published the first error correcting codes in 1950 [14].

The principle of error correction coding is to add redundancy (parity bits) to the information stream. This redundancy enables a decoder to detect and/or correct transmission errors. According to Shannon's noisy channel coding theorem [14], by properly choosing error correcting codes, an arbitrarily low bit error rate can be achieved as long as the data rate is less than the channel capacity. Practically, higher performance requires more redundancy. In real-time communications, the cost is more bandwidth.

In UWB systems, due to the low power emission restriction, the signal-to-noise ratio E_b/N_0 is low, which results in a poor bit error rate in uncoded systems. Thus error correcting codes are necessary to provide adequate performance. A well-designed error correcting code can achieve excellent performance without significantly increasing the transmitted power.

2.1 BCH Codes

There are two major families of error correcting codes, block codes and trellis (convolutional) codes [15]. Codes can also be divided into linear codes and nonlinear codes. BCH codes are cyclic linear block codes. According to the definition from [15], block codes refer to codewords of length n each of which corresponds to a message block of length m. The codeword symbols are taken from an alphabet of size q, and the message symbols are taken from an alphabet of size d, which satisfy $d^m \leq q^n$. Linear codes refer to a linear mapping from the space of the message blocks to the space of the codewords. Cyclic codes are defined as linear block codes for which a cyclic shift of any codeword is also a codeword.

BCH codes have been widely studied due to their error correction capabilities and efficiency. The advantages of BCH codes include outstanding performance especially for short-to-moderate block lengths with small code alphabet sizes; numerous choices of block lengths and code rates; and efficient decoding algorithms. In addition, short-to-moderate BCH codes fit well with real-time high data rate wireless communications requirements because of their low-complexity and short delay [16]. BCH codes have been shown to improve the bit error rate of spread spectrum communication systems [17].

BCH Code Definition

BCH codes employ successive powers of an alphabet element as zeros of the generator polynomial. From [15], the definition of a BCH code is as follows.

> Given a field $GF(q)$, a block length $n \geq 3$, which is a divisor of $q^m - 1$ for some m, and $3 \leq \delta \leq n$, an (n, k) BCH code over $GF(q)$ is a cyclic code

generated by

$$g(x) = \text{LCM}[m_{\alpha^j}(x), m_{\alpha^{j+1}}(x), m_{\alpha^{j+2}}(x), \ldots, m_{\alpha^{j+\delta-2}}(x)], \qquad (2.1)$$

where $GF(q)$ denotes the Galois field of order q; δ is the minimum distance of the BCH code; $g(x)$ is the generator polynomial; $\{m_{\alpha^t}(x)\}(j \leq t \leq j+\delta-2)$ are the minimal polynomials of $\delta - 1$ consecutive powers of a primitive nth root of unity α in an extension field $GF(q^m)$; j is a nonnegative integer; LCM denotes the least common multiple of all the indicated minimal polynomials.

Basic Concepts

In order to understand BCH codes more thoroughly, some essential concepts need to be clarified.

A field is a set of objects F on which two operations $+$ (addition) and $\cdot$ (multiplication) are defined [14] : $\alpha \cdot (\beta + \gamma) = (\alpha \cdot \beta) + (\alpha \cdot \gamma), (\alpha, \beta, \gamma \in F)$; F forms a commutative group under $+$ with the additive identity element $\{0\}$; $F - \{0\}$ forms a commutative group under $\cdot$ with the multiplicative identity element $\{1\}$. A Galois field is a field of finite order (cardinality). For any prime q there exists a finite field of q elements, denoted $GF(q)$. It is also possible to extend the prime field $GF(q)$ to the field $GF(q^m)$ for any positive integer m.

The Hamming distance between two codewords is defined as the number of coordinates in which the two codewords differ. The minimum distance d_{min} of a BCH code is the minimum Hamming distance between any two codewords. A BCH code with minimum distance d_{min} can correct up to $\lfloor (d_{min} - 1)/2 \rfloor$ errors or detect up to $d_{min} - 1$ errors.

A generator polynomial for a BCH code is defined as the unique monic polynomial $g(x)$

with degree $n-k$ in an (n,k) BCH code. Every code polynomial $c(x)$ can be expressed as $c(x) = g(x)m(x)$, where $m(x)$ is a message polynomial of degree less than k.

A minimal polynomial with respect to the field $GF(q)$ is the smallest-degree nonzero polynomial $m_\alpha(x)$ in $GF(q)[x]$ such that $m_\alpha(\beta) = 0, (\beta \in GF(q))$.

The BCH bound is a very important property of BCH codes. Let C be an (n,k) cyclic code with generator polynomial $g(x)$ over $GF(q)$. Let m be the smallest integer such that $n|q^m - 1$, and let $\alpha \in GF(q^m)$ be a primitive nth root of unity. For some integers $b \geq 0$ and $\delta \geq 2$, $g(\alpha^j) = 0, (j = b, b+1, \ldots, b+\delta-2)$. Then the minimum distance is $d_{min} \geq \delta$ if $g(x)$ has $(\delta - 1)$ successive powers of α as zeros. The parameter δ is called the design distance. If $b = 1$, the BCH code is called narrow-sense. If $n = q^m - 1$ (m is some positive integer), the BCH code is called primitive.

BCH Code Design

Using the previous description of BCH codes, a detailed procedure to design a BCH code is given in Figure 2.1. Note that the real minimum Hamming distance d_{min} may be greater than the design distance δ, in which case an optimum decoder can correct more errors than standard BCH decoding algorithms [15]. However, it is known that all primitive single and double error correcting BCH codes have a minimum distance exactly the same as the design distance [18].

Based on Figure 2.1, we give an example of the construction of a 2-error correcting BCH code of length 31 over $GF(2)$.

let $t = 2, q = 2, n = 31$

$\Rightarrow$ *find the minimal* m *such that* $31|2^m - 1$

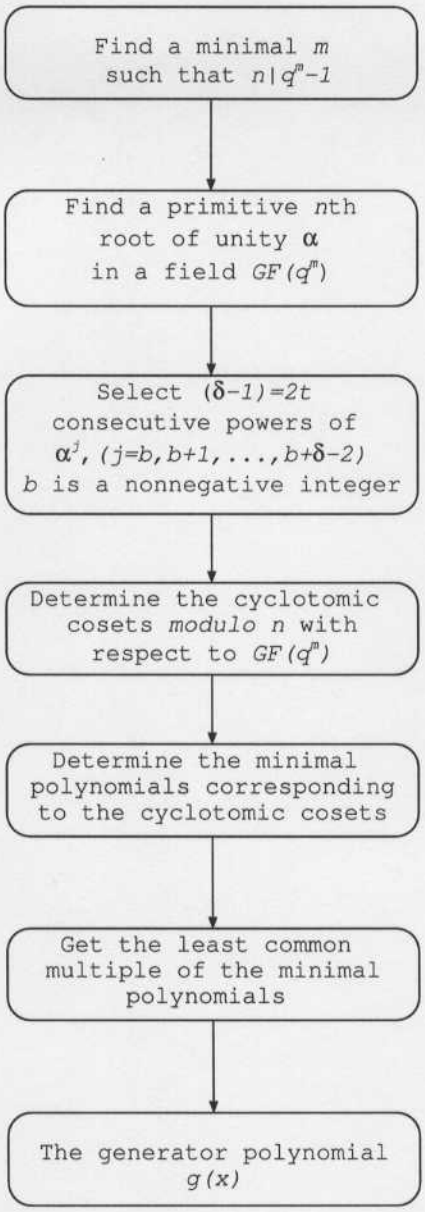

Figure 2.1. *BCH code design procedure.*

$\Rightarrow m = 5$

$\Rightarrow$ *let* α *be a primitive* $31st$ *root of unity in* $GF(2^5)$

$t = 2 \Rightarrow \delta - 1 = 2t = 4$

Let $b = 1 \Rightarrow$ *four consecutive powers of* α *are the roots of the generator polynomial* : $\alpha, \alpha^2, \alpha^3, \alpha^4$.

Cyclotomic Cosets	*Conjugacy Class*	*Associated Minimal Polynomial*
$\{0\}$	$\{1\}$	$M_0(x)$
		$= x - 1 = x + 1$
$\{1, 2, 4, 8, 16\}$	$\{\alpha, \alpha^2, \alpha^4, \alpha^8, \alpha^{16}\}$	$M_1(x)$
		$= (x - \alpha)(x - \alpha^2)(x - \alpha^4)(x - \alpha^8)(x - \alpha^{16})$
		$= x^5 + x^2 + 1$
$\{3, 6, 12, 24, 17\}$	$\{\alpha^3, \alpha^6, \alpha^{12}, \alpha^{24}, \alpha^{17}\}$	$M_3(x)$
		$= (x - \alpha^3)(x - \alpha^6)(x - \alpha^{12})(x - \alpha^{24})(x - \alpha^{17})$
		$= x^5 + x^4 + x^3 + x^2 + 1$
$\{5, 10, 20, 9, 18\}$	$\{\alpha^5, \alpha^{10}, \alpha^{20}, \alpha^9, \alpha^{18}\}$	$M_5(x)$
		$= (x - \alpha^5)(x - \alpha^{10})(x - \alpha^{20})(x - \alpha^9)(x - \alpha^{18})$
		$= x^5 + x^4 + x^2 + x + 1$
$\{7, 14, 28, 25, 19\}$	$\{\alpha^7, \alpha^{14}, \alpha^{28}, \alpha^{25}, \alpha^{19}\}$	$M_7(x)$
		$= (x - \alpha^7)(x - \alpha^{14})(x - \alpha^{28})(x - \alpha^{25})(x - \alpha^{19})$
		$= x^5 + x^3 + x^2 + x + 1$
$\{11, 22, 13, 26, 21\}$	$\{\alpha^{11}, \alpha^{22}, \alpha^{13}, \alpha^{26}, \alpha^{21}\}$	$M_{11}(x)$
		$= (x - \alpha^{11})(x - \alpha^{22})(x - \alpha^{13})(x - \alpha^{26})(x - \alpha^{21})$
		$= x^5 + x^4 + x^3 + x + 1$
$\{15, 30, 29, 27, 23\}$	$\{\alpha^{15}, \alpha^{30}, \alpha^{29}, \alpha^{27}, \alpha^{23}\}$	$M_{15}(x)$
		$= (x - \alpha^{15})(x - \alpha^{30})(x - \alpha^{29})(x - \alpha^{27})(x - \alpha^{23})$
		$= x^5 + x^3 + 1$

$\Rightarrow$ *obtain the minimal polynomials* $M_1(x)$ *having roots* $\{\alpha, \alpha^2, \alpha^4\}$ *and* $M_3(x)$

having root $\{\alpha^3\}$.

$\Rightarrow$ *the generator polynomial is*

$g(x) = \text{LCM}(M_1(x), M_3(x)) = M_1(x)M_3(x) = x^{10} + x^9 + x^8 + x^6 + x^5 + x^3 + 1$

From this example, we find that in order to minimize the redundancy that is added into the data stream while achieving a given error correcting capability or to maximize the code rate, the degree of the generator polynomial should be minimized. This corresponds to minimizing the number of zeros of the generator polynomial while keeping the necessary number of consecutive powers of a primitive nth root of unity as zeros. The extra roots of the generator polynomial are actually the conjugates of the required roots. This suggests proper selection of b to construct the most efficient BCH code (with the highest code rate $R_c = k/n$).

2.2 BCH Decoding

The first explicit decoding scheme for BCH codes was published by Peterson in 1960. It was designed for binary BCH codes. Since then, many other decoding schemes have been studied and implemented. Generally, decoding schemes are either hard-decision or soft-decision.

With hard-decision decoding, the detection algorithm only distinguishes the received symbol according to the transmitted symbols. For binary BCH codes, this means that "0" and "1" are the choices the detection algorithm can select from. Typically, a threshold is set midway between the values of "0" and "1", and the detection algorithm determines the received symbol by comparing it to the threshold. The advantages of hard-decision decoding are low complexity and low delay.

However, hard-decision decoding does not make use of all the information in the re-

ceived symbols, which can improve the overall performance. For instance, assuming the value "0" is the threshold to determine between the two transmitted symbol values "+1" and "-1", the received values "+10", "+1" and "+0.1" are all assigned to symbol "+1". Obviously, the likelihood of correctly assigning a received value to symbol "+1" ranges from high to low according on the distance between the received value and the threshold.

A soft-decision receiver employs an expanded set of values to allocate the received symbols. The simplest soft-decision receiver uses erasures to denote received values that are in doubt (close to the threshold). These are used in conjunction with a BCH decoding algorithm. In this thesis, we use the well known Berlekamp-Massey decoding algorithm for errors-only and errors-and-erasures (soft-decision) decoding.

2.2.1 The Berlekamp-Massey Decoding Algorithm

The Berlekamp-Massey decoding algorithm is a hard-decision decoding algorithm. It is one of the most efficient decoding algorithms in terms of complexity [14]. This algorithm is derived from Berlekamp's algorithm and Massey's shift-register-based interpretation [14].

A t-error-correcting binary BCH code is constructed by first identifying the smallest field $GF(2^m)$ that contains a primitive nth root of unity α. The generator polynomial $g(x)$ then has $2t$ consecutive powers of α as roots

$$g(\alpha^i) = 0, (i = b, b+1, \ldots, b+2t-1), \tag{2.2}$$

where b is a nonnegative integer.

Assume the transmitted codeword polynomial is

$$c(x) = \sum_{i=0}^{n-1} c_i x^i, \tag{2.3}$$

where $c(x)$ corresponds to the codeword $(c_0, c_1, \ldots, c_{n-1})$. The received polynomial is

$$r(x) = c(x) + e(x), \tag{2.4}$$

where $e(x) = \sum_{i=1}^{k} e_{p_i} x^{p_i}$, $(k \leq t, p_i < p_j$ when $i < j)$ is the error polynomial with error positions $(p_1, p_2, \ldots, p_k)$. Define the syndrome series $s_j, j = 1, 2, \ldots, 2t$ in $GF(2^m)$. For simplicity, a narrow-sense code $(b = 1)$ is considered

$$s_j = r(\alpha^j) = e(\alpha^j) = \sum_{i=1}^{k} e_{p_i} \alpha^{jp_i}, j = 1, 2, \ldots, 2t, k \leq t. \tag{2.5}$$

The computations in (2.5) are performed in $GF(2^m)$. Because the coefficients of the error polynomial are in $GF(2)$ for a binary BCH code, $e_{p_i} = 1, (i = 1, 2, \ldots, k)$, where k is the number of errors. Then the syndrome series can be expressed as

$$s_j = \sum_{i=1}^{k} e_{p_i} \alpha^{jp_i} = \sum_{i=1}^{k} l_i^j, j = 1, 2, \ldots, 2t, k \leq t, \tag{2.6}$$

where $l_i = \alpha^{p_i}, (i = 1, 2, \ldots, k)$ is the error locator for the ith error. These are a sequence of $2t$ syndrome equations in terms of the k unknown error location values $\{l_i\}$. The next step is to define an error locator polynomial that has as its roots the inverse of the k error locators

$$M(x) = \prod_{i=1}^{k} (1 - l_i x) = M_0 + M_1 x + M_2 x^2 + \cdots + M_k x^k, \tag{2.7}$$

where

$$M_i = \sum_{j_1 < j_2 < \cdots < j_i} l_{j_1} l_{j_2} \cdots l_{j_i}.$$

Combining (2.6) and (2.7), the following polynomials can be derived

$$\begin{aligned} s_1 + M_1 &= 0 \\ s_2 + s_1 M_1 + 2M_2 &= 0 \\ &\vdots \\ s_k + s_{k-1} M_1 + \cdots + s_1 M_{k-1} + kM_k &= 0 \\ s_{k+1} + s_k M_1 + \cdots + s_1 M_k &= 0 \\ &\vdots \\ s_{2t} + s_{2t-1} M_1 + \cdots + s_{2t-k} M_k &= 0 \end{aligned}$$

In $GF(2^m)$, $(\sum_{i=1}^{t} \alpha_i)^{2^u} = \sum_{i=1}^{t} \alpha_i^{2^u}$ for $u = 1, 2, 3, \ldots,$, so that $s_{2i} = s_i^2$ [14]. The resulting simplified equations are

$$\begin{aligned} s_1 + M_1 &= 0 \\ s_3 + s_2 M_1 + s_1 M_2 + M_3 &= 0 \\ &\vdots \\ s_{2t-1} + s_{2t-2} M_1 + \cdots + s_{2t-k-1} M_k &= 0 \end{aligned}$$

These can also be expressed as a function of the coefficients of the error locator polynomial $M(x)$ and the syndromes $s_{i-1}, \ldots, s_{i-k}$ in recursive form

$$s_i = \begin{cases} -(s_{i-1} M_1 + s_{i-2} M_2 + \cdots + s_{i-k} M_k) & \text{if } i > k \\ -(s_{i-1} M_1 + s_{i-2} M_2 + \cdots + s_1 M_{i-1} + M_i) & \text{if } 1 \leq i \leq k\,, \end{cases} \tag{2.8}$$

Massey provided a linear feedback shift register (LFSR) interpretation of the solution of (2.8). Figure 2.2 shows its physical structure.

In Massey's interpretation, decoding involves finding an LFSR of minimum length for which the first $2t$ outputs are the same as the syndromes $s_1, s_2, \ldots, s_{2t}$. Then the LFSR taps

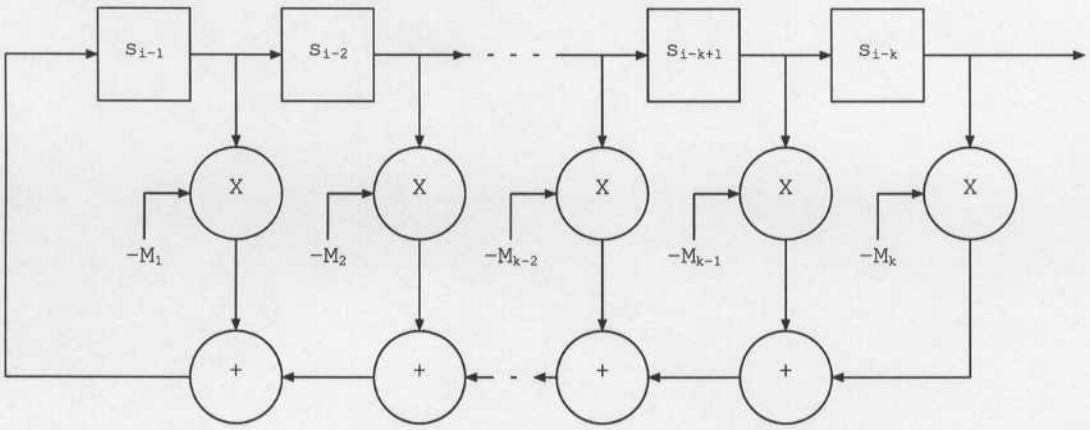

Figure 2.2. *A linear feedback shift register.*

are the coefficients of the corresponding error locator polynomial $M(x)$. The Berlekamp-Massey algorithm is a recursive algorithm. It starts with $M^{(0)}(x) = M_0 = 1$. Then M_1 is found such that $M^{(1)}(x) = M_0 + M_1 x$ creates the first syndrome element s_1. The LFSR construction continues to create the second element such that the second syndrome s_2 is output. The discrepancy between the output and s_2 is used to update the LFSR. This process continues until all $2t$ syndromes are output. The resulting error locator polynomial $M(x)$ is unique provided that the number of errors is not greater than t [14].

Figure 2.3 is a flowchart of the Berlekamp-Massey decoding algorithm. Here $s_1, \ldots, s_{2t}$ is the syndrome sequence calculated using (2.5); i is the index variable; N is the length of the LFSR; $M^{(i)}(x)$ is the error locator polynomial corresponding to index i; $p(x)$ is the adaptation polynomial; and $d^{(i)}$ is the discrepancy. In each iteration, if the discrepancy is zero, the error locator polynomial will be the same as in the previous iteration. The maximum number of iterations is $2t$.

In this thesis, we employ the Berlekamp-Massey algorithm for binary BCH decoding.

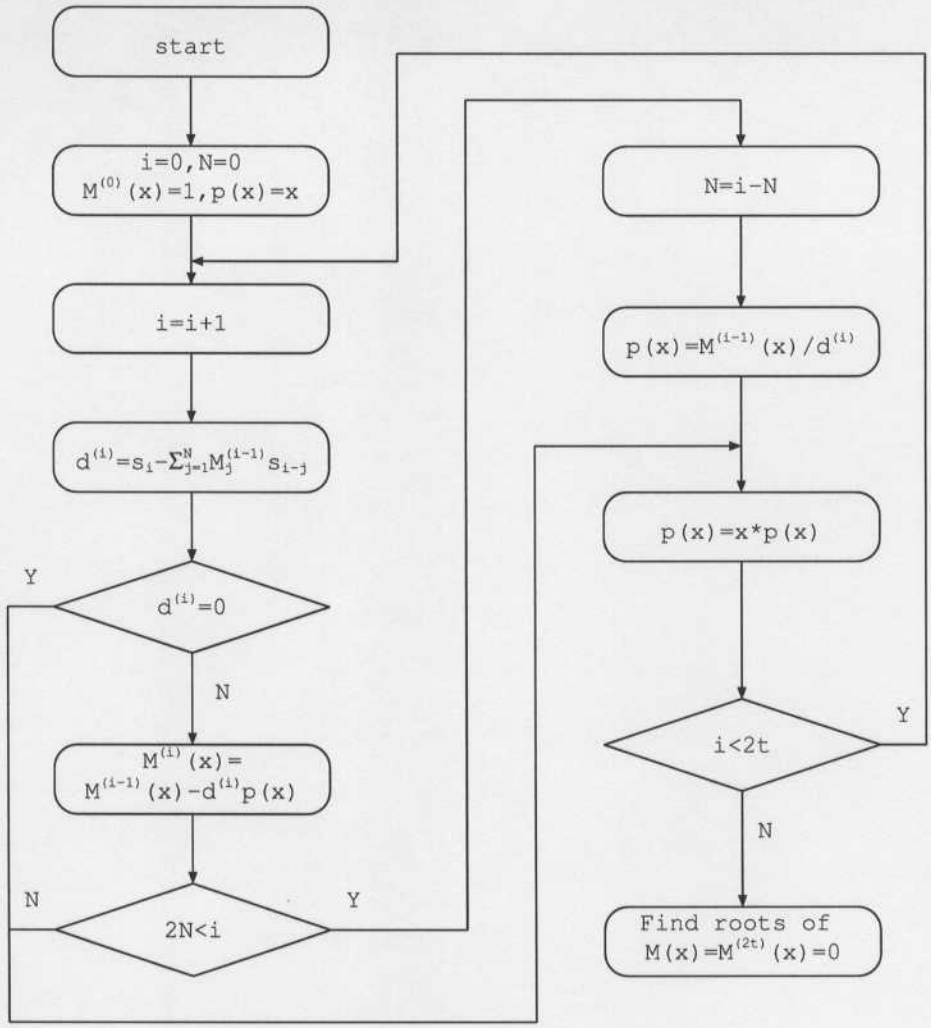

Figure 2.3. *The Berlekamp-Massey decoding algorithm.*

2.2.2 Errors-and-Erasures Decoding

In a binary DS-SS PPM UWB communications system, the symbol choices at the receiver are limited to "0" and "1". With hard-decision decoding, a received symbol will only be categorized as "0" or "1" no matter what the received value is. A soft-decision decoding scheme takes advantage of the "wasted" information to improve the probability of correct decoding.

Among soft-decision decoding schemes, errors-and-erasures decoding is very simple and efficient. In the binary case, some doubtful received symbols will be indicated by erasures instead of "0" or "1". Let δ be the minimum distance of the BCH code; e the number of errors and r the number of erasures. The received symbols will be decoded successfully if

$$2e + r \leq \delta - 1, \tag{2.9}$$

is satisfied.

This shows that if the number of errors is zero, up to $\delta - 1$ erasures can be corrected. Thus erasures decoding provides a higher error correcting capability if all error locations are covered by erasures. Figure 2.4 shows the errors-and-erasures decoding algorithm. In Figure 2.4, the algorithm starts by setting the number of erasures to r. Then in the received word R, the r symbols that are least likely to be correct (those closest to the threshold), are marked as erasures. Note that a received symbol with the same value as the threshold has a 50% probability of being a "0" or "1". In the following two steps, two words are decoded, the received word R with all its erasures replaced by "0", and the received word R with all its erasures replaced by "1". The final decision is made by comparing the Hamming distances between the resulting code words and the received word. The smaller distance corresponds to the correct codeword if (2.9) is satisfied. The reason for this is as follows. We require that $2e+r \leq \delta-1$ as indicated in (2.9). Assuming r_0 and r_1 are the errors introduced by replacing the erasures with "0" and "1", respectively,

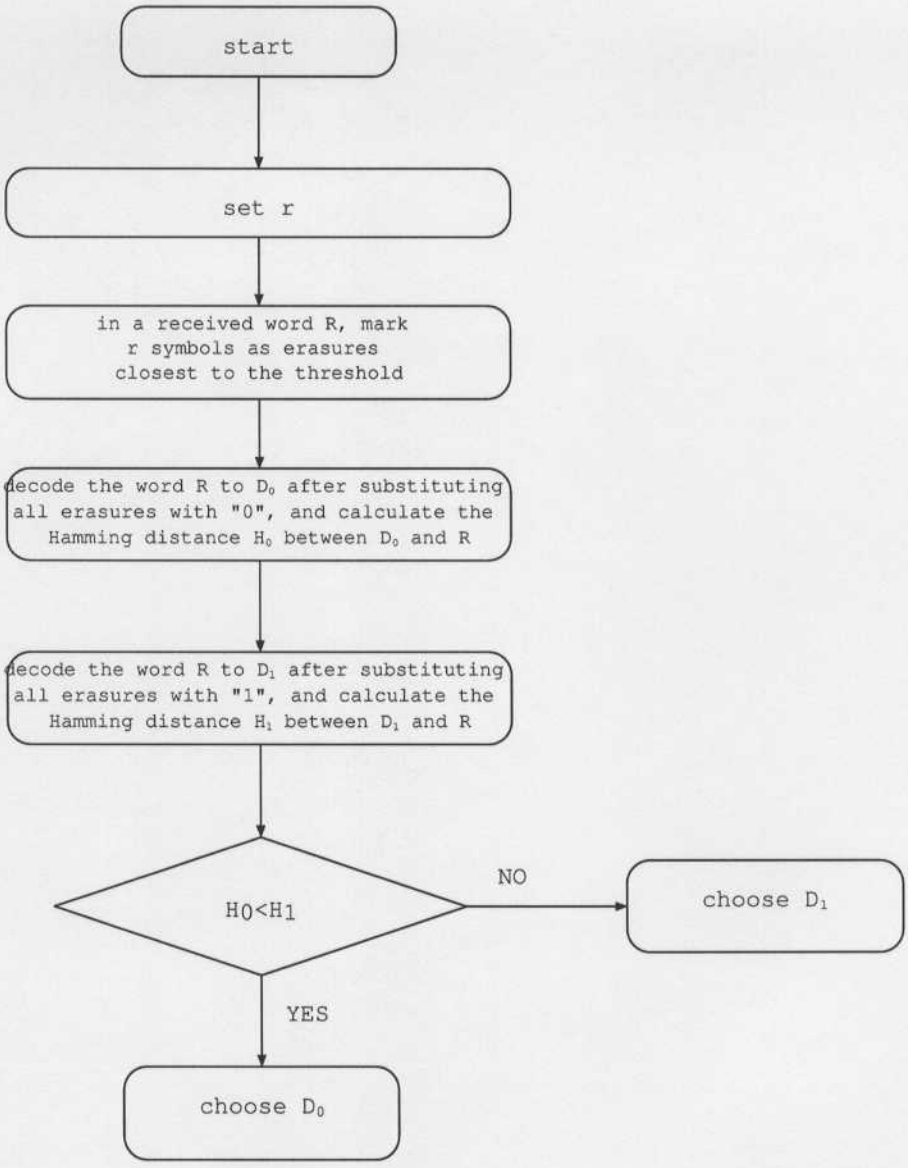

Figure 2.4. *Binary errors-and-erasures decoding algorithm.*

the total number of errors will be $(e + r_0)$ for D_0 and $(e + r_1)$ for D_1. As $r_0 + r_1 = r$, $(e + \min(r_0, r_1)) \leq (e + r/2) \leq (\delta - 1)/2$, which means that the correction will be successful. If the number of errors is greater than $\lfloor(\delta - 1)/2\rfloor$, decoding will either fail or result in an incorrect codeword.

2.3 Discussion

Because of their strong error correcting capability and high efficiency, BCH codes play an important role in digital communications systems. In UWB systems, the low signal power levels and channel fading make it necessary to employ error correction coding. BCH codes are a large family of codes with a variety of blocklengths and code rates. Tradeoffs exist among the data rate, code rate, blocklength, multi-access capacity, signal to noise ratio, and bit error rate.

A hard-decision decoding algorithm, the Berlekamp-Massey algorithm, was presented along with an efficient technique for errors-and-erasures decoding. Errors-and-erasures decoding makes better use of the received information. However, because each received codeword is decoded twice, the decoding time and/or the decoding hardware is increased. This may be a concern for some high data rate real-time UWB systems due to the extra delay, but as will be seen in the next chapter, some performance gains can be achieved.

We will study the performance of BCH codes with various blocklengths and code rates in a typical UWB system (DS-SS PPM UWB). Both AWGN and fading channels will be considered along with multi-access communications.

Chapter 3

DS-SS PPM UWB System Performance in AWGN

In UWB systems, DS-SS is a very popular multiplexing technique by which multiple users can simultaneously communicate in the same frequency band with tolerable cross interference [19]. It has been used in military and commercial applications for decades. By adopting Gold codes as the pseudo-random spreading sequences, DS-SS can alleviate the effects of cross interference due to their good autocorrelation and cross-correlation properties of these codes [15].

In this chapter, an AWGN channel is considered. The effects of fading are considered in the next chapter. The performance of a DS-SS PPM UWB system will be analyzed and the improvement using different BCH codes will be verified and studied.

3.1 System Model over An AWGN Channel

In a binary DS-SS PPM UWB system, the information data stream for each user is first BCH encoded. Then the codeword bits are mapped into a number of impulse waveforms by introducing a time shift delay δ that is decided by the bit value. The phase is modified by the Gold code sequence designated to the user. At the receiver, a pulse correlator is employed to recover the received bits. Next BCH decoding provides the received information data

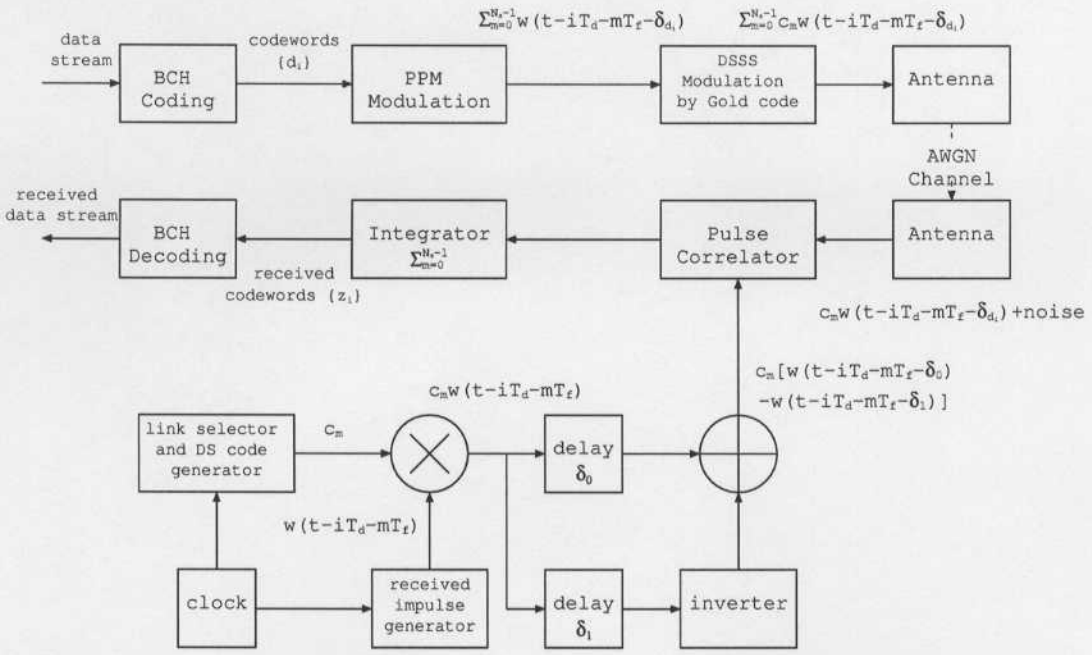

Figure 3.1. *A binary DS-SS PPM UWB system with BCH coding over an AWGN channel.*

stream. Figure 3.1 illustrates this system. In this diagram, the transmitted DS-SS PPM signal is given by

$$S^{(v)}(t) = \sum_{v=1}^{\infty} \sum_{m=0}^{N_s-1} c_m^{(v)} w(t - iT_d - mT_f - \delta_{d_i^{(v)}}), \tag{3.1}$$

where $S^{(v)}$ is the signal for the vth user; $w(t)$ is the impulse waveform; $\{c_m^{(v)}\}$ is the Gold code sequence for user v; N_s is the number of impulses modulated by each data bit; T_f is the impulse repetition interval; m is the mth interval; T_d is the data bit interval; $\delta_{d_i^{(v)}}$ is the delay corresponding to the data bit value.

The impulse waveform $w(t)$ we use is a normalized Gaussian monocycle as presented in (3.2) [20]

$$w(t) = [1 - 4\pi(\frac{t - 0.35}{0.2877})^2] \exp[-2\pi(\frac{(t - 0.35)}{0.2877})^2], \tag{3.2}$$

with center at $t = 0.35ns$ and time duration $T = 7 \times (0.2877/\sqrt{4\pi}) = 0.568ns$ symmetrically distributed [4].

In Figure 3.1, the composite received signal with N_u users is given by

$$R(t) = \sum_{v=1}^{N_u} r^{(v)}(t) + n(t), \tag{3.3}$$

where $n(t)$ is additive white Gaussian noise and

$$r^{(v)}(t) = \sum_{i=1}^{\infty} \sum_{m=0}^{N_s-1} c_m^{(v)} w(t - iT_d - mT_f - \delta_{d_i^{(v)}}). \tag{3.4}$$

Then the pulse correlator decision rule for errors-only decoding for the first user is

$$"z_i^{(1)} = 0" \Longleftrightarrow D_i^{(1)} = \sum_{m=0}^{N_s-1} \int_{mT_f}^{(m+1)T_f} R(t) w_\Delta^{(1)}(t - mT_f) dt > 0, \tag{3.5}$$

where $w_\Delta^{(1)}(t) = c_m^{(1)}[w(t - iT_d - \delta_0) - w(t - iT_d - \delta_1)]$ is the correlator sequence.

For errors-and-erasures decoding, assuming $\{z_i^{(1)}\}(i = 1, 2, \ldots, n)$ is the received word, if

$$|D_{u_1}^{(1)}| \leq |D_{u_2}^{(1)}| \leq \cdots \leq |D_{u_n}^{(1)}|, (u_i \in \{1, 2, \ldots, n\} \; and \; u_p \neq u_q \; for \; p \neq q), \tag{3.6}$$

then $\{z_{u_1}^{(1)}, z_{u_2}^{(1)}, \ldots, z_{u_r}^{(1)}\}$ will be categorized as erasures where r is the number of erasures. The other bits will be determined according to (3.5).

For binary $BCH(n, k, t)$ codes, the code rate R_c is defined as $R_c = k/n$. It has been shown that BCH codes with rates $1/3$ to $3/4$ provide the best coding gains [21]. The bit error rate can be severely degraded if the code rate is either very high or very low [22]. Therefore, in this thesis we consider primitive binary BCH codes with parameters $(31, 26, 1)$, $(31, 16, 3)$, $(31, 11, 5)$, $(127, 99, 4)$ and $(127, 85, 6)$.

The simulations were done on SunBlade 1500 workstations employing Matlab v6.5. On average, each point was based on 3 runs of 1-10 million bits each.

3.2 Simulation Results

In this section, we compare the performance of uncoded and coded DS-SS PPM UWB systems using BCH codes over an AWGN channel. In particular, the relationship between the BER improvement and the code rate is evaluated. We focus on the performance improvement due to BCH coding. Furthermore, the effects of different BCH decoding algorithms are also analyzed, specifically errors-only and errors-and-erasures decoding. The length of the Gold code sequences for DS-SS is chosen to be 31, which is produced by modulo 2 adding the outputs of two shift registers of length 5. Two scenarios are employed: synchronous and asynchronous. With synchronous communications, all the users are synchronized in time.

3.2.1 Synchronous Communications

Figure 3.2 shows the uncoded performance for one, five and ten users, respectively. When E_b/N_0 is zero in the single-user case, the BER is about 10^{-1}, which is much better than the performance without spreading [11]. The reason is that there are 31 waveforms transmitted for each data bit. Among the three curves, the single-user performance is best, followed by that with 5-users and 10-users, which is reasonable. However, the degradation from single-user to 5-users, and from 5-users to 10-users, is small. This can be explained as follows. According to (3.3), (3.4) and (3.5), the pulse correlator decision for one data bit of the first user can be expressed by

$$D^{(1)} = \sum_{v=1}^{N_u} \Delta D^{(1,v)} + \Delta D^{(1)}_{noise}, \tag{3.7}$$

where $\Delta D^{(1,v)} = \sum_{m=0}^{N_s-1} \int_{mT_f}^{(m+1)T_f} [c_m^{(v)} w(t - mT_f - \delta_{d^{(v)}})]\{c_m^{(1)}[w(t - mT_f - \delta_0) - w(t - mT_f - \delta_1)]\}dt$; $\Delta D^{(1)}_{noise} = \sum_{m=0}^{N_s-1} \int_{mT_f}^{(m+1)T_f} n(t)\{c_m^{(1)}[w(t - mT_f - \delta_0) - w(t - mT_f - \delta_1)]\}dt$; $w(t)$ is the impulse waveform; $\{c_m^{(v)}\}$ is a Gold code sequence for user v; $n(t)$ is

AWGN noise. In this case, $N_s = 31$, so that

$$\Delta D^{(1,v)} = \begin{cases} -\frac{1}{31}\Delta D^{(1,1)}, & \text{if } \delta_{d^{(v)}} = \delta_{d^{(1)}} \text{ and } v \neq 1, \\ \frac{1}{31}\Delta D^{(1,1)}, & \text{if } \delta_{d^{(v)}} \neq \delta_{d^{(1)}} \text{ and } v \neq 1, \end{cases} \tag{3.8}$$

because $\delta_{d^{(v)}}(v \neq 1)$ is independent of $\delta_{d^{(1)}}$, so the probability that $\delta_{d^{(v)}} = \delta_{d^{(1)}}$ is $1/2$. Therefore, the cross interference in the pulse correlator is $\{\frac{N_u-1-2i}{31}\Delta D^{(1,1)}\}$ (i is the number of the users that transmit the same data bit as the first user) with probability $\left\{\binom{N_u-1}{i}(\frac{1}{2})^{N_u-1}\right\}$. In (3.7), we see how the cross interference impacts the decision. As $\Delta D^{(1,1)}$ is the energy of the first user bit, a positive cross interference will increase the effective bit energy for the first user, and a negative cross interference will decrease this energy. From this result, we see that the cross interference from other users is mostly cancelled, which explains why multi-user performance has only a slight degradation.

Figure 3.3 shows the performance of the $BCH(31, 26, 1)$, $BCH(31, 16, 3)$, $BCH(31, 11, 5)$, $BCH(127, 99, 4)$ and $BCH(127, 85, 6)$ codes for the single-user case. Compared to the performance of the uncoded system, the performance of the coded systems is improved when the BER is lower than 10^{-2}. This is because when the BER is high, the number of errors often exceeds the error correcting capability of the code and decoding may introduce additional errors.

As the BER decreases (E_b/N_0 increases), the coded systems show accelerated improvement with respect to the uncoded system. Among the BCH codes of length 31, for a BER between 10^{-2} and 10^{-4}, $BCH(31, 11, 5)$ is always the best, $BCH(31, 16, 3)$ is the second best, and $BCH(31, 26, 1)$ is the weakest. The coding gains become more obvious as the BER decreases. At a BER of 10^{-4}, $BCH(31, 11, 5)$ gives the most coding gain of 1.9dB, $BCH(31, 16, 3)$ gives a coding gain of 1.7dB and $BCH(31, 26, 1)$ gives the least coding gain of 1.2dB. For the BCH codes of length 127, at a BER of 10^{-4}, $BCH(127, 85, 6)$ has a coding gain of 2.9dB and $BCH(127, 99, 4)$ has a coding gain of 2.5dB. The stronger code

$BCH(127, 85, 6)$ always shows better performance than $BCH(127, 99, 4)$ between BERs of 10^{-2} and 10^{-4}. The advantage of $BCH(127, 85, 6)$ becomes more obvious as the BER decreases. Furthermore, the BCH codes of length 127 have better performance than the BCH codes of length 31 when the BER is below 10^{-2}.

Figure 3.3 shows the performance with errors-only decoding. In order to enhance the performance without decreasing the code rate, we also consider errors-and-erasures decoding. Figures 3.4, 3.5 and 3.6 show the performance for the single-user case using 2, 4 and 6 erasures, respectively. These figures confirm that errors-and-erasures decoding improves the performance as explained in Chapter 2. Though the coding scheme and the channel conditions are the same, errors-and-erasures decoding makes better use of the information in the received bits by substituting erasures for the least reliable bits.

Figure 3.7 presents the performance of $BCH(31, 26, 1)$, where we see that $BCH(31, 26, 1)$ and $BCH(31, 26, 1, 2)$ show about 1dB coding gain that is the least coding gain among the five codes due to the lower error correcting capability. However, it has a higher code rate than the other two BCH codes of length 31. $BCH(31, 26, 1, 2)$ provides only a trivial performance improvement compared to that with $BCH(31, 26, 1)$ because the number of erasures is only one higher than the single correctable error, and the code can no longer correct unerased bits.

Figure 3.8 shows the performance of $BCH(31, 16, 3)$, where we find that $BCH(31, 16, 3, 2)$ has a greater improvement over $BCH(31, 16, 3)$ than $BCH(31, 16, 3, 6)$. It indicates that sufficient error correcting capability should exist for unerased bits. Beyond this point, the performance is worse than without erasures. This is because as the number of erasures approaches its maximum, the new erasures have less probability of being in errors, whereas fewer bits in error that were not erased can be corrected. Figures 3.9 for $BCH(31, 11, 5)$, 3.10 for $BCH(127, 99, 4)$ and 3.11 for $BCH(127, 85, 6)$, all show similar results to the

previous figure. When the number of erasures is less than the maximum $2e$, where e is the error correcting capability, better performance is obtained by decoding with more erasures though the marginal improvement is smaller. At a BER of 10^{-4}, the extra coding gains with erasure decoding over no erasures is approximately 0.5dB, which translates into a 12% reduction in power (except for $BCH(31, 26, 1, 2)$ and $BCH(31, 16, 3, 6)$, which are at the maximums).

For the multiple-user case, we have simulated 5-user and 10-user systems using the same BCH codes and numbers of erasures. In the 5-user case, Figures 3.12, 3.13, 3.14 and 3.15 show similar performance to that with a single user. No significant degradation in performance occurs. This is because the interference from other users is essentially cancelled according to (3.8). In the 10-user case, Figures 3.16, 3.17, 3.18 and 3.19 also show similar performance to that with a single user. The degradation is about 0.3dB at a BER of 10^{-4} compared to the single-user case. Thus the discussion given above also applies to these cases.

3.2.2 Asynchronous Communications

With asynchronous communications, Figure 3.20 shows the uncoded performance for a single-user, 5-user and 10-user. The single-user case is identical to that with synchronous communications. Compared to the single-user performance, the 5-user case has a degradation of about 1.8dB and the 10-user case has a degradation of about 2.3dB at a BER of 10^{-4}, which corresponds to a 34% effective power reduction for the 5-user case and 41% effective power reduction for the 10-user case. The degradations of these asynchronous multi-user cases are about 1.5dB for the 5-user case and 1.8dB for the 10-user case worse than the synchronous ones. There are several reasons for this increased degradation. Consider the expression of the pulse correlator decision for one data bit of the first user

$$D_a^{(1)} = \sum_{v=1}^{N_u} \Delta D_a^{(1,v)} + \Delta D_{noise}^{(1)} \tag{3.9}$$

where

$$\Delta D_a^{(1,v)} = \sum_{m=0}^{N_s-1}[\int_{mT_f}^{(m+1)T_f-\beta^{(v)}} c^{(v)}_{m+\alpha^{(v)}} w(t-mT_f-\delta_{d^{(v)}_{m+\alpha^{(v)}}}+\beta^{(v)})w_c^{(1)}dt + \int_{(m+1)T_f-\beta^{(v)}}^{(m+1)T_f} c^{(v)}_{m+\alpha^{(v)}+1} w(t-(m+1)T_f-\delta_{d^{(v)}_{m+\alpha^{(v)}+1}}+\beta^{(v)})w_c^{(1)}dt] \quad (3.10)$$

$$w_c^{(1)} = c_m^{(1)}[w(t-mT_f-\delta_0)-w(t-mT_f-\delta_1)] \quad (3.11)$$

and the vth user is $(\alpha^{(v)}T_f+\beta^{(v)})$ $(0 \le \alpha^{(v)} \le N_s-1, 0 \le \beta^{(v)} < T_f)$ ahead of the first user in a data bit period.

This situation is more complicate than the synchronous one. By calculation, we know that the cross correlation between one specific Gold sequence and a shifted version of another Gold code sequence can be much larger than the cross correlation without any shift. The maximum value of the former is 9 times as much as the value of the latter. This weakens the Gold code sequences' resistance to interference, but it is still much better than the situation without using Gold code sequences. In addition, the cross correlation values from the correlator fluctuate from the greatest value of the waveform autocorrelation V to the smallest $-V$. The $-V$ case occurs when the waveform shifts by $\frac{1}{2}T_f$ and overlaps with the another information bit position. This further weakens the system immunity to cross interference. However, according to the simulation results given in Figure 3.20, the DS-SS PPM UWB system still exhibits very good immunity to cross interference.

Figure 3.21 shows the performance of the $BCH(31,26,1)$, $BCH(31,16,3)$, $BCH(31,11,5)$, $BCH(127,99,4)$ and $BCH(127,85,6)$ codes with 5-users. The coded system surpasses the uncoded system performance when the BER is lower than 2×10^{-2}. The coded performance difference between the asynchronous and the synchronous systems is insignificant from 0dB to 4dB. This is because in this region, the channel noise plays a more important role than the cross interference. With hard-decision decoding, we find that the BER is about twice that with a synchronous system between 4dB to 6dB, where the cross interference

becomes more dominant than the channel noise. In addition, the gaps between the asynchronous systems and synchronous ones increases as E_b/N_0 increases.

In Figures 3.22, 3.23 and 3.24, the errors-and-erasures decoding performance is given when the number of erasures is 2, 4 and 6, respectively. The improvement using erasures is similar to that with the synchronous system. The fact that $BCH(31, 26, 1, 2)$ provides only a slight improvement over $BCH(31, 26, 1)$, and $BCH(31, 16, 3, 6)$ is worse than $BCH(31, 16, 3)$ can be attributed to the maximum erasure phenomenon, as explained in the discussion regarding synchronous communications.

In the 10-user case, Figures 3.25, 3.26, 3.27 and 3.28 show that the degradation at a BER of 10^{-4} is about 1.2dB and 1.7dB compared to the synchronous 10-user case and the single user case, respectively. This can be attributed to the asynchronous cross interference that reduces the Gold code sequences' resistance to interference.

3.3 Discussion and Summary

From the performance results in an AWGN channel, we find that BCH codes are very effective to improve the performance of DS-SS PPM UWB systems. In the single-user case, generally the BCH codes of length 127 have better performance than the BCH codes of length 31 in the region where coded performance surpasses uncoded performance. Amongst the same length BCH codes, the stronger error correcting capability exhibits better performance. The tradeoff is more redundancy or lower code rate. Specifically, for the codes of length 127, at a BER of 10^{-4}, $BCH(127, 85, 6)$ has 3dB coding gain (allowing for 50% power reduction). It has a code rate of 0.67, which is lower than the 0.78 of $BCH(127, 99, 4)$. $BCH(127, 99, 4)$ provides 2.5dB of coding gain at this BER. With the codes of length 31, at a BER of 10^{-4}, $BCH(31, 11, 5)$ provides 2dB coding gain (allowing for about 37% power reduction), but the code rate is only 0.35. $BCH(31, 26, 1)$ provides

1.2dB of coding gain at this BER with a code rate of 0.84. The coding gain and code rate of $BCH(31, 16, 3)$ are between those of the other two codes.

In the 5-user case, the coded system has coding gains similar to that for the single-user synchronous case. In the asynchronous case, the coding gains are more pronounced. At a BER of 10^{-4}, $BCH(127, 85, 6)$ provides 4dB coding gain (allowing for 60% power reduction), which is an outstanding improvement. For $BCH(31, 11, 5)$, there is a 3dB coding gain. Overall, the asynchronous coding gains are greater than the synchronous ones in the simulation results.

In the 10-user case, the coded system performance is very close to the 5-user performance in the synchronous case. In the asynchronous case, the coded system performance is worse than the 5-user case in proportion to the uncoded one. However, the coding gains in the 5-user case are very similar to those with 10 users.

By using erasures, at a BER of 10^{-4}, an extra coding gain of 0.5dB to 1dB can be achieved for the BCH codes considered. When the number of erasures increases, the performance improves provided that the number of erasures does not reach the maximum. The marginal coding gain decreases as the number of erasures increases. When the number of erasures reaches its maximum, there is only a trivial improvement or even a reduction in performance compared to the non-erasure case. Furthermore, the synchronous DS-SS PPM UWB system exhibits better performance than the asynchronous ones with multiple users. In the 10-user case, the advantage is more obvious than in the 5-user case.

From the simulation results, we find that there are some tradeoffs among them. The first tradeoff is that BCH codes of length 127 have better performance than BCH codes of length 31 with similar code rate, but longer codes have more decoding delay than the shorter ones. If the requirement for real-time communication is high while the quality requirement is

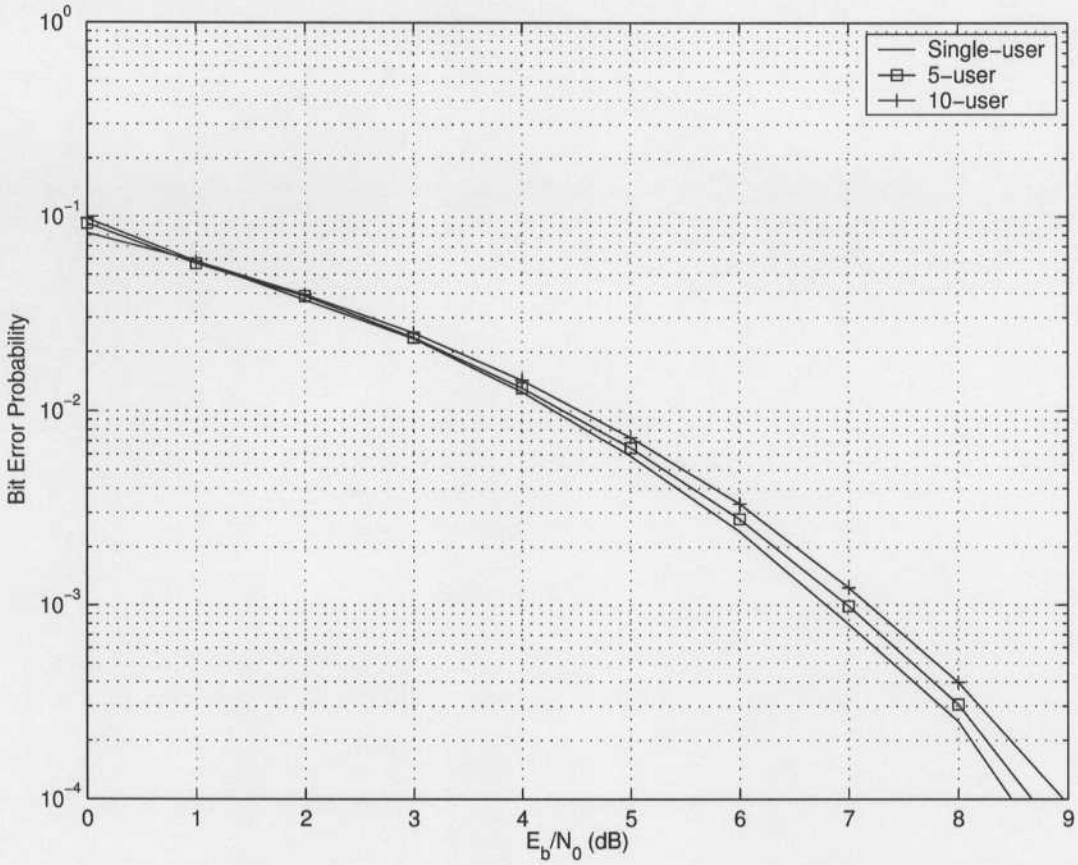

Figure 3.2. *Uncoded synchronous DS-SS PPM UWB performance over an AWGN channel.*

not high, shorter codes may be preferable. The second tradeoff is that erasure decoding provides an improvement over non-erasure decoding, but erasure decoding also introduces additional delay as it needs twice the decoding time. The coding choice also depends on the real-time requirements, data quality and transmission power.

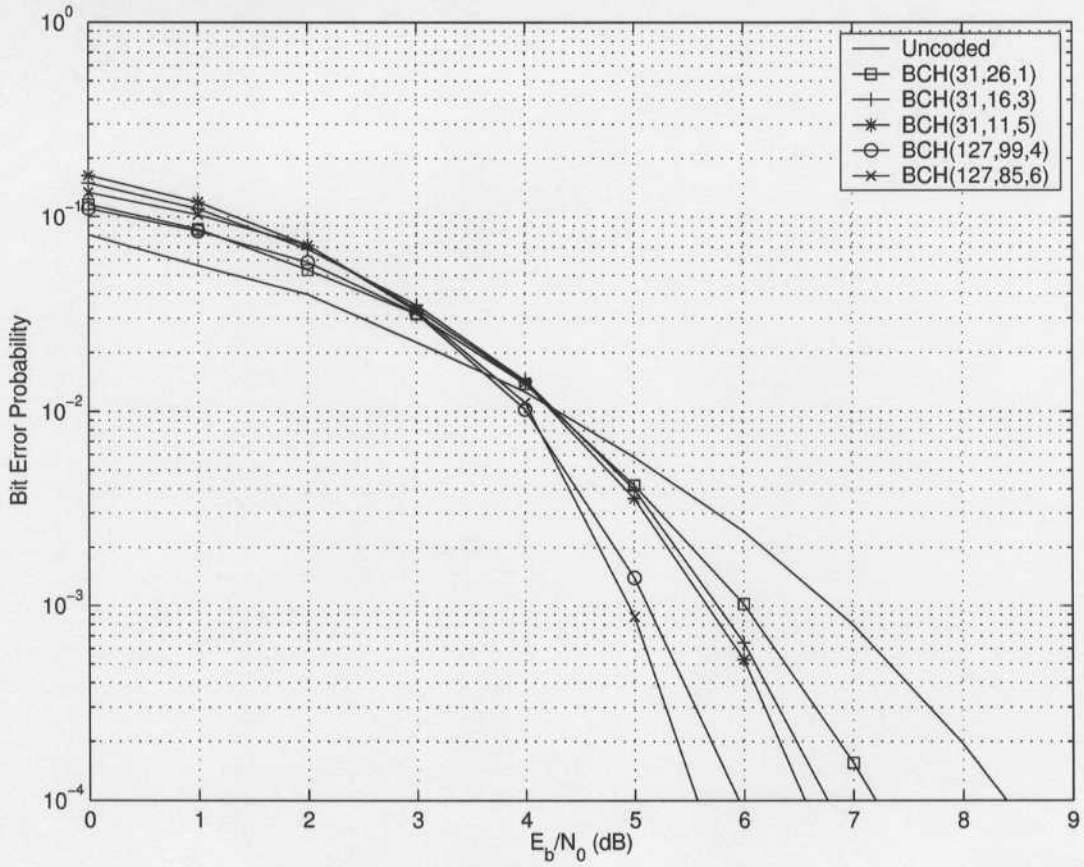

Figure 3.3. *Single-user DS-SS PPM UWB system performance with BCH coding over an AWGN channel.*

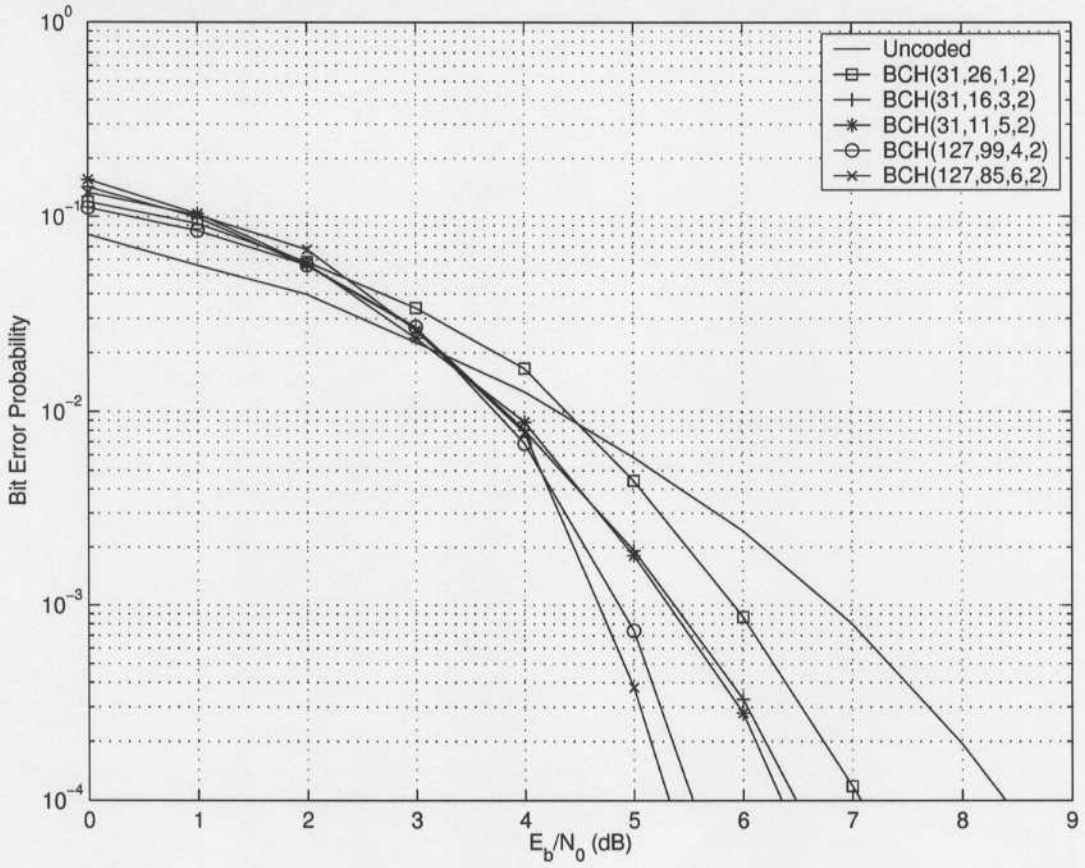

Figure 3.4. *Single-user DS-SS PPM UWB system performance with BCH coding and 2 erasures over an AWGN channel.*

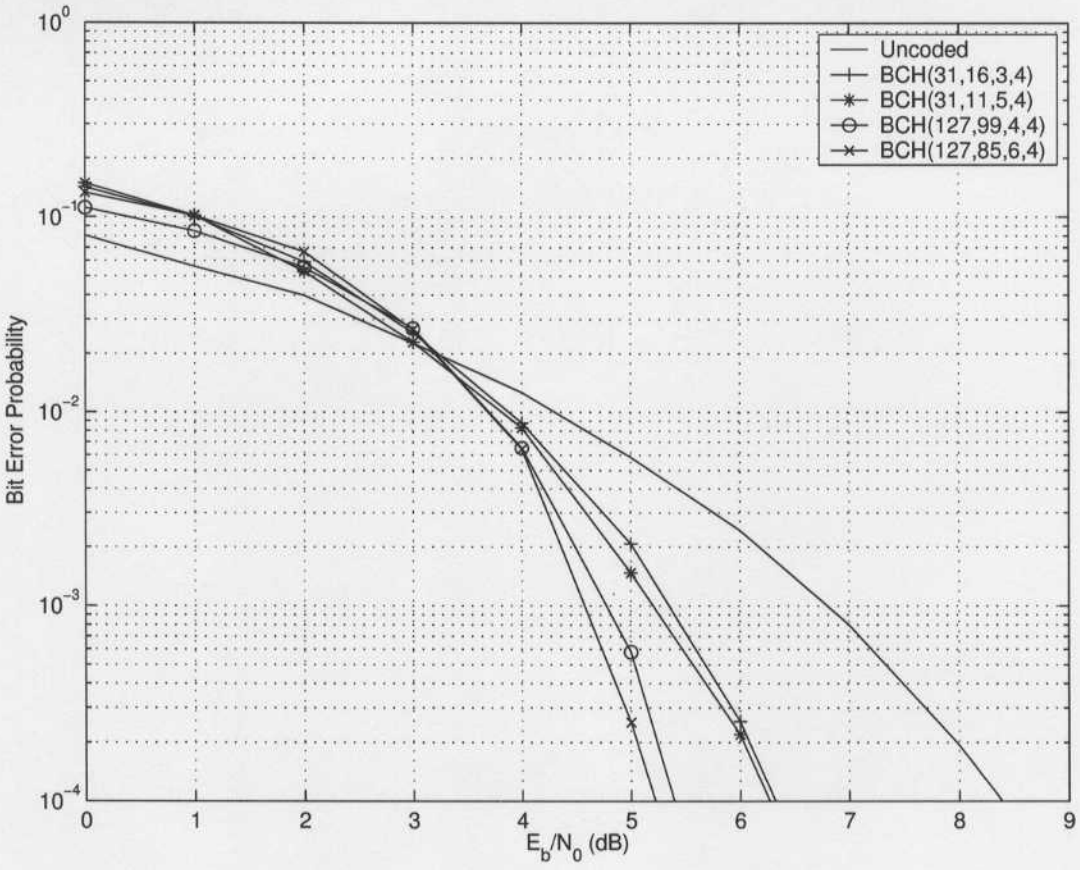

Figure 3.5. *Single-user DS-SS PPM UWB system performance with BCH coding and 4 erasures over an AWGN channel.*

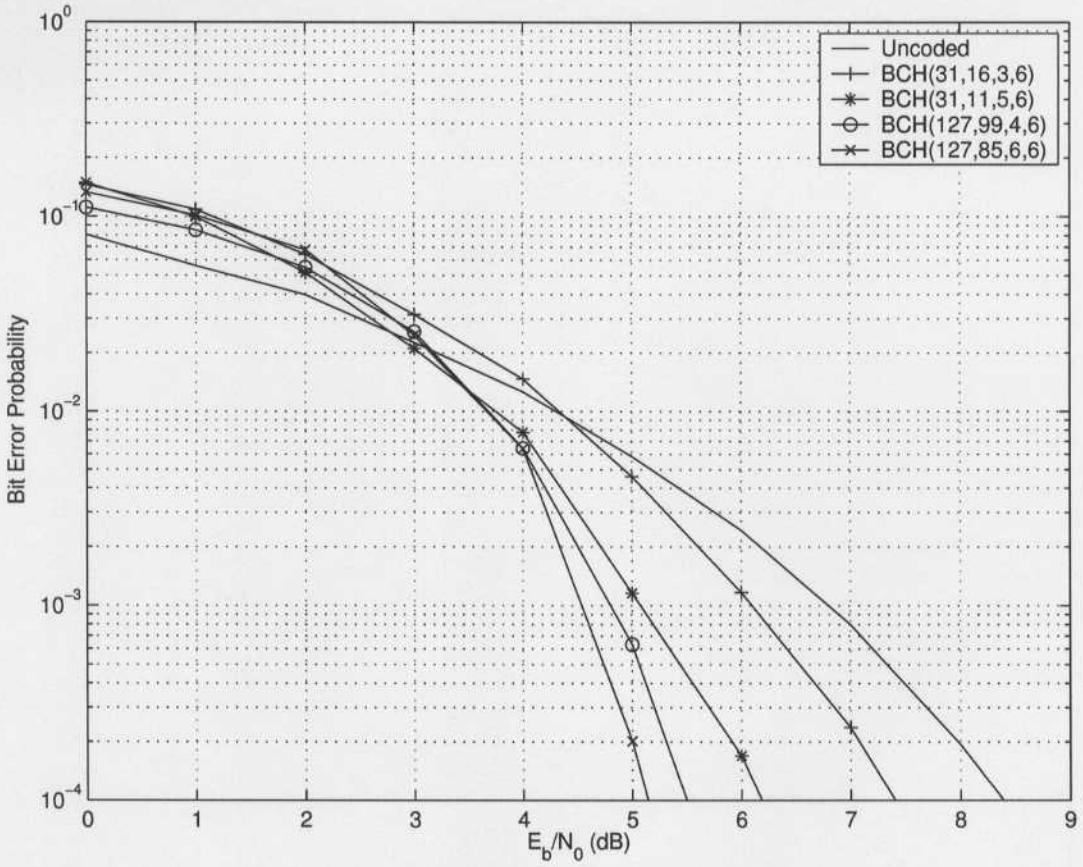

Figure 3.6. *Single-user DS-SS PPM UWB system performance with BCH coding and 6 erasures over an AWGN channel.*

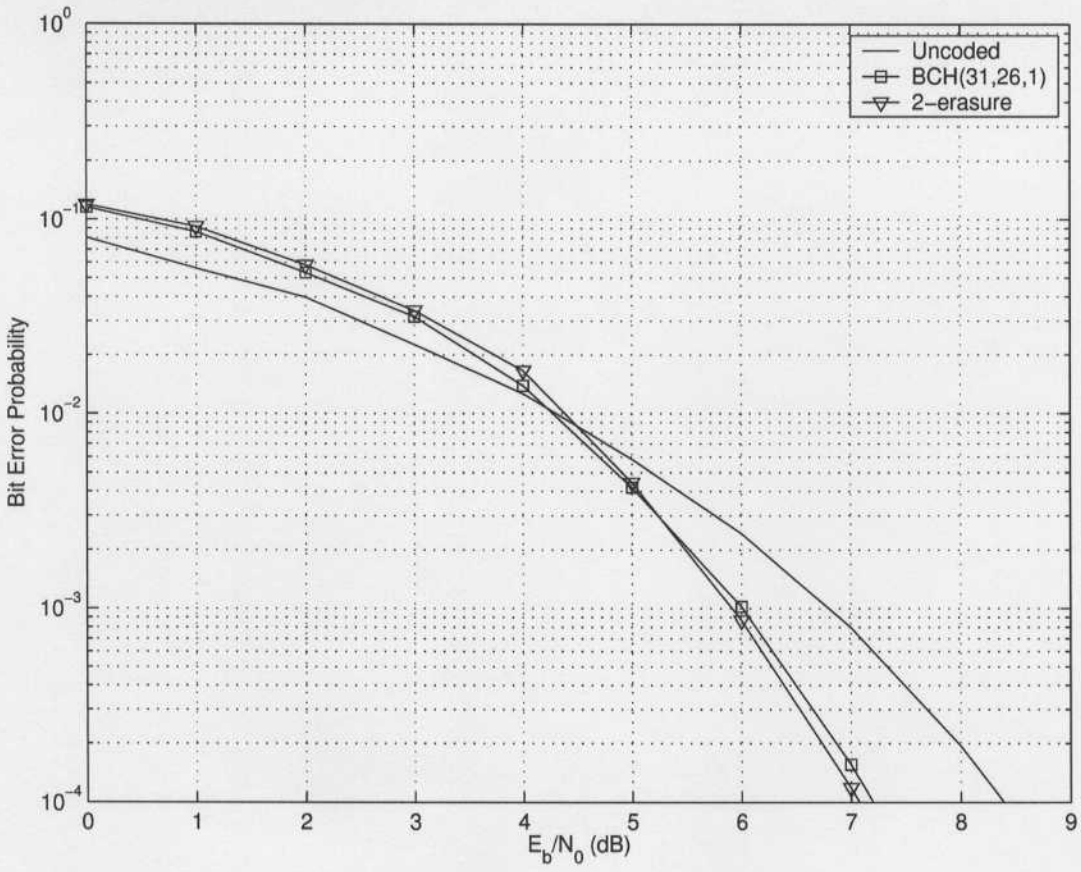

Figure 3.7. *Single-user DS-SS PPM UWB system performance with BCH(31,26,1) over an AWGN channel.*

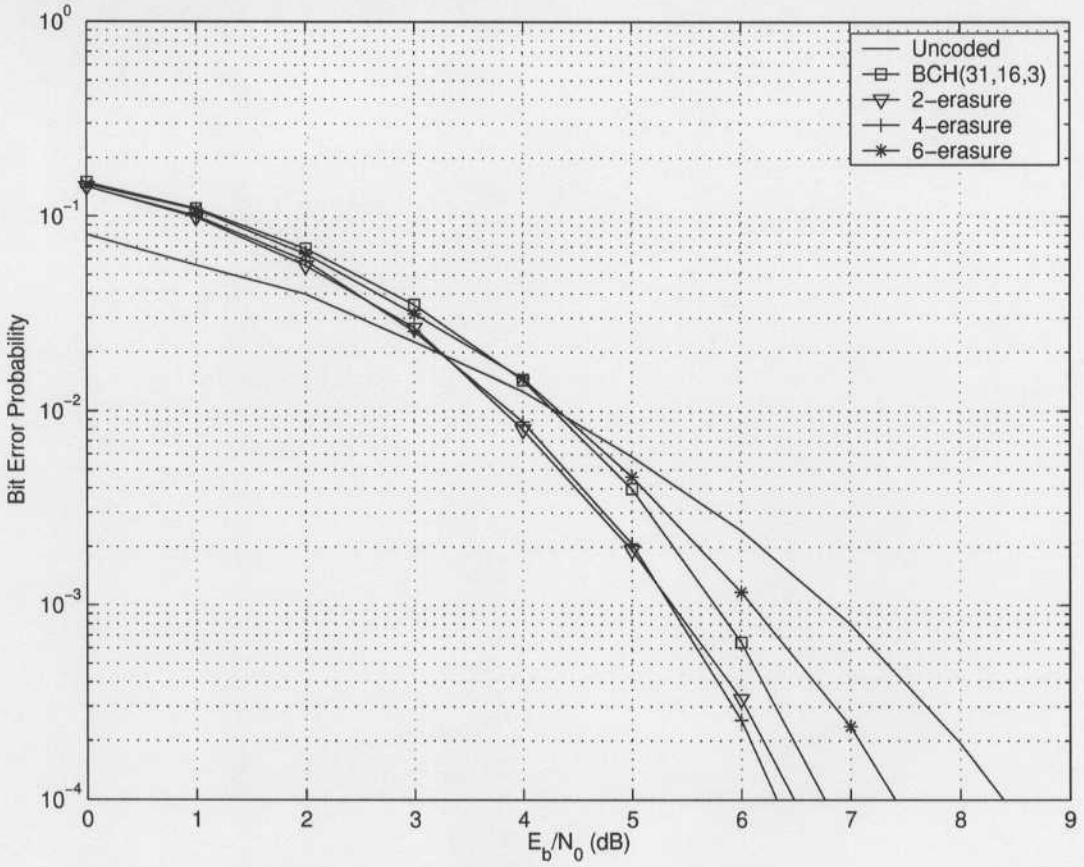

Figure 3.8. *Single-user DS-SS PPM UWB system performance with BCH(31,16,3) over an AWGN channel.*

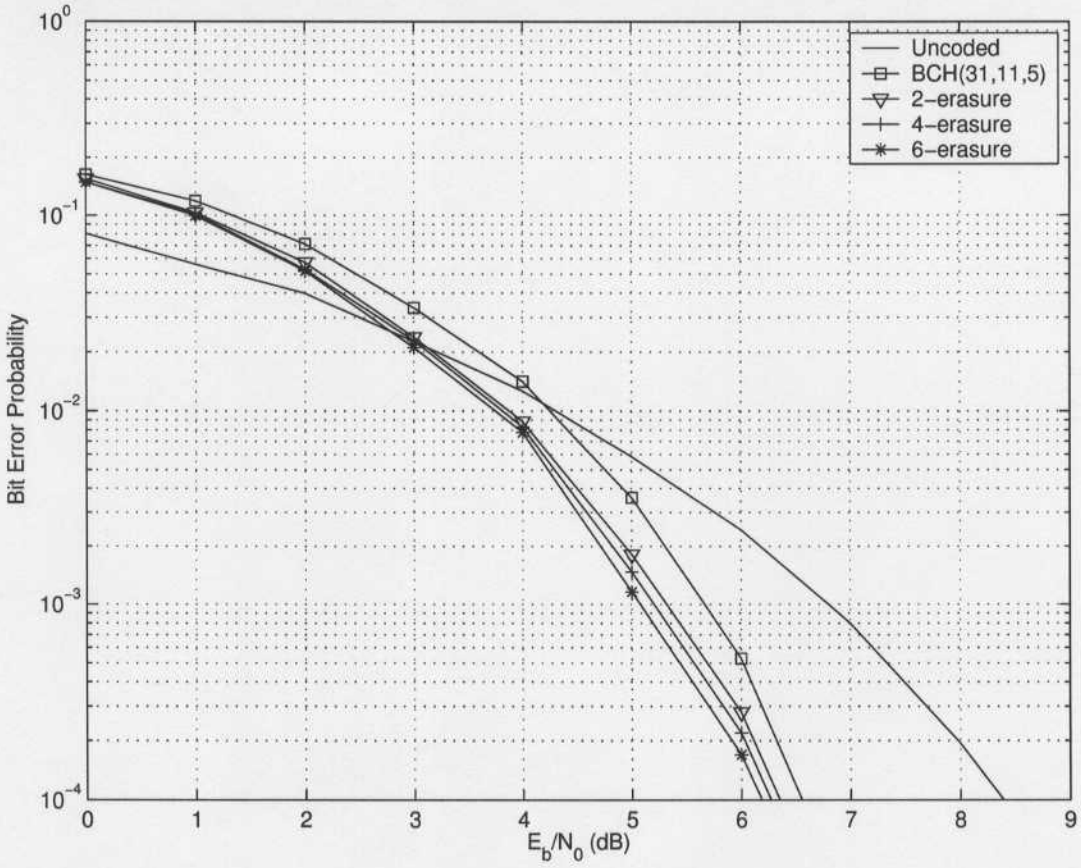

Figure 3.9. *Single-user DS-SS PPM UWB system performance with BCH(31,11,5) over an AWGN channel.*

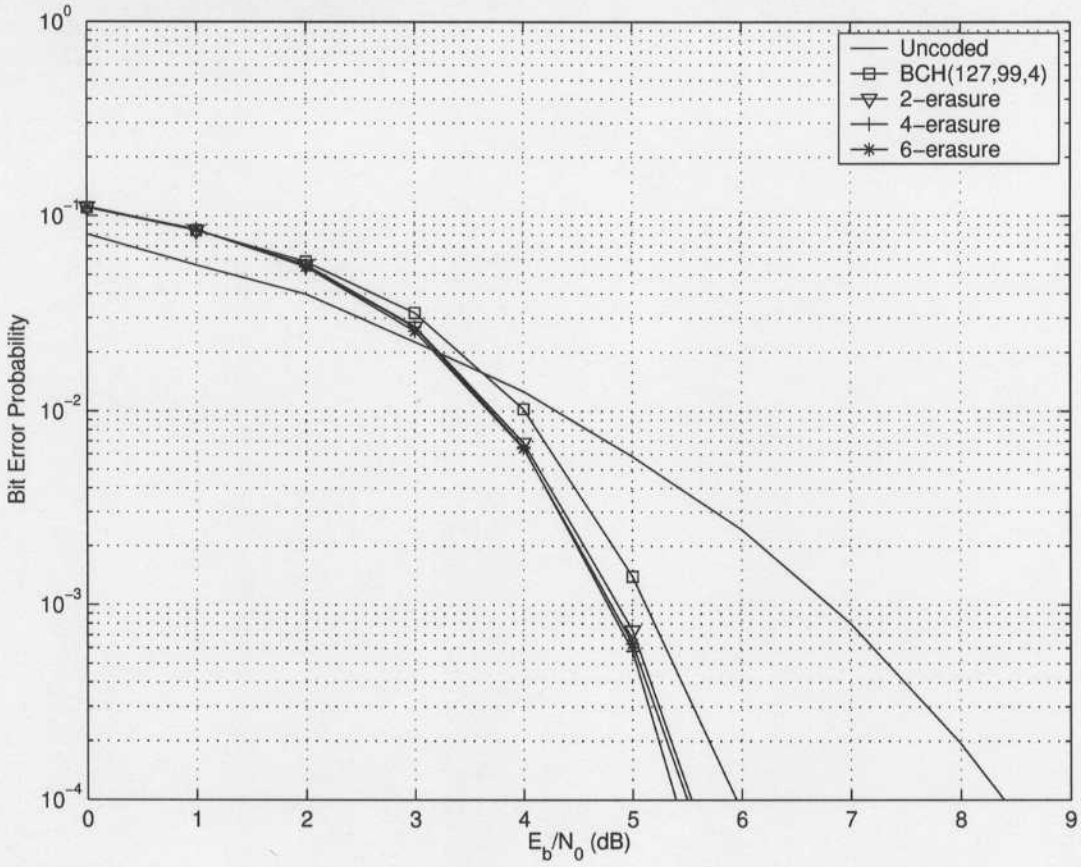

Figure 3.10. *Single-user DS-SS PPM UWB system performance with BCH(127,99,4) over an AWGN channel.*

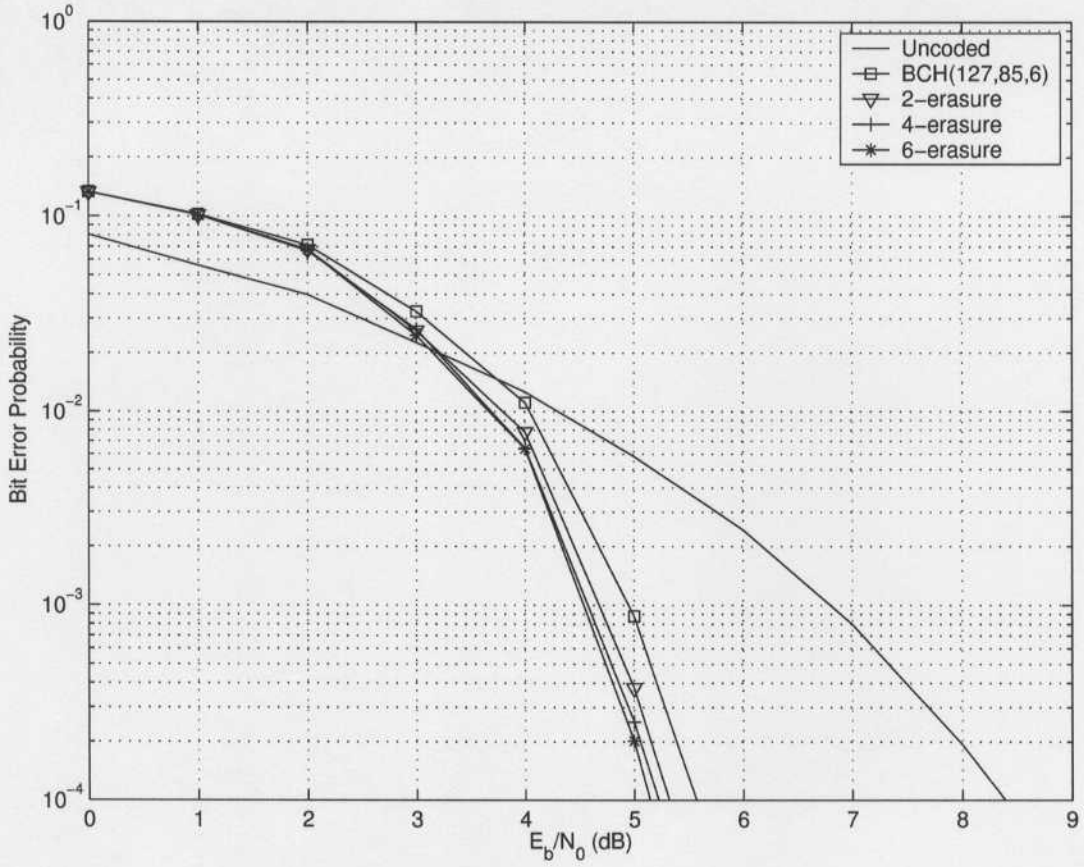

Figure 3.11. *Single-user DS-SS PPM UWB system performance with BCH(127,85,6) over an AWGN channel.*

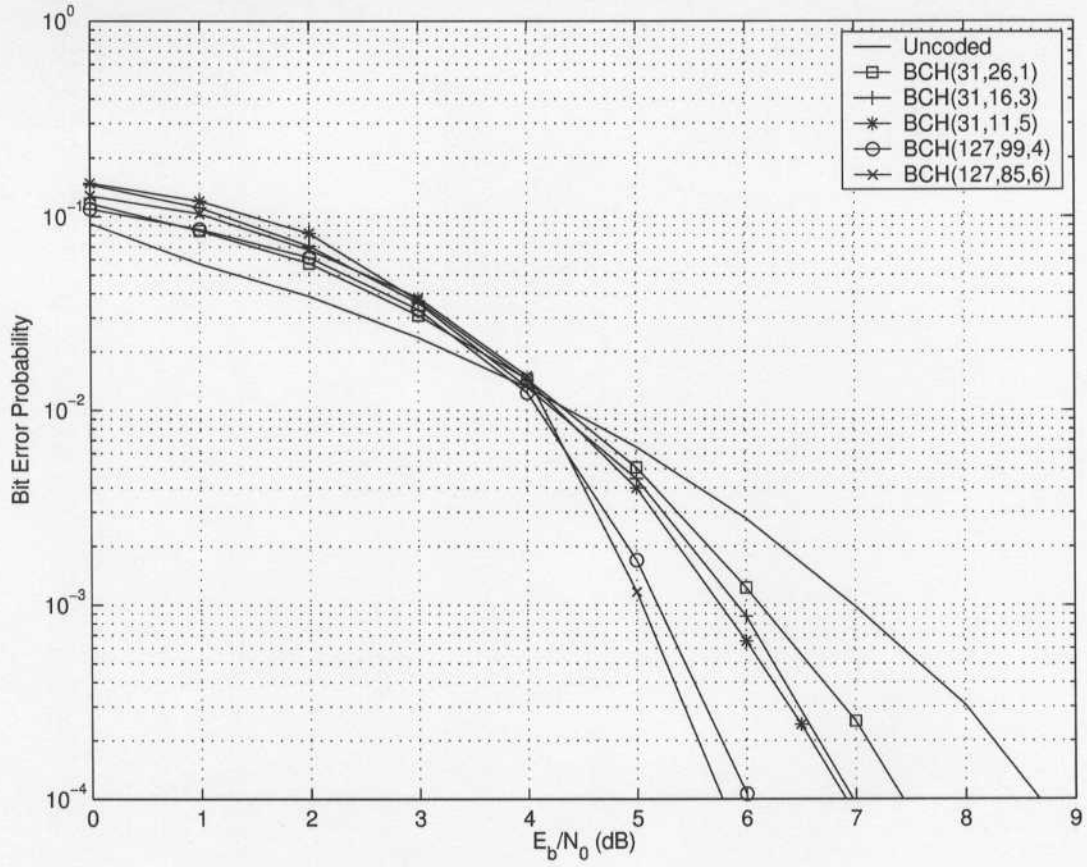

Figure 3.12. *Performance with five users in a synchronous DS-SS PPM UWB system with BCH coding over an AWGN channel.*

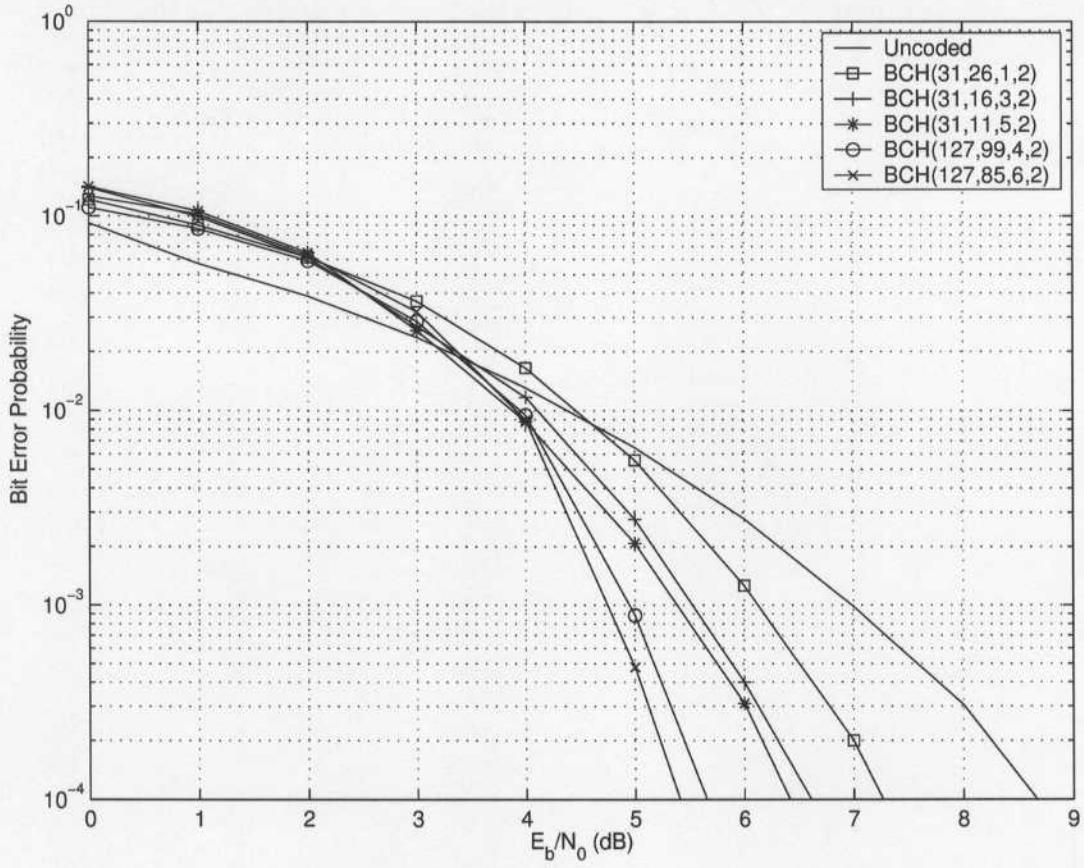

Figure 3.13. *Performance with five users in a synchronous DS-SS PPM UWB system with BCH coding and 2 erasures over an AWGN channel.*

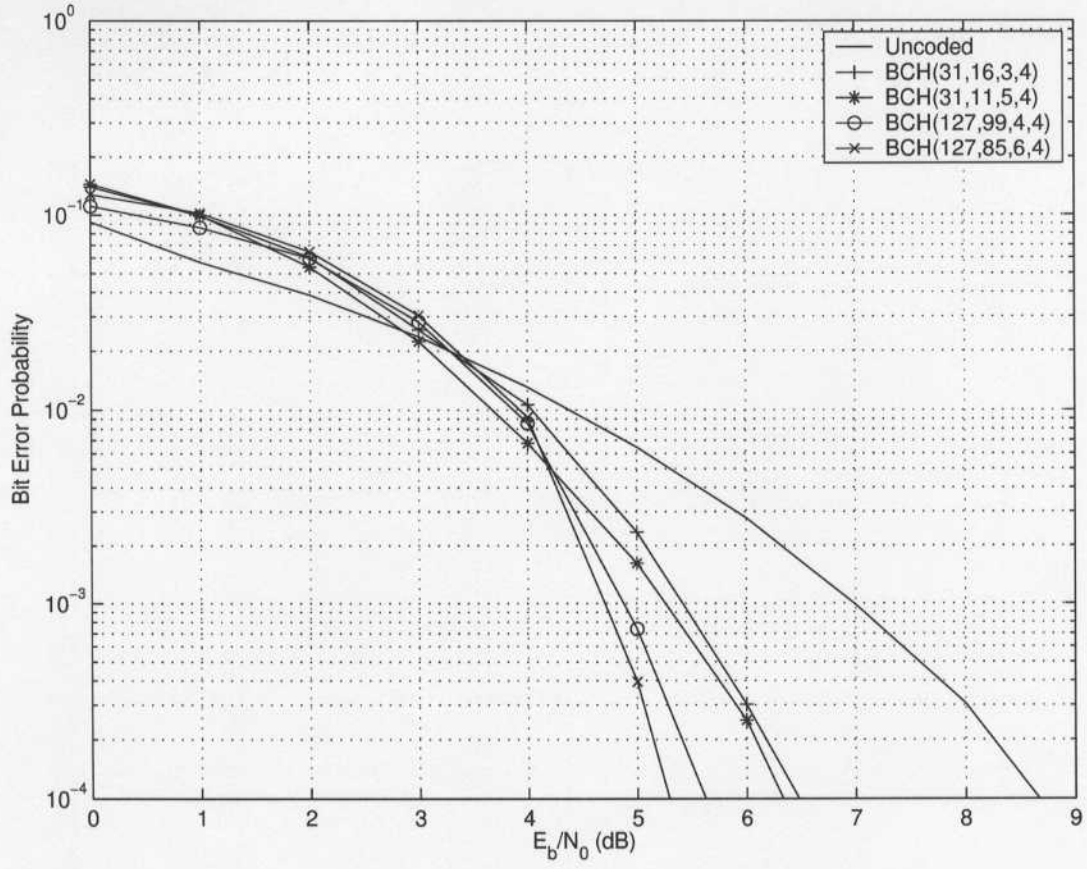

Figure 3.14. *Performance with five users in a synchronous DS-SS PPM UWB system with BCH coding and 4 erasures over an AWGN channel.*

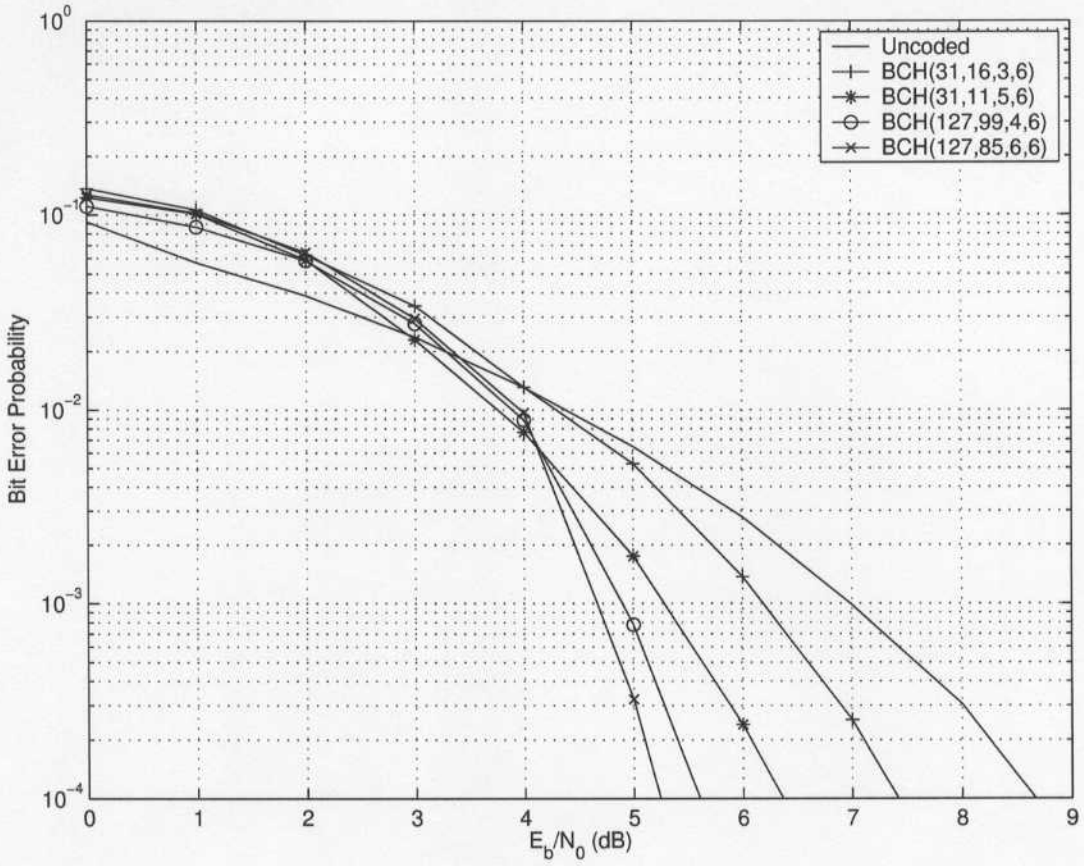

Figure 3.15. *Performance with five users in a synchronous DS-SS PPM UWB system with BCH coding and 6 erasures over an AWGN channel.*

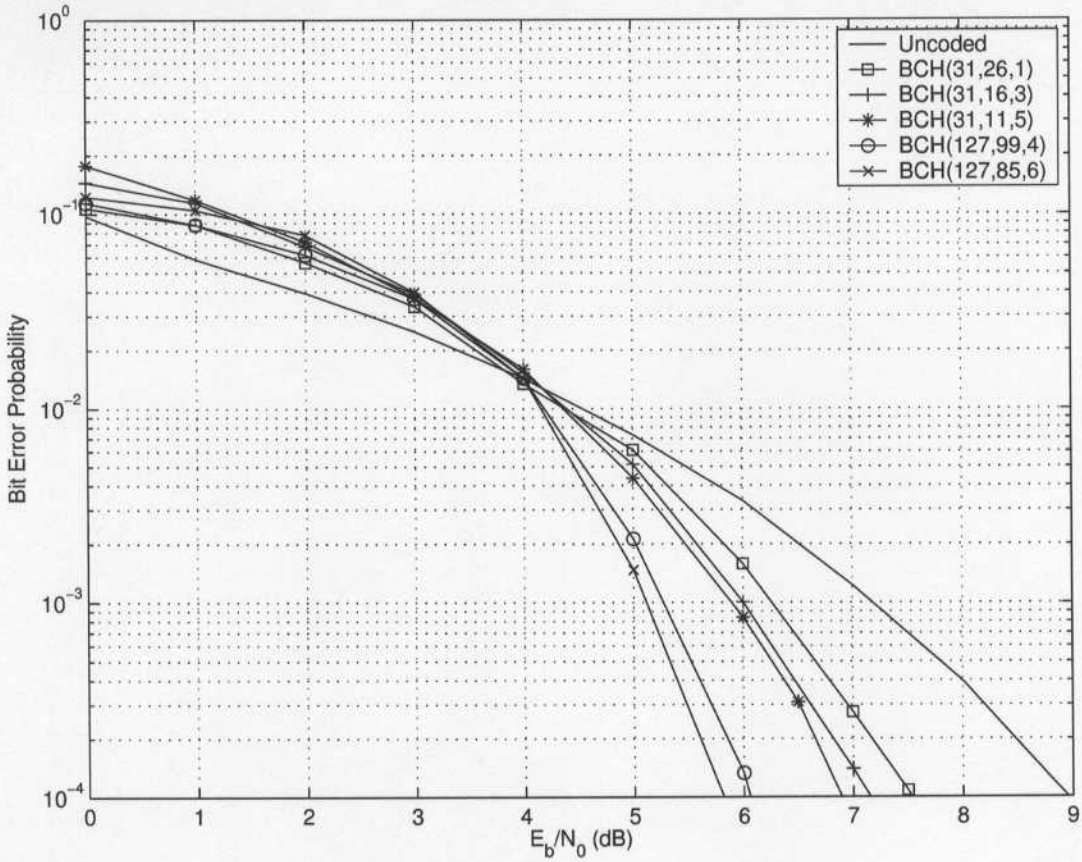

Figure 3.16. *Performance with ten users in a synchronous DS-SS PPM UWB system with BCH coding over an AWGN channel.*

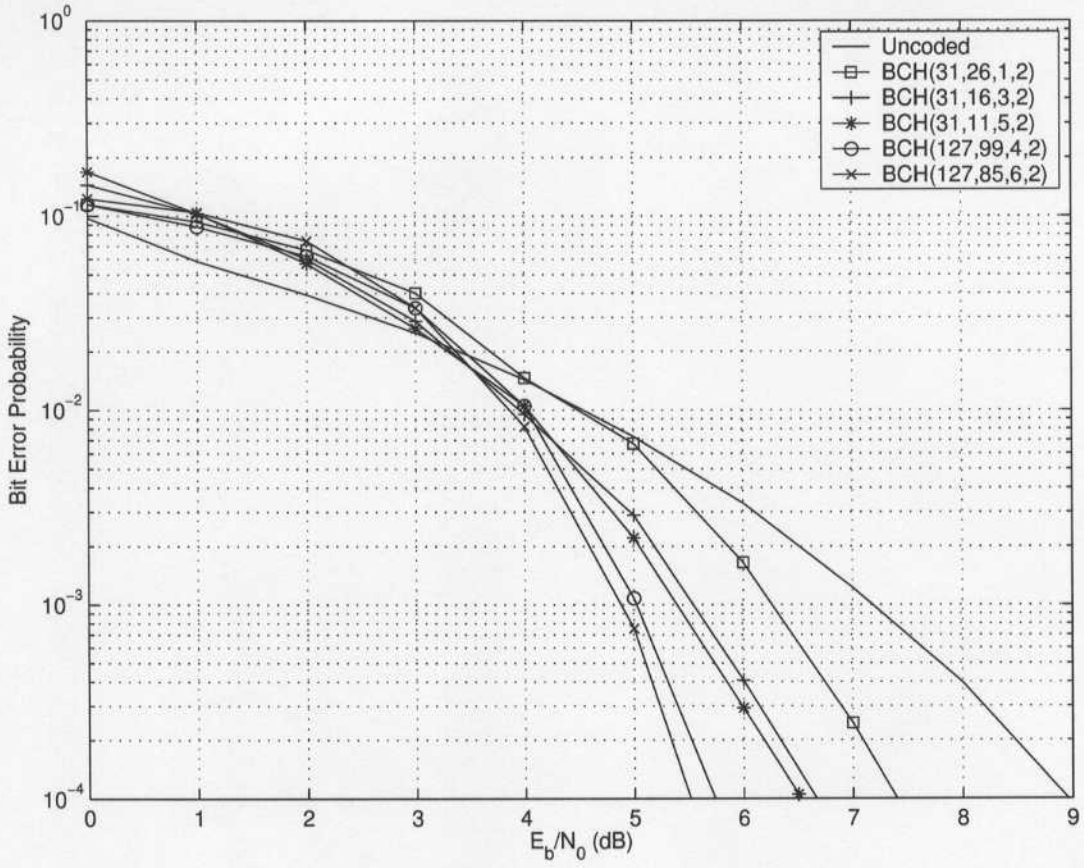

Figure 3.17. *Performance with ten users in a synchronous DS-SS PPM UWB system with BCH coding 2 erasures over an AWGN channel.*

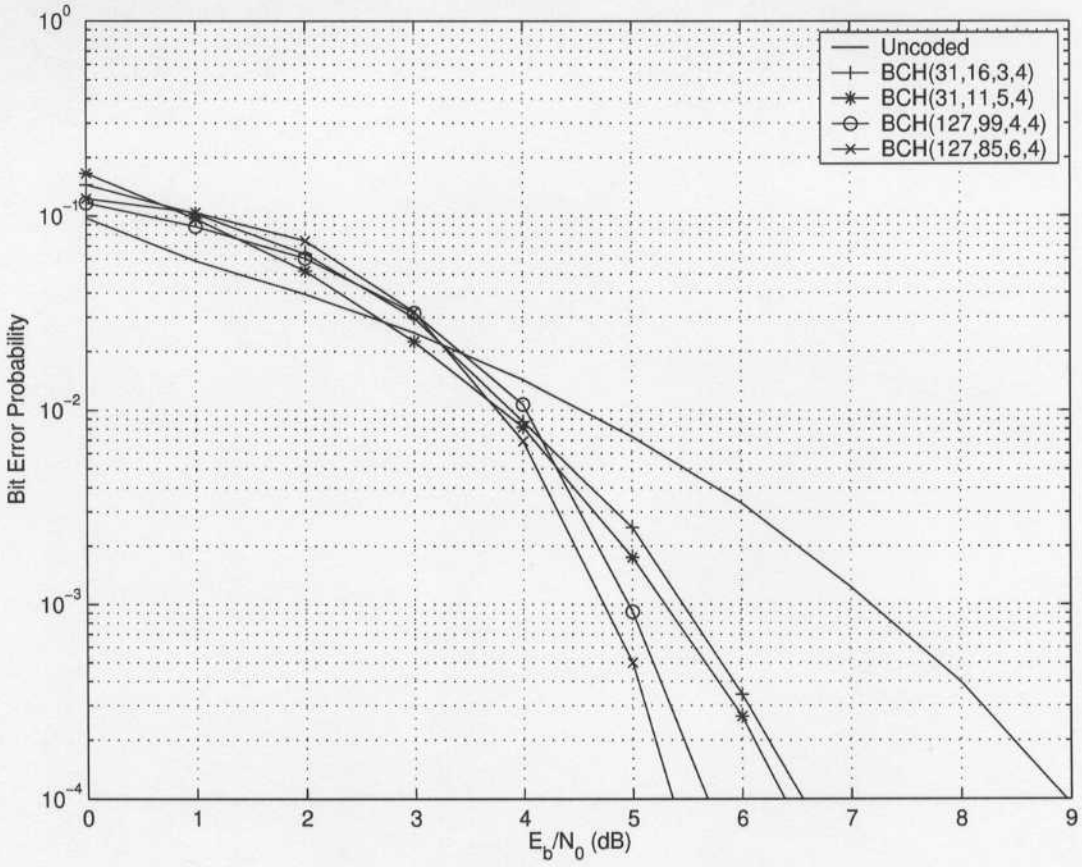

Figure 3.18. *Performance with ten users in a synchronous DS-SS PPM UWB system with BCH coding and 4 erasures over an AWGN channel.*

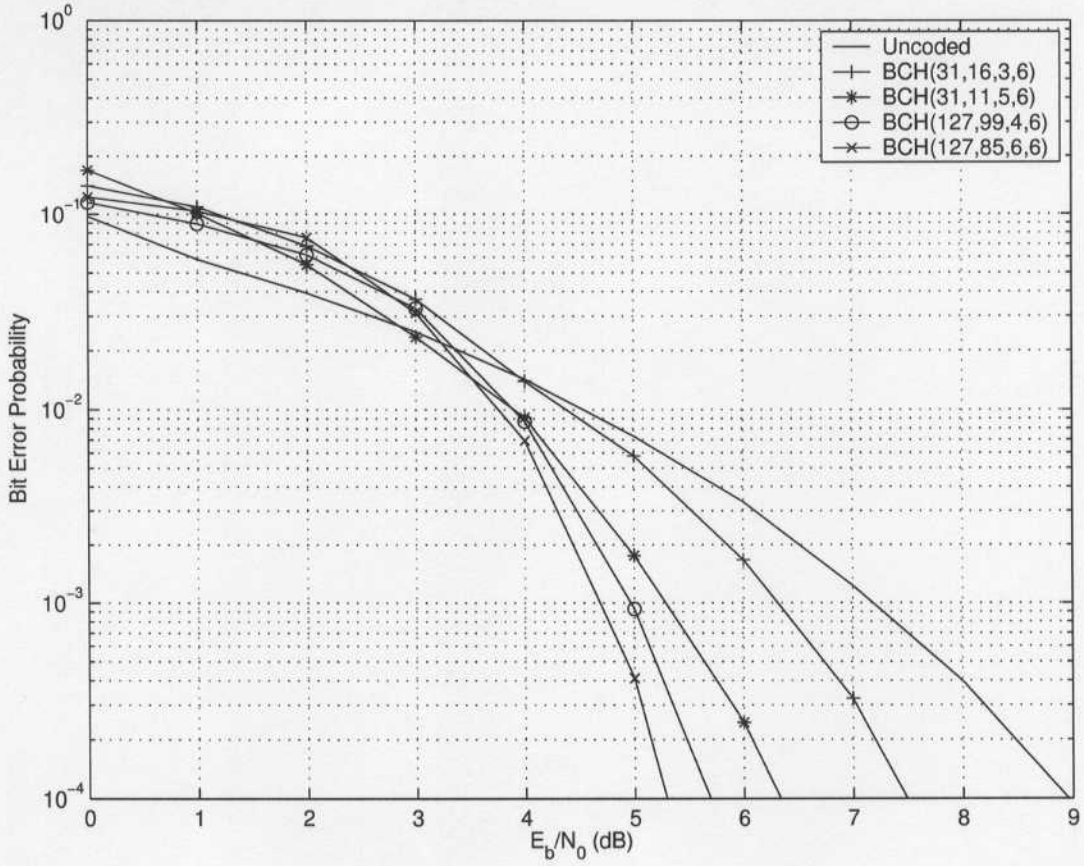

Figure 3.19. *Performance with ten users in a synchronous DS-SS PPM UWB system with BCH coding and 6 erasures over an AWGN channel.*

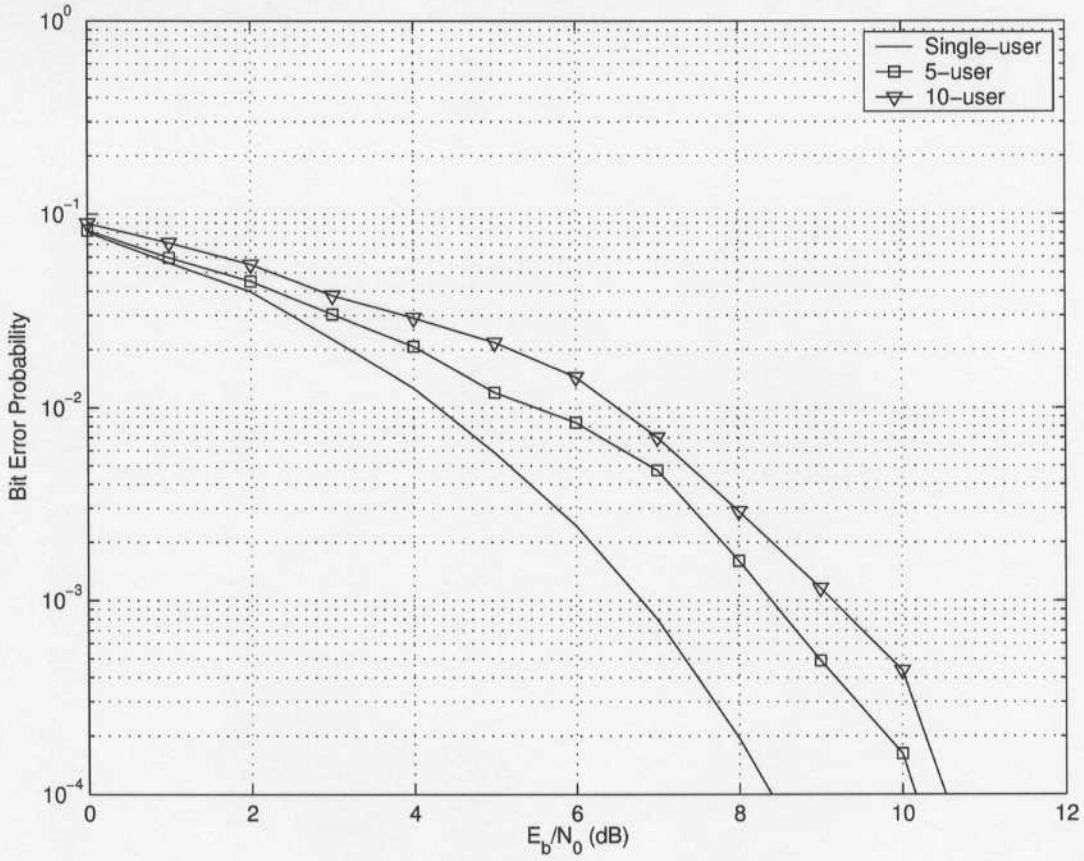

Figure 3.20. *Performance in an asynchronous uncoded DS-SS PPM UWB system over an AWGN channel.*

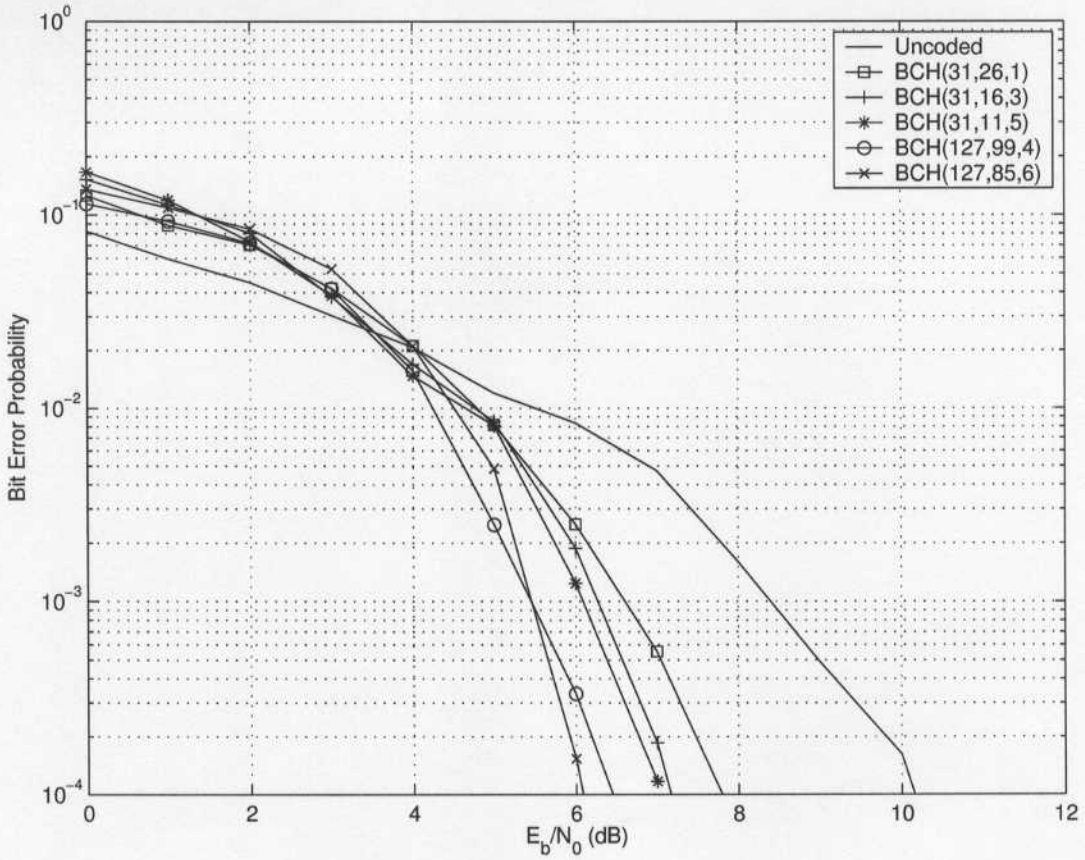

Figure 3.21. *Performance with five users in an asynchronous DS-SS PPM UWB system with BCH coding over an AWGN channel.*

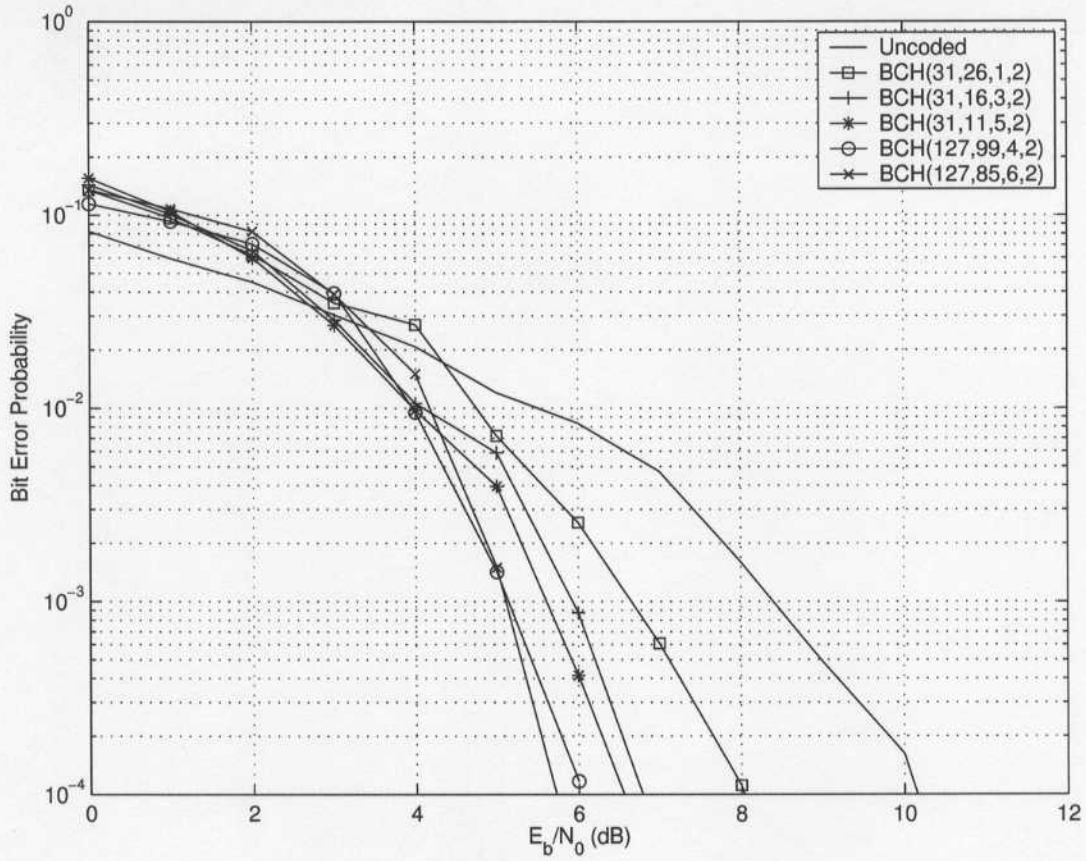

Figure 3.22. *Performance with five users in an asynchronous DS-SS PPM UWB system with BCH coding and 2 erasures over an AWGN channel.*

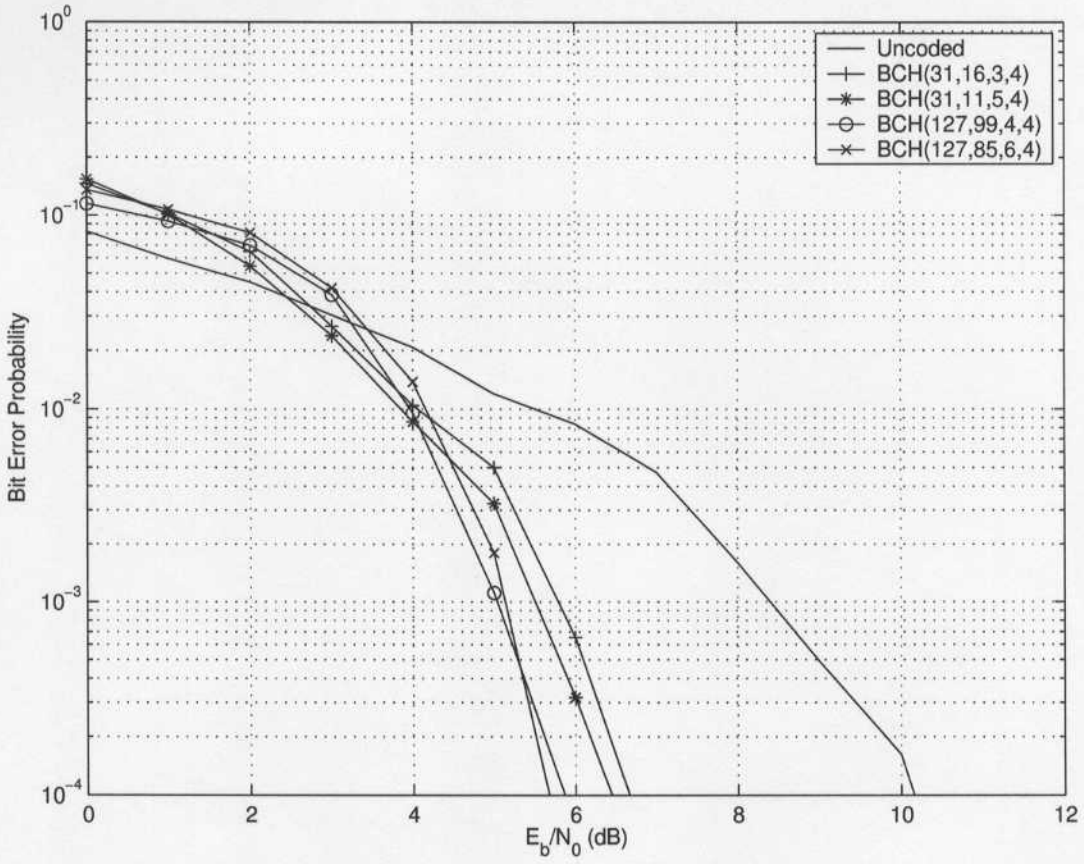

Figure 3.23. *Performance with five users in an asynchronous DS-SS PPM UWB system with BCH coding and 4 erasures over an AWGN channel.*

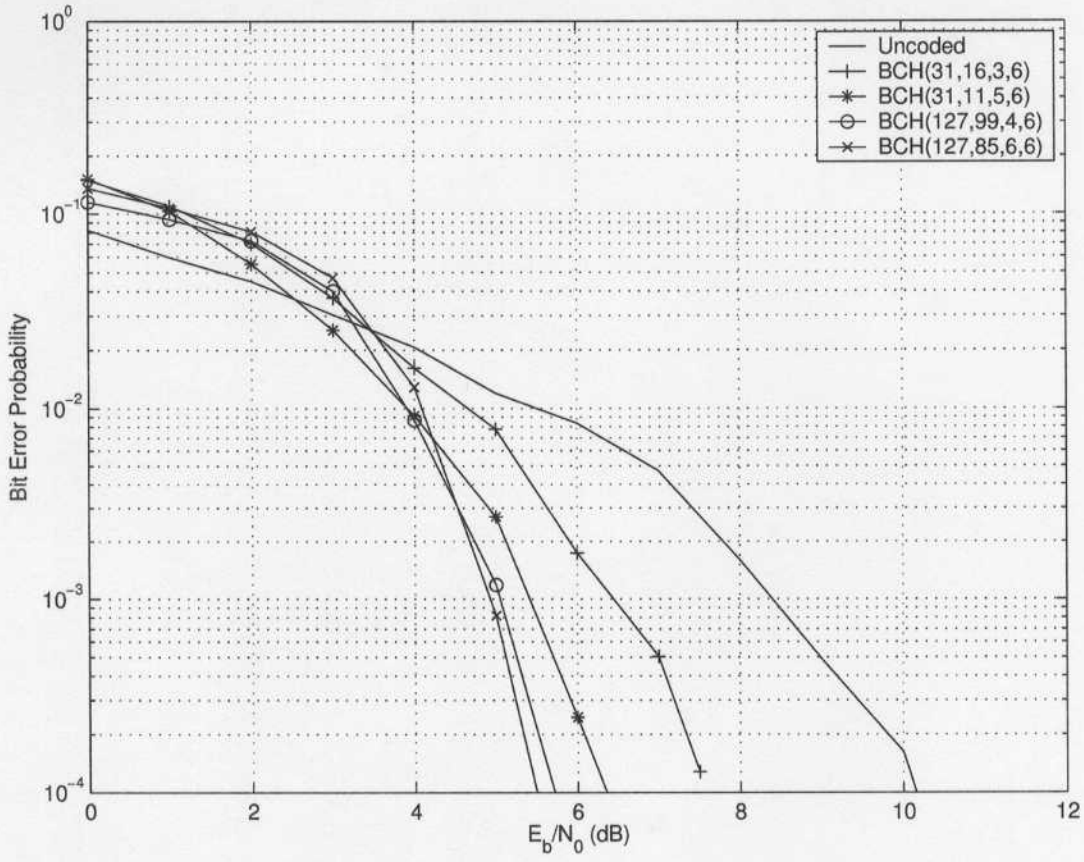

Figure 3.24. *Performance with five users in an asynchronous DS-SS PPM UWB system with BCH coding and 6 erasures over an AWGN channel.*

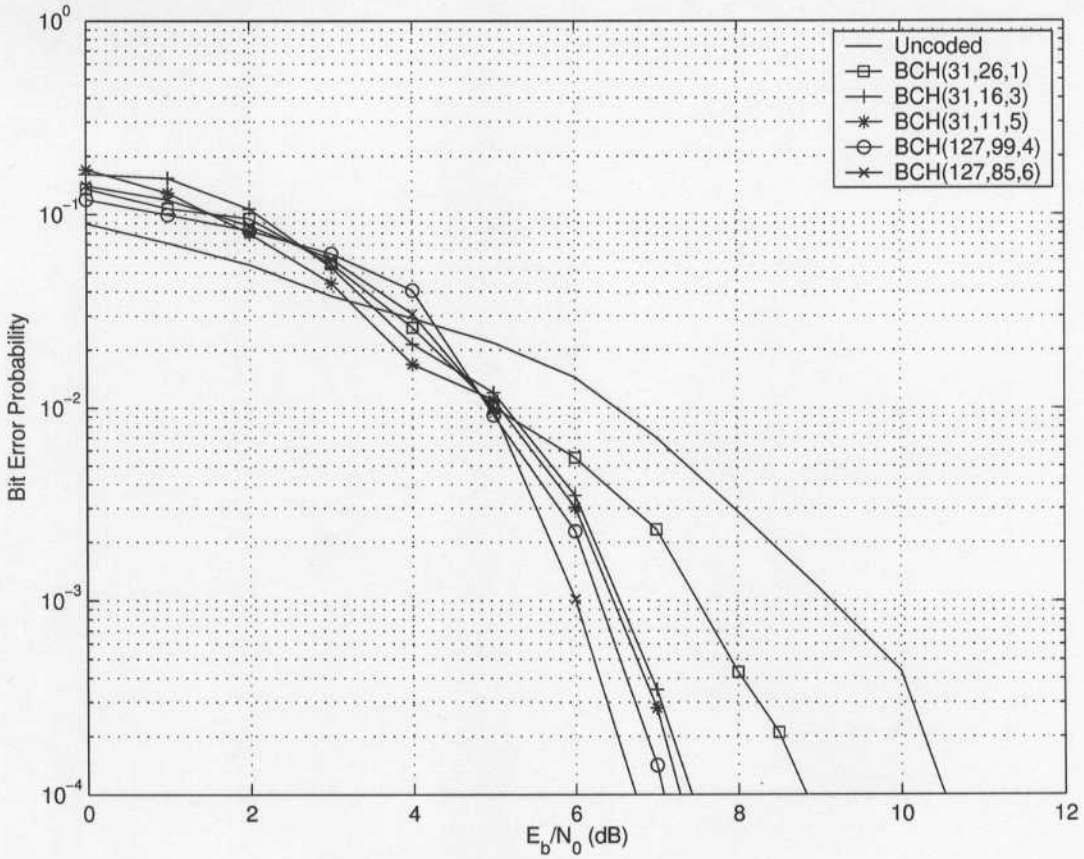

Figure 3.25. *Performance with ten users in an asynchronous DS-SS PPM UWB system with BCH coding over an AWGN channel.*

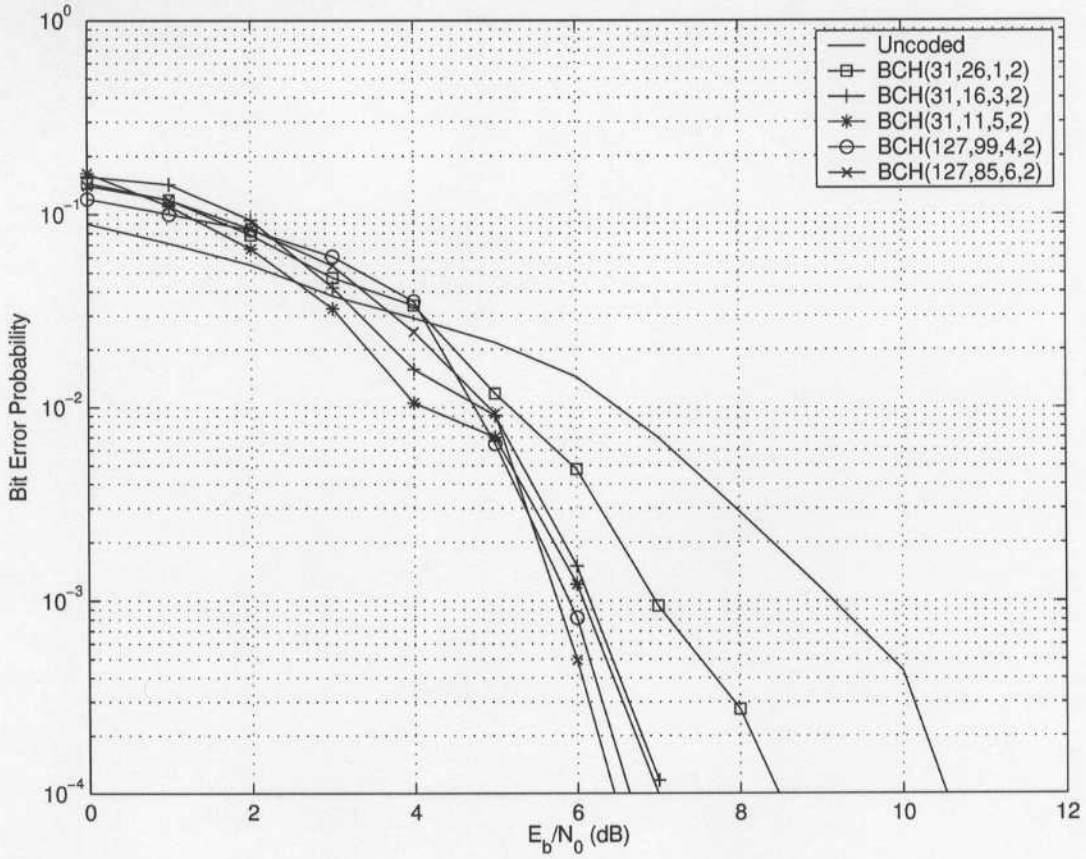

Figure 3.26. *Performance with ten users in an asynchronous DS-SS PPM UWB system with BCH coding and 2 erasures over an AWGN channel.*

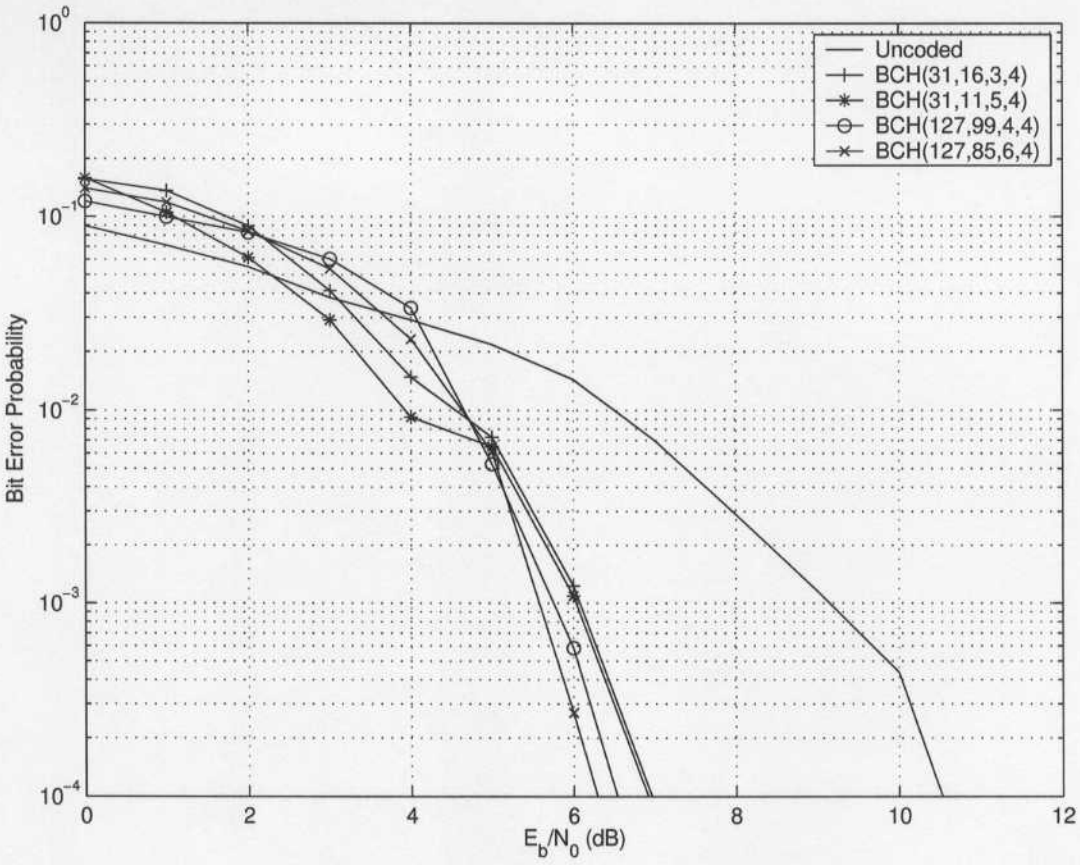

Figure 3.27. *Performance with ten users in an asynchronous DS-SS PPM UWB system with BCH coding and 4 erasures over an AWGN channel.*

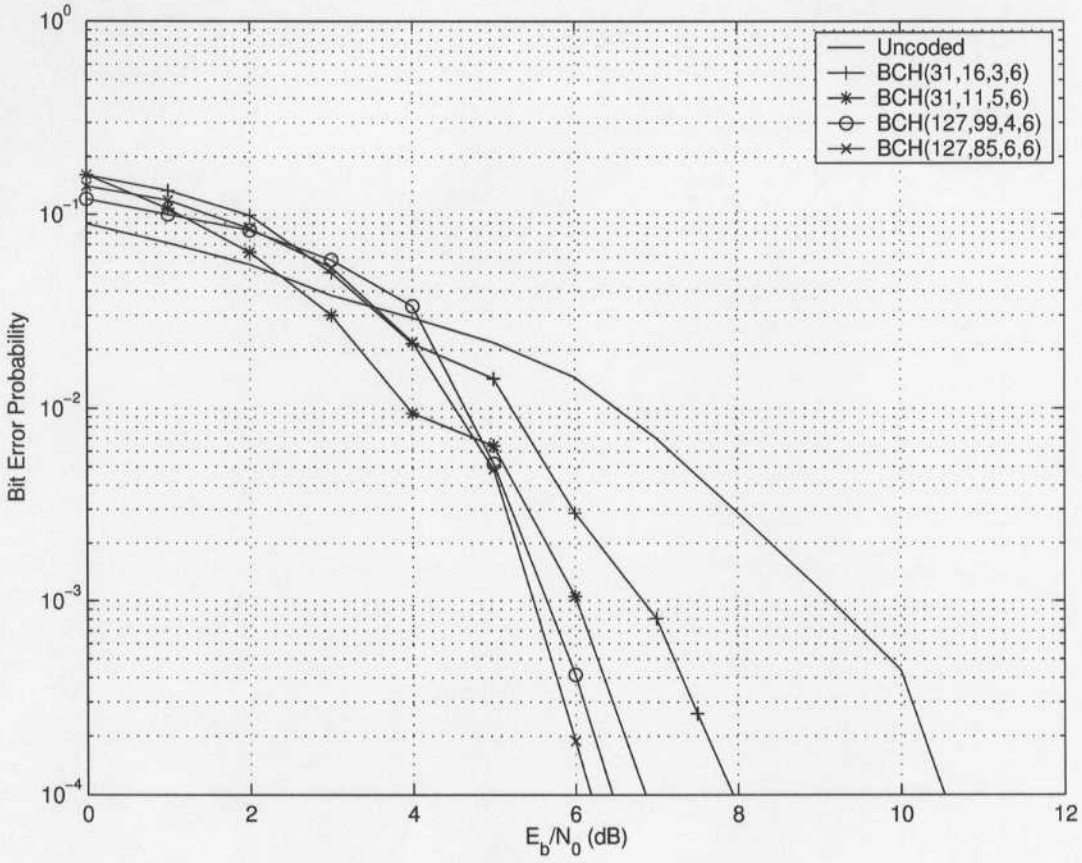

Figure 3.28. *Performance with ten users in an asynchronous DS-SS PPM UWB system with BCH coding and 6 erasures over an AWGN channel.*

Chapter 4

DS-SS PPM UWB Performance over a Fading Channel

In this Chapter, we consider the same DS-SS PPM UWB system as described in Chapter 3, but over a UWB fading channel. In an AWGN channel, additive white Gaussian noise is considered to be the only channel effect impacting performance. However, severe channel fading exists in UWB channels, thus we implement a statistical UWB indoor fading channel model with AWGN to simulate a more realistic channel environment [23].

4.1 The Fading Channel Model

A fading channel is a channel model with time-varying recombination of signals having different time delays after reflection from objects [24]. This is called time-varying multi-path propagation.

Because of the restriction on measurement bandwidth and the high resolution of the UWB system in the time domain, narrowband channel models are not suitable for UWB systems. In the simulations, we adopt a statistical channel model for the UWB indoor environment [23]. It is a stochastic tapped delay-line (STDL) propagation model, and is based on an extensive channel measurements in a typical office building. The averaged power delay profile can be characterized by a single exponential decay and a statistically

Table 4.1. *UWB Statistical Fading channel Model Parameters*

Parameters	Formula
Path Loss	$20.4log_{10}(\frac{d}{d_0}) \quad d \leq 11m$
	$-56 + 74log_{10}(\frac{d}{d_0}) d > 11m$
Shadowing	$\overline{F_{tot}} \sim \Lambda_N(-PL; 4.3)$
Decay Constant	$\alpha \sim \Lambda_N(16.1; 1.27)$
Power Ratio	$\beta \sim \Lambda_N(-0.4; 0.3)$
Energy Gains	$F_k \sim \Gamma(\overline{F_k}; m_k)$
m values	$m_k \sim \tau_N(\mu_m(\tau_k; \sigma_m^2(\tau_k))$
	$\mu_m(\tau_k) = 3.5 - \tau_k/73$
	$\sigma_m^2(\tau_k) = 1.84 - \tau_k/160$

distributed decay constant. The statistical model parameters are listed in the Table 4.1 [25].

The unit of Path Loss is dB and $d_0 = 1m$ is the base reference distance between the transmitter and receiver. $\overline{F_{tot}}$ is the total mean energy at a distance of d. $\Lambda_N(\mu; \sigma)$ denotes the lognormal distribution with μ (the mean) and σ (the standard deviation). $\overline{F_k}$ is the average power in the kth delay bin (the distance between the adjacent multipaths) over the small-scale fading. It can be expressed as

$$\overline{F_k} = \begin{cases} \frac{\overline{F_{tot}}}{1+\beta Q(\alpha)} & \text{if } k = 1 \\ \frac{\overline{F_{tot}}}{1+\beta Q(\alpha)} \beta e^{-\frac{(\tau_k - \tau_2)}{\alpha}} & \text{if } k = 2, \ldots, l, \end{cases} \tag{4.1}$$

where

$$Q(\alpha) = \frac{1}{1 - e^{-\Delta\tau/\alpha}}. \tag{4.2}$$

Here α is the decay constant that is a random variable with a lognormal distribution

$$\alpha \sim \Lambda_N(16.1; 1.27) \tag{4.3}$$

The unit of α is nanosecond. β is the power ratio $\beta = \overline{F_2}/\overline{F_1}$. It is also a random variable

with a lognormal distribution

$$\beta \sim \Lambda_N(-0.4; 0.3) \tag{4.4}$$

From the above equations, the average power in each delay bin is exponentially decaying.

Assuming $\Delta\tau = 2ns$ is the resolution of the UWB system, we set the observation window to 5α, which stands for 100 delay bins on average [25]. In each delay bin, the statistical model of the small-fading is built up by a Gamma distribution with mean $\overline{F_k}$ and the parameter m_k [25]. The unit of τ_k is nanoseconds.

We use the above UWB fading channel model to simulate a more practical environment compared to the environment in Chapter 3 where only AWGN was considered. Because UWB propagation creates many multipaths with significant cross interference and multipath interference, a large performance degradation is expected compared to that with just AWGN. The same BCH codes as in the previous chapter, namely $(31, 26, 1)$, $(31, 16, 3)$, $(31, 11, 5)$, $(127, 99, 4)$ and $(127, 85, 6)$, will be considered to improve the performance.

In the simulations, the same Gaussian impulse waveform as in Chapter 3 was used. Matlab v6.5 was employed on SunBlade 1500 workstations. On average, each point had 3 runs of only 0.1-1 million bits each due to the significantly increased running time.

4.2 Simulation Results

In this section, we simulate asynchronous uncoded and coded DS-SS PPM UWB systems using BCH codes over a UWB fading channel. The single-user and 5-user cases have been implemented. Due to the long simulation time (2-3 months per curve) caused by the large number of multipath signals, in the 5-user case only hard-decision decoding was considered. The incremental improvements due to errors-and-erasure decoding was quantified in the last chapter. Because the multipath signals are not synchronized with the original

waveforms, asynchronous interference will alway dominate performance. Because of this and the fact the an asynchronous system is more realistic, a synchronous system is not considered in this chapter.

4.2.1 Single-User Performance

The single-user case in a UWB fading channel is very different from the one in an AWGN channel. In an AWGN channel, the white Gaussian noise is the only source of errors. In a fading channel, besides the white Gaussian noise, there is also interference from multipath signals. As these signals are evoked by the former waveforms of the single user, we call this self-interference. Furthermore, because fading distributes the power into numerous bins, the useful waveform power in the first bin is also greatly decreased.

Figure 4.1 shows the performance of the uncoded and coded DS-SS PPM UWB systems with a full duty cycle. It can be seen that at a E_b/N_0 of 0dB the uncoded and coded BER is between 0.4 to 0.5, which indicated almost the worst situation. Compared to the single-user case in an AWGN channel in Figure 3.3, this performance is much worse due to the severe effects of fading.

When the BER is lower than 10^{-2}, the coded system performance starts to surpass the uncoded system, which is similar to the AWGN channel case. However, the E_b/N_0 is about 20 dB compared to 4 dB for the AWGN channel at a BER of 10^{-2}. The signal power is 16 dB or 40 times higher than in the AWGN channel. There are two main reasons for the large performance degradation. The first reason is that according to (4.1) the waveform power in the first bin is much less than the original waveform power. In order to attain the same performance in a fading channel, the transmit power must be greatly increased to compensate for the power reduction in the first bin and the self-interference. On average, the power in the first bin is about $1/20$ of the original power for full duty cycle transmission, which means an additional 13 dB of power is needed to obtain the same performance without

considering the self-interference. The second reason is the self-interference from delayed versions of previous waveforms. The average number of multipath signals that create interference is about 100 according to the UWB fading model parameters. Though the power in each multipath signal is exponentially decreasing, the accumulated self-interference still greatly impacts the performance. The performance is even much worse than the 10-user asynchronous AWGN case as shown in Figure 3.25. At a BER of 10^{-4}, the signal power is about 19 dB higher than the single-user AWGN case or 17 dB higher than the 10-user asynchronous AWGN case. This is because on average the accumulated self-interference power is about 20 times the power in the first bin that is used to determine the bit value. In comparison the cross interference in the 10-user asynchronous AWGN case is 9 times the useful power of the desired user.

The coding gains at a BER of 10^{-4} is similar to the AWGN case. The BCH codes of length 127 have better performance than the codes of length 31. The coding gain for the best code, $BCH(127, 85, 6)$, is about 5.5 dB and the coding gain for the weakest code, $BCH(31, 26, 1)$, is about 3 dB. All coding gains are slightly higher than those ones for the 10-user AWGN case.

In Figures 4.2, 4.3 and 4.4, the simulation results are shown for 2, 4 and 6 erasures, respectively. The improvement using erasures over no erasures is not significant. In more detail, consider the most powerful erasure decoding for each BCH code. There is 1 dB extra coding gain at a BER of 10^{-4} for $BCH(31, 26, 1, 2)$, as shown in Figure 4.5, $BCH(31, 11, 5, 6)$ as shown in Figure 4.7, $BCH(127, 99, 4, 6)$ as shown in Figure 4.8 and $BCH(127, 85, 6, 6)$ as shown in Figure 4.9. There is 1.7 dB extra coding gain for $BCH(31, 16, 3, 4)$ in Figure 4.6. These extra coding gains are greater than those in an AWGN channel.

In the above figures, we also find that the marginal coding gains decrease as the num-

ber of erasures increases for a specific coded system. When the number of erasures is at its maximum, the performance may be degraded. For example, the performance of $BCH(31, 16, 3, 6)$ is worse than the performance of $BCH(31, 16, 3)$. This is the same as in the AWGN channel, and the same explanation as for the AWGN channel applies to the fading channel.

4.2.2 Five Users Performance

In fading, the effects of the multipath propagation significantly increase the self-interference and decrease the useful signal power. As described for the single-user case, the power of the user's self-interference is about 20 times the power of the useful signal on average. In the 5-user case, assuming the transmit power is the same for each user, the power of the cross interference can be about 80 times the desired user's signal.

Figure 4.10 shows the performance of the 5-user asynchronous DS-SS PPM UWB system with a full duty cycle over a fading channel. From these results, we can see that the uncoded performance does not fall below 10^{-2} no matter how high the E_b/N_0 is. This is because at high E_b/N_0, the interference dominates the performance. The improvement with coding differs for each code. However, due to the high interference, all the curves except for $BCH(127, 85, 6)$ shows a BER error floor higher than 10^{-4}. It is not surprising that $BCH(127, 85, 6)$ is the best and $BCH(31, 26, 1)$ is the worst, which matches with the results in other cases.

In order to reduce the interference, we can reduce the duty cycle. In Figure 4.11, the performance with a 10% duty cycle is shown without changing the other parameters. In this case, the uncoded performance has dramatically improved compared to the full duty cycle case. At the BER of 10^{-4}, the E_b/N_0 is about 22.5 dB, which is even lower than the one in the single-user full duty cycle case. The reason is that the self-interference power from the previous waveforms become much smaller in average because the average power

in the delayed versions of the signal decreases exponentially. Therefore, the total self-interference becomes much smaller in the 10% duty cycle case. This also applies to the cross interference.

We can explain this in another way. In the full duty cycle case, all the multipath signals starting from the second bin have bad effects or interference to the following useful waveforms as long as the communication is proceeding. While in the 10% duty cycle case, only 10% of the multipath signals interfere with future useful waveforms. The remaining 90% fall into "non-signal" zones and do not affect the performance. Therefore, the interference will be reduced by more than 90% from the full duty cycle case. However, there is a trade-off as the data rate will also be decreased by 90% if we use the same waveform width.

For the coded systems, at E_b/N_0 of 0 dB the BERs of all coded systems are between 0.35 to 0.45. The uncoded performance is the best at this point because the number of errors exceeds the BCH codes' error correcting capability. For most of the codes, the crossovers happen at about a BER of 2×10^{-2}. At a BER of 10^{-4}, the coded systems performance follows the same pattern as in the previous cases. The best code $BCH(127, 85, 6)$ has about 4 dB coding gain and the weakest code $BCH(31, 26, 1)$ has 2 dB coding gain. This means that the transmit power for $BCH(127, 85, 6)$ can be reduced by 60% from the uncoded case for the same performance. Even $BCH(31, 26, 1)$ allows for a 37% reduction in power.

4.3 Discussion and Summary

In this chapter, we considered uncoded and coded systems in a statistical UWB indoor fading channel model. In the single user case, both errors only and errors-and-erasures decoding performance was evaluated with a full duty cycle. In the multiple user case, 5 users with a full duty cycle and a 10% duty cycle were simulated. Due to the significant simulation time spent on these fading cases, errors-and-erasures decoding was not considered for

multiple users.

In the single-user case, the improvement with BCH coding mirrors that in an AWGN channel, but the coding gains are more significant. For example, $BCH(127, 85, 6)$ has 6 dB coding gain in fading but only 3 dB in AWGN; $BCH(31, 26, 1)$ has 2.5 dB coding gain in fading but only 1.2 dB in AWGN. On the other hand, due to the severe self-interference and fading effects, the required E_b/N_0 is significantly higher than in an AWGN channel. In order to decrease the E_b/N_0, a partial duty cycle was used to reduce self-interference. The data rate will decrease with a diminished duty cycle provided that the waveform width does not change. The performance will still be worse than in AWGN, even if the duty cycle is very small, because the useful signal power in the first bin is approximately $1/20$ of the original signal power on average according to the UWB fading model, which is about a 13 dB loss in E_b/N_0.

By using erasures, at a BER of 10^{-4} an extra coding gain of 1 to 1.7 dB can be obtained with the BCH codes considered provided that the number of erasures does not reach their maximums. Here the improvement using erasures is more obvious than in an AWGN channel. The decrease in marginal coding gains in fading verifies the explanation given in Chapter 3.

In the 5-user case, the system performance was significantly degraded compared to the single-user case with a full duty cycle. Besides the effects from the white Gaussian noise and fading, the cross interference from other users results in a significant degradation. Statistically, the cross interference power from the other four users is 4 times the desired user's self-interference power. As most of the BCH codes cannot reach a low BER regardless of how high the E_b/N_0 is, the multiple-user applications are limited. In order to improve the performance, a partial duty cycle can be employed to reduce both the self-interference and the cross interference.

The 5-user case with a 10% duty cycle shows significantly better performance. It is even better than in the single-user case with a full duty cycle because the interference is reduced by more than 90%. Here we find that the effective combined interference power is about 10 times the useful signal power. This interference power is comparable to that in Figure 3.25 which shows the asynchronous 10-user AWGN case. Apart from the fading effects that decrease the useful waveform power to $1/20$ of that transmitted waveform, their results are similar. For example, at the BER of 10^{-4}, the E_b/N_0 for the uncoded systems is 10.5dB for 10-user AWGN case and 22.5dB for 5-user fading case with 10% duty cycle. By removing the reduced useful power effect of 13dB, the E_b/N_0 is very close.

From the simulation results discussed above, we find that the two tradeoffs described in the AWGN case still exist in the fading case. One is that BCH codes of length 127 have better performance than codes of length 31 with a similar code rate, but the longer codes have more decoding delay. The other one is that erasure decoding can achieve better performance as long as the number of erasures does not reach the maximum, but erasure decoding doubles the decoding delay. Because of the multipath signals, the fading is always asynchronous regardless of whether the users are synchronized or not. The third tradeoff is the performance and the data rate. By reducing the waveform duty cycle, the performance can be improved, but the data rate decreases in proportion to the duty cycle. The fourth tradeoff is the performance versus the number of users, as increasing the number of users significantly degrades performance. A balance between performance, number of users and data rate must be carefully considered in real applications. Furthermore, the number of users is limited by the number of Gold code sequences. In this thesis, the Gold code sequences of length 31 can accommodate a maximum 32 multiple access users.

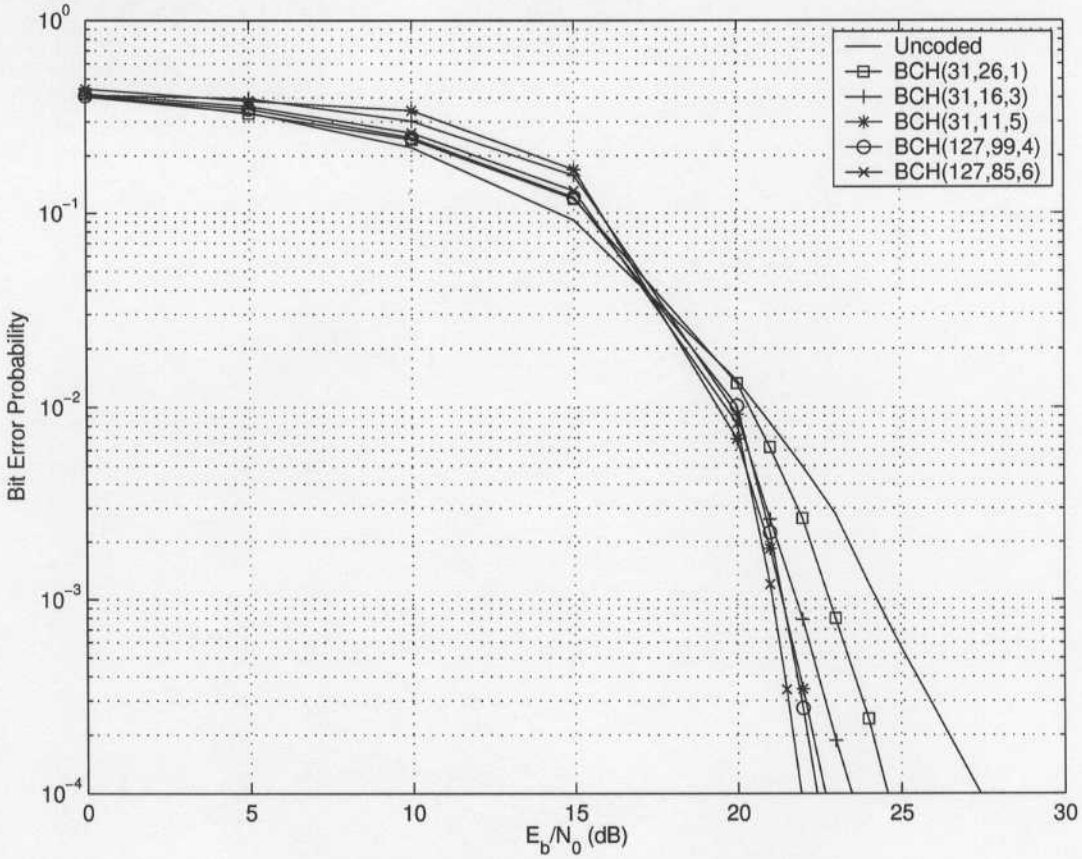

Figure 4.1. *Single-user DS-SS PPM UWB system performance with BCH coding over a fading channel.*

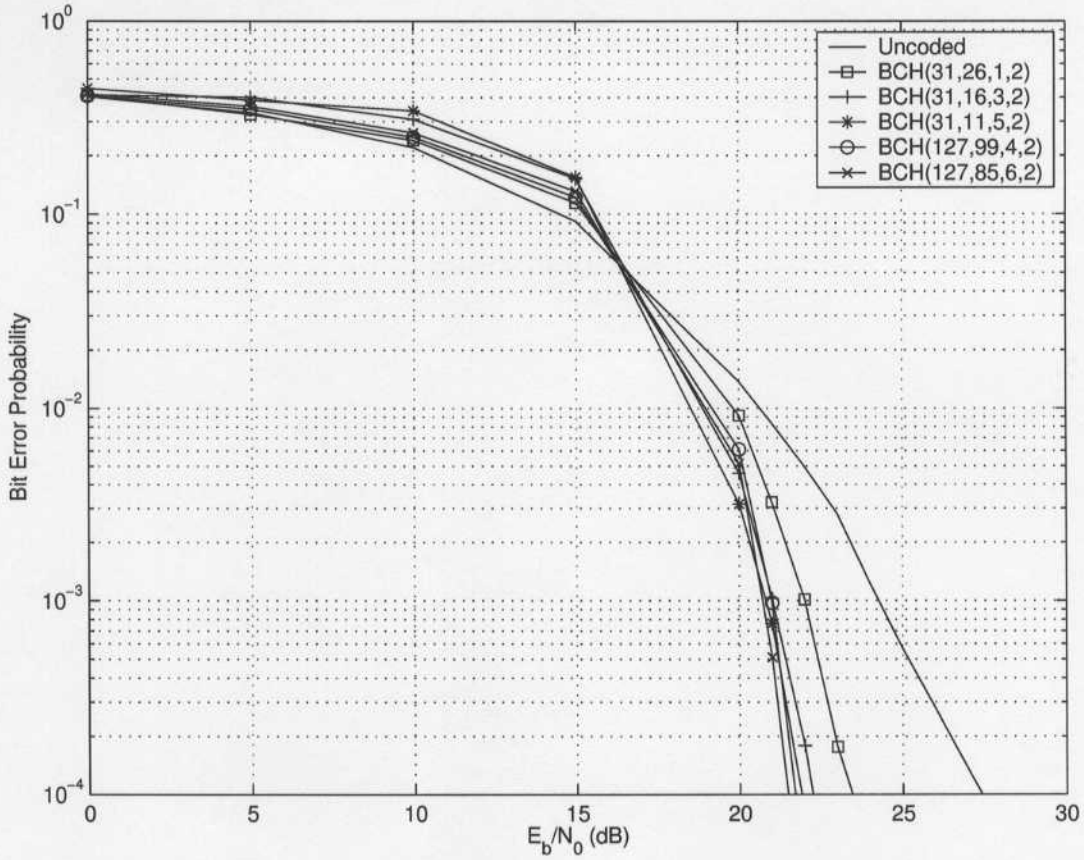

Figure 4.2. *Single-user DS-SS PPM UWB system performance with BCH coding and 2 erasures over a fading channel.*

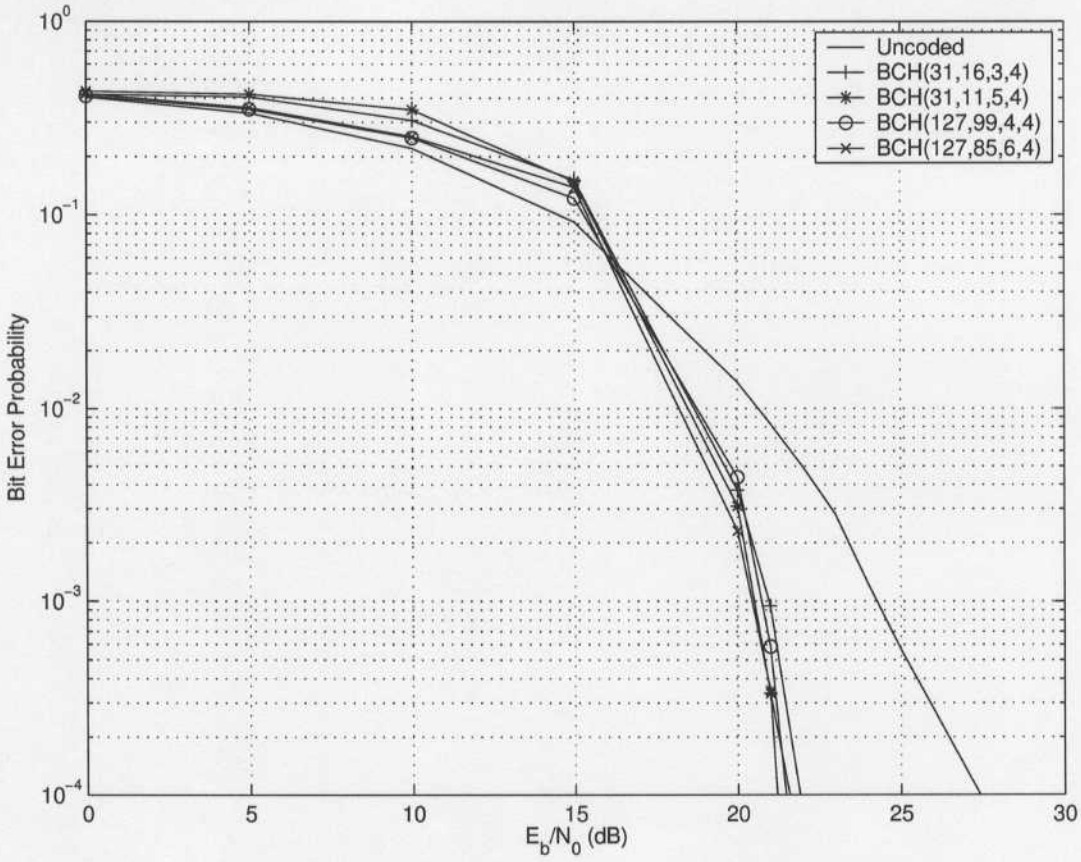

Figure 4.3. *Single-user DS-SS PPM UWB system performance with BCH coding and 4 erasures over a fading channel.*

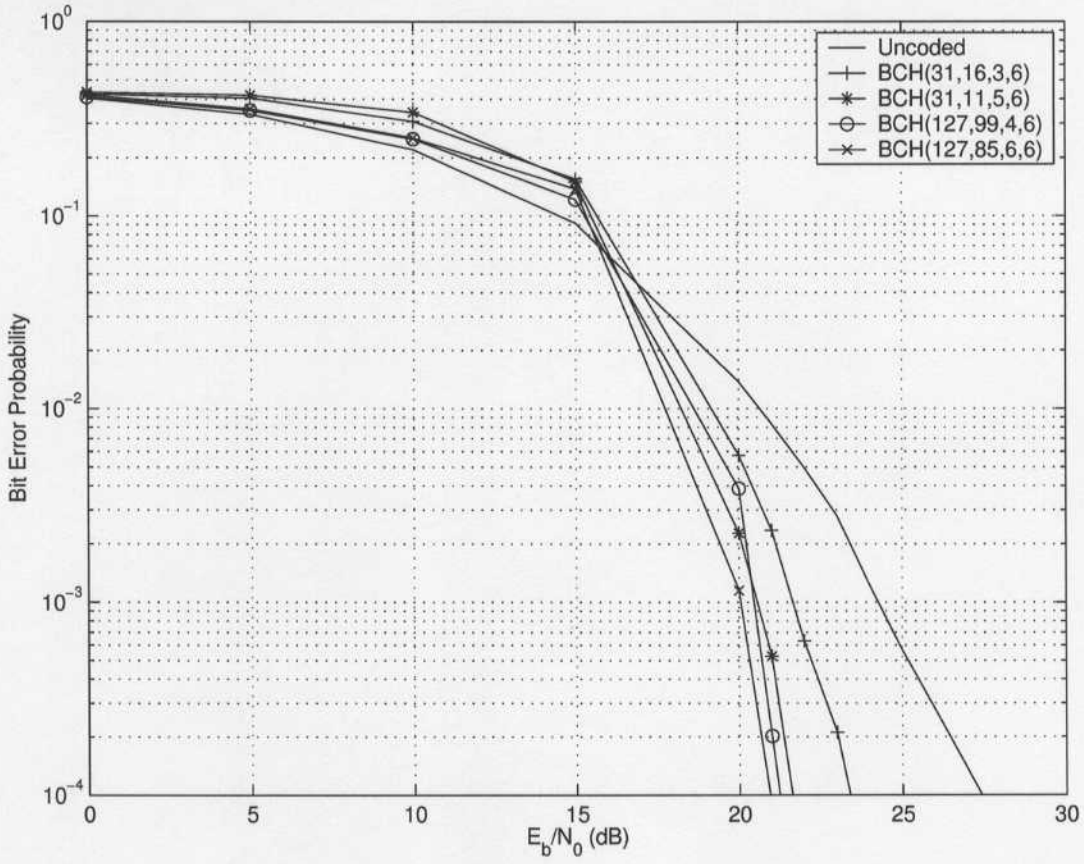

Figure 4.4. *Single-user DS-SS PPM UWB system performance with BCH coding and 6 erasures over a fading channel.*

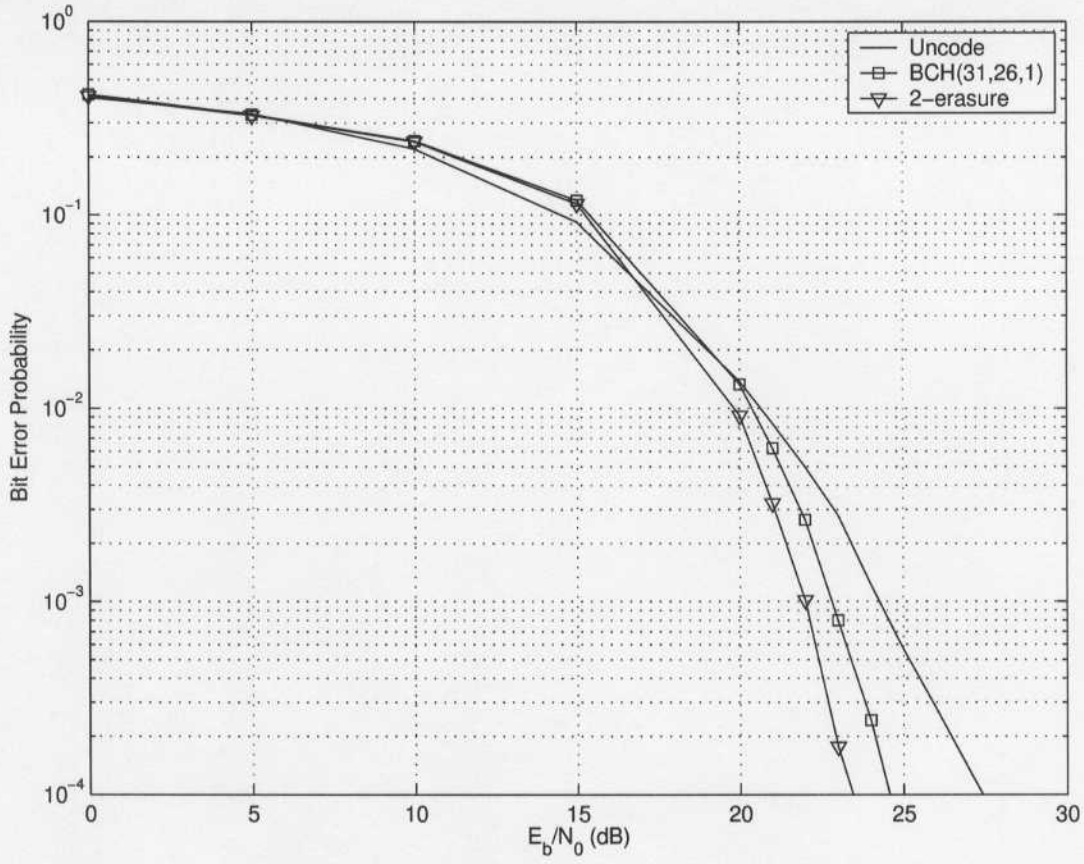

Figure 4.5. *Single-user DS-SS PPM UWB system performance with BCH(31,26,1) over a fading channel.*

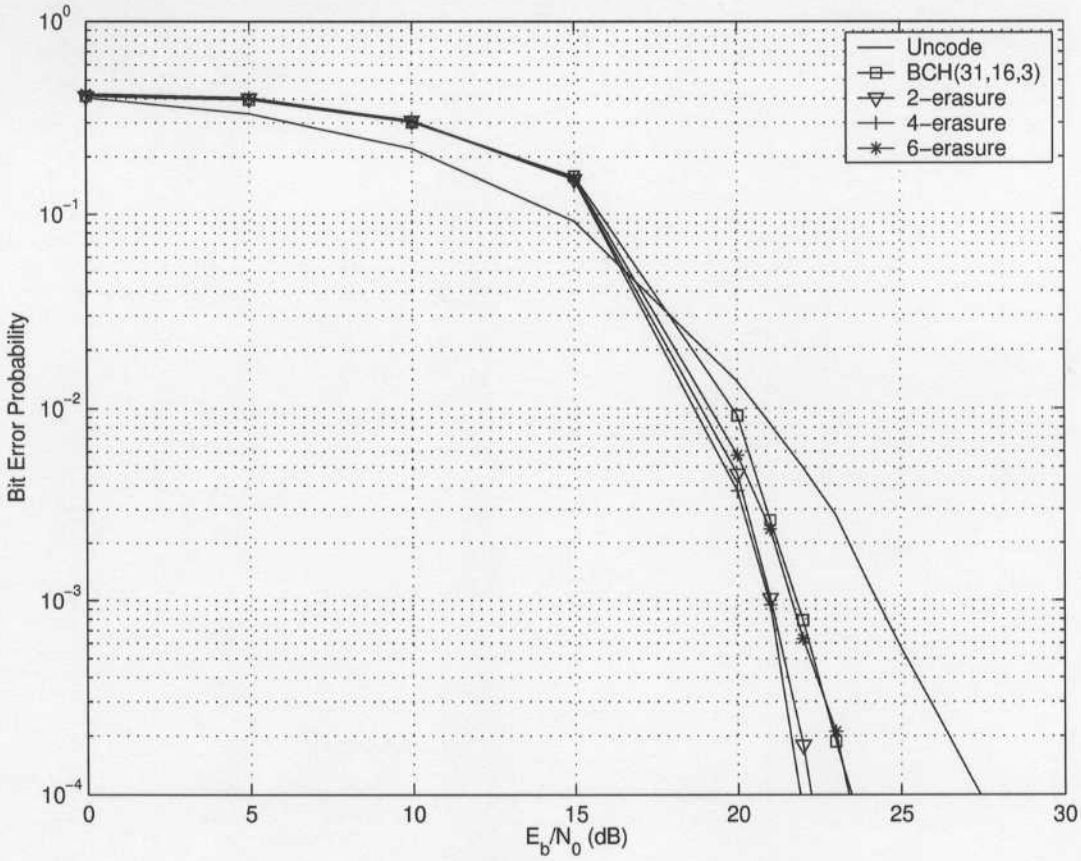

Figure 4.6. *Single-user DS-SS PPM UWB system performance with BCH(31,16,3) over a fading channel.*

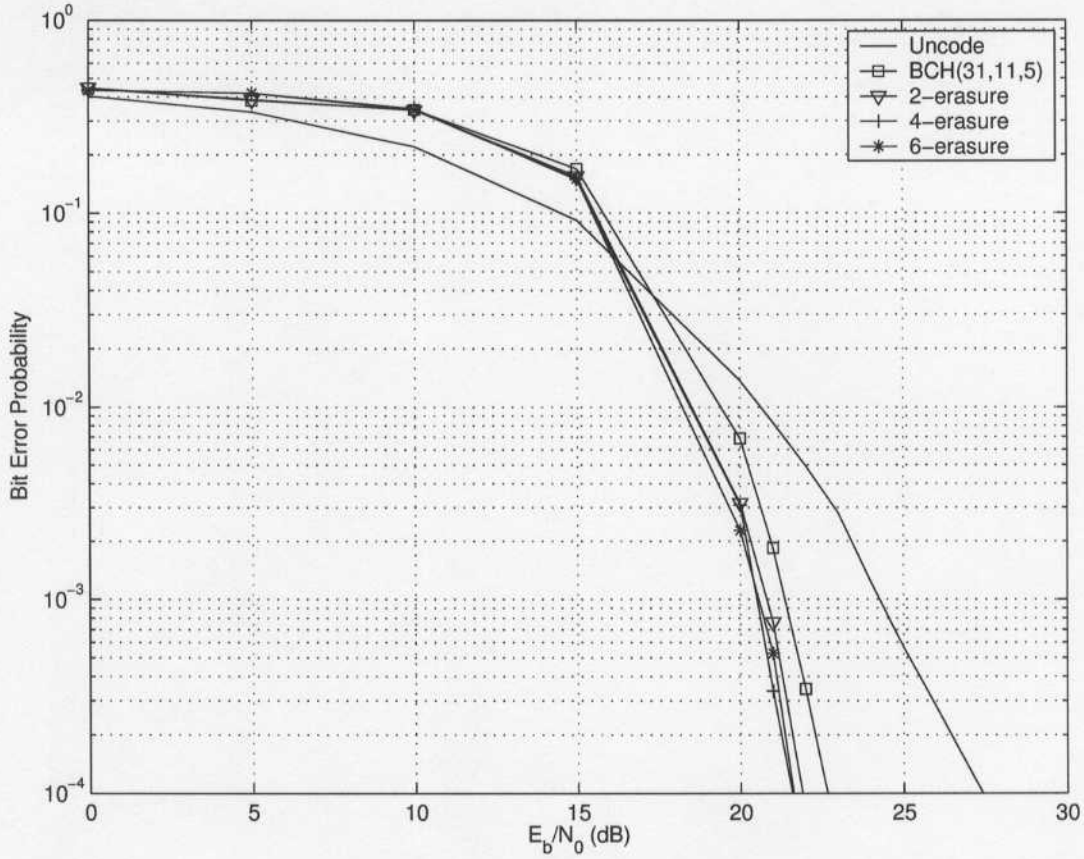

Figure 4.7. *Single-user DS-SS PPM UWB system performance with BCH(31,11,5) over a fading channel.*

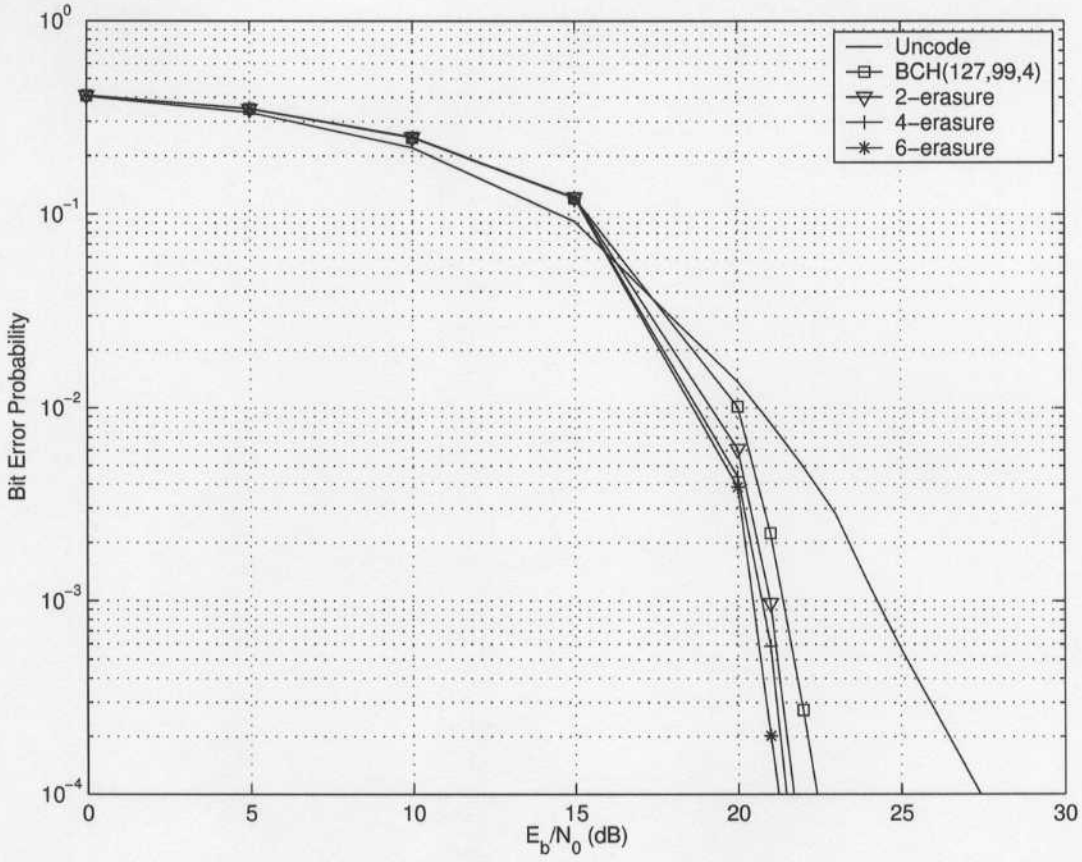

Figure 4.8. *Single-user DS-SS PPM UWB system performance with BCH(127,99,4) over a fading channel.*

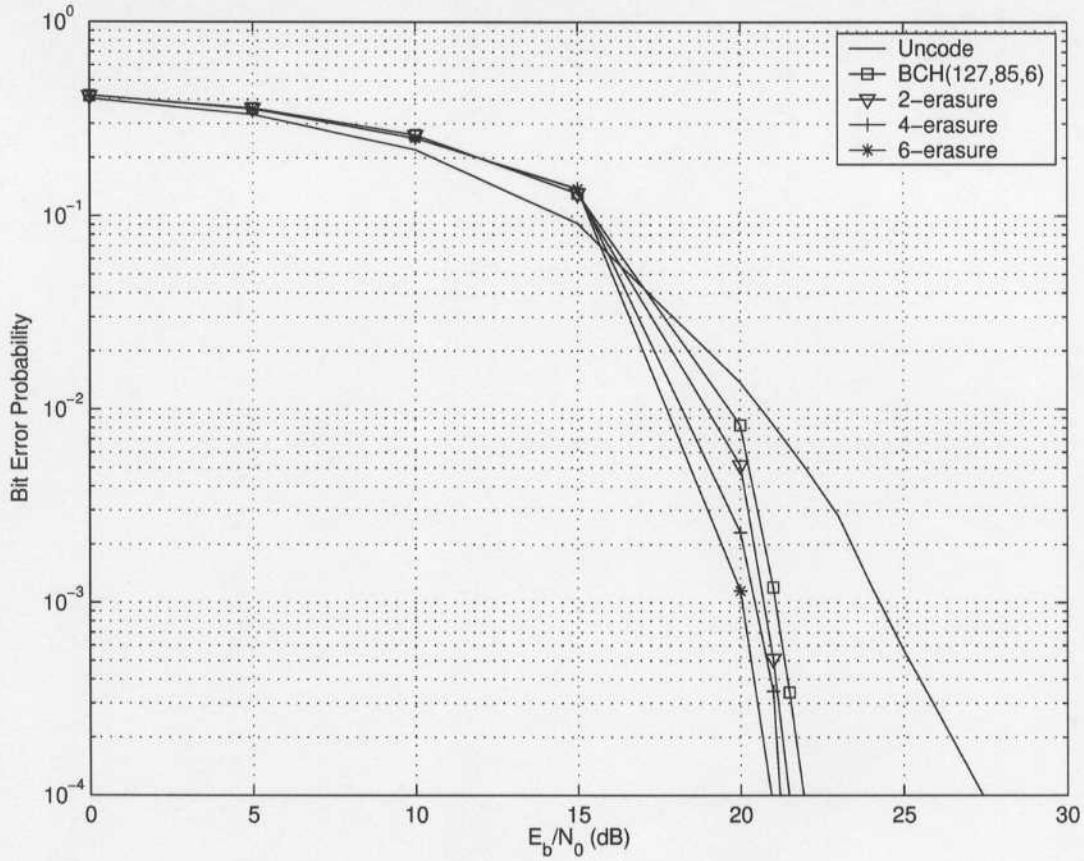

Figure 4.9. *Single-user DS-SS PPM UWB system performance with BCH(127,85,6) over a fading channel.*

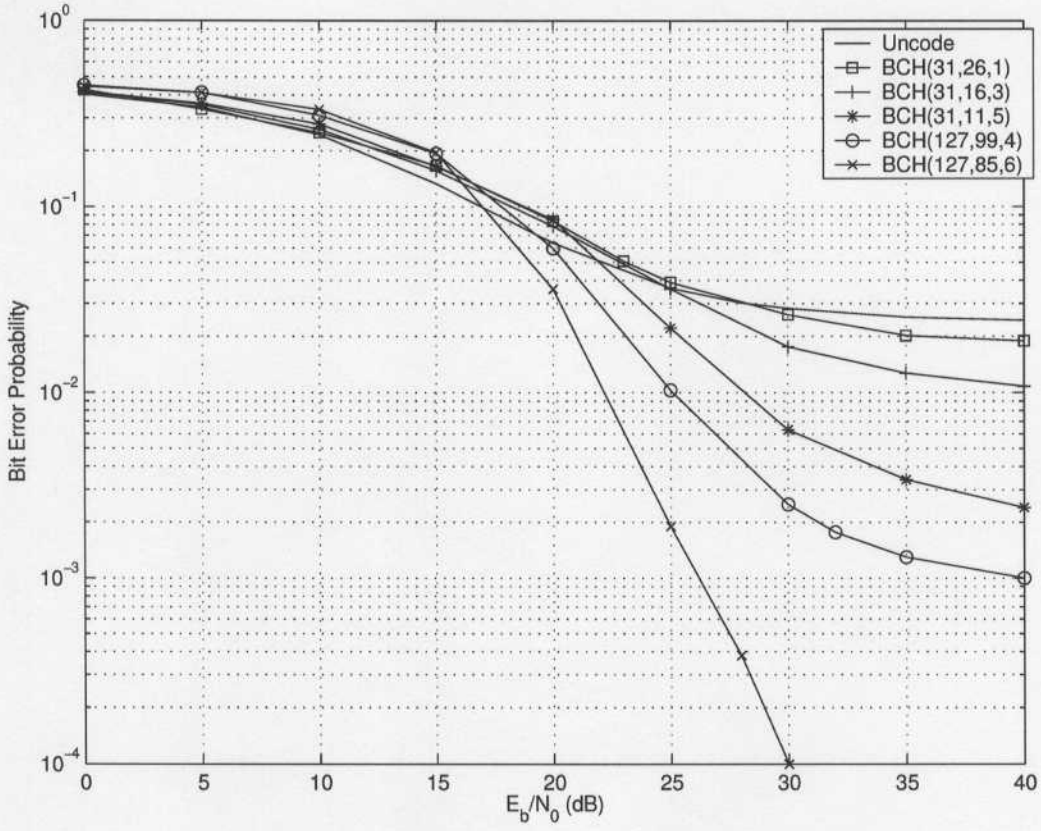

Figure 4.10. *Performance with five users in an asynchronous DS-SS PPM UWB system with BCH coding over a fading channel.*

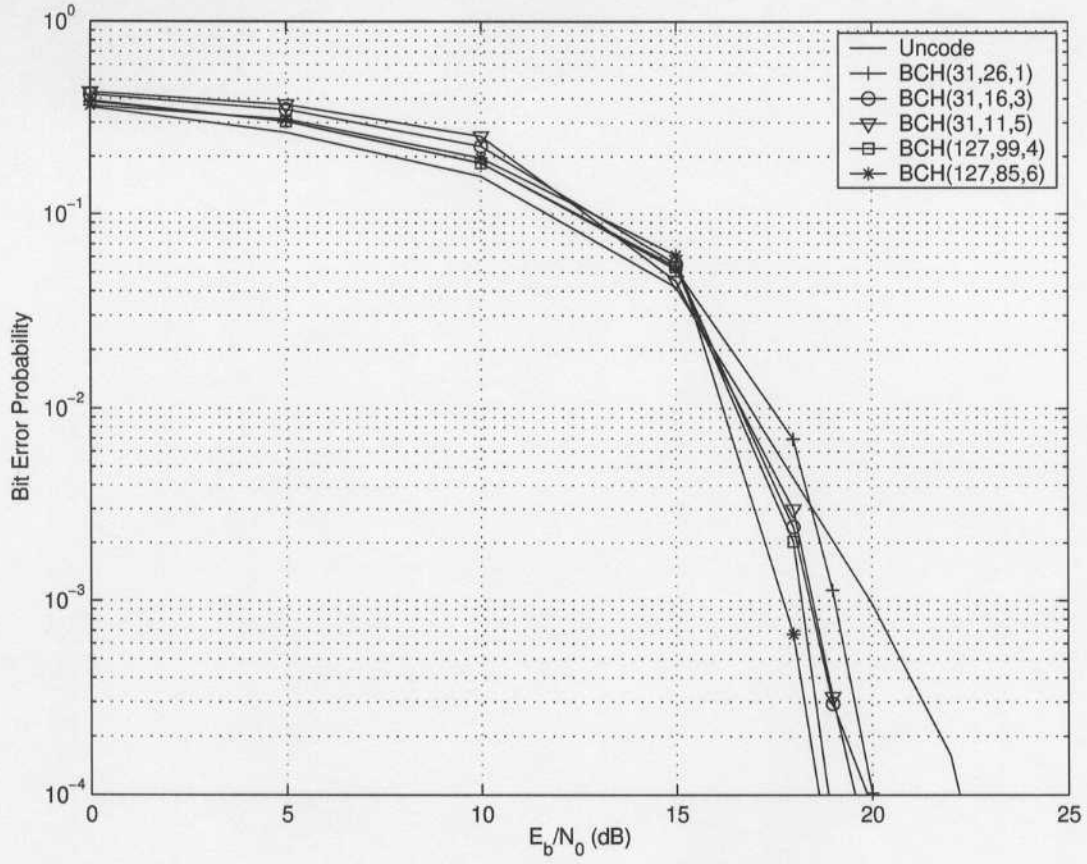

Figure 4.11. *Performance with five users in an asynchronous DS-SS PPM UWB system with BCH coding over a fading channel(10% duty cycle).*

Chapter 5

Conclusions and Future Work

5.1 Conclusions

Ultra-Wideband (UWB) communication is an emerging wireless technology with uniquely attractive features. By using spread-spectrum techniques, it is ideally suited for future indoor wireless communications. In dense multipath environments, it can provide high data rates, low transmission power, low interference with existing narrow-band radio systems, robustness to severe multipath and low cost [26, 27, 28, 29, 30]. Spread spectrum techniques are used for multiple access communications. There are four typical modulation techniques applicable to UWB systems: DS-SS PPM, DS-SS PAM, TH-SS PPM and TH-SS PAM. This thesis considered only DS-SS PPM modulation as the emphasis was on the effects of error-correcting codes.

To enhance the performance of UWB systems, BCH error correcting codes were employed due to their excellent performance and low decoding complexity. Several block-lengths and error correcting capabilities were used to quantify the improvement. The Berlekamp-Massey decoding algorithm was implemented due to its efficiency. Furthermore, errors-and-erasures decoding was considered to further improve the performance.

Both additive white Gaussian (AWGN) and fading channels were considered. In the AWGN case, both synchronous and asynchronous users were evaluated. In the fading

case, only asynchronous users were considered because the asynchronous multipath interference dominates the performance. The simulation results show that significant performance improvements are possible using BCH codes. The most powerful code considered, $BCH(127, 85, 6)$, provides 3-4 dB coding gain at a BER of 10^{-4} in AWGN, and more than 5 dB in fading. Even for the weakest code, $BCH(31, 26, 1)$, provided 1-2 dB coding gain in AWGN and 3 dB coding gain in fading at a BER of 10^{-4}. Therefore, to reach an accepted transmission quality, significant transmit power reduction can be achieved. Alternatively, the performance can be improved tremendously without increasing the transmit power.

Besides errors-only decoding, errors-and-erasures decoding was also employed. This makes better use of the received information by erasing the least reliable bits. Two decoding iterations are required in this case, but the simulation results show 0.5-1 dB extra coding gain in AWGN and 1-2 dB extra coding gain in fading over errors-only decoding at a BER of 10^{-4}.

In fading, we find that with a full duty cycle, 5-user performance is not acceptable even with a high E_b/N_0. By decreasing the duty cycle to 10%, the performance is significantly improved due to the multipath interference reduction. In addition, the reason that multi-access synchronous AWGN systems have only a slight degradation while multi-access asynchronous AWGN systems have a larger degradation compared to the single-user case is because the cross interference is mostly cancelled in the synchronous case while in the asynchronous case the cross correlation between the shifted spreading sequences can be much larger.

The reason that the fading system performance is much worse than the AWGN systems was also explained. It can be attributed to the fact that fading significantly reduces the useful signal power and greatly increases self-interference power.

Furthermore, we discussed the tradeoffs between BCH length vs. delay. The BCH codes of length 127 show better performance than the codes of length 31 while the former has longer delay in decoding. For errors-only decoding and errors-and-erasures decoding, errors-and-erasures decoding has better performance but has more delay. For performance improvement, a reduced duty cycle can have better performance, but it will decrease the data rate.

5.2 Future Work

In this thesis we introduced binary BCH error correcting coding for a typical UWB communication model. The simulation results show great performance improvements over the uncoded system. As only DS-SS PPM was employed, this work can be extended to DS-SS PAM, TH-SS PPM and TH-SS PAM models with a variety of waveform choices.

The relationship between the performance and the duty cycle can be considered further. A quantitative analysis based on the UWB statistical fading model will clarify the effects of data rate, number of users and transmit power on the performance.

For the errors-and-erasures decoding algorithm, the marginal coding gains as the number of erasures increases can be quantitatively analyzed. Moreover, more powerful error correcting coding techniques can be applied such as turbo code or low density parity check codes. In addition, as all work done thus far is based on binary codes, future research can also explore the use of non-binary codes such as Reed-Solomon codes to enhance the transmission efficiency. As these codes are more complicated than BCH code, the penalty will be increased delay and more cost/implementation complexity.

Channel capacity is another topic that can be investigated. Based on the UWB fading model, parameters such as duty cycle occupancy, transmit power and error correcting code

can be modified to improve the channel capacity. This work can be done for all four UWB data transmission models.

Bibliography

[1] L. Yang and G. B. Giannakis, "Ultra-wideband communications - An idea whose time has come," *IEEE Signal Process. Mag.*, vol. 21, no. 6, pp. 26–54, Nov. 2004.

[2] I. Oppermann, M. Hamalainen, and J. Iinatti, *UWB Theory and Applications*, 2nd ed. John Wiley & Sons, Inc., 2004.

[3] "First report and order in the matter of revision of part 15 of the commission's rules regarding ultra-wideband transmission systems, ET Docket 98-153, Federal Communications Commission, FCC 02-48," Apr. 22, 2002.

[4] W. Zhuang, X. Shen, and Q. Bi, "Ultra-wideband wireless communications," *Wireless Commun. and Mobile Computing*, vol. 3, pp. 663–685, 2003.

[5] R. A. Scholtz, "Multiple access with time-hopping impulse modulation," *Proc. IEEE Military Commun. Conf.*, pp. 447–450, Oct. 1993.

[6] M. Z. Win and R. A. Scholtz, "Characterization of ultra-wide bandwidth wireless indoor channels: a communication-theoretic view," *IEEE J. Select. Areas Commun.*, vol. 20, pp. 1613–1627, Dec. 2002.

[7] ——, "On the robustness of ultra-wide bandwidth signals in dense multipath environments," *IEEE Commun. Letters*, vol. 2, pp. 51–53, Feb. 1998.

[8] T. Barrett, "History of ultra wideband (UWB) radar and communications: Pioneers and innovators," *Proc. Progress in Electromagnetics Symp.*, 2002.

[9] "Assessment of ultra-wideband (UWB) technology, OSD/DARPA, Ultra-Wideband Radar Review Panel, R-6280," July 13, 1990.

[10] H. Chen, W. Li, T. A. Gulliver, and H. Zhang, "DS-PPM ultra-wideband systems with BCH coding," *Proc. IEEE Pacific Rim Conf. on Commun., Computers and Signal Process.,*, pp. 17–20, Aug. 2005.

[11] B. Sklar, *Digital Communications Fundamentals and Applications*, 2nd ed. Prentice Hall, Inc., 2001.

[12] J. Fakatselis, "Processing gain for direct sequence spread spectrum communication systems and PRISM," *Intersil Corp. Application Note 9633*, Aug. 1996.

[13] M. G. M. Hussain, "Principles of space-time array processing for ultrawide-band im-

pulse radar and radio communications," *IEEE Trans. Vehic. Tech.*, vol. 51, pp. 393–403, 2002.

[14] S. B. Wicker, *Error Control Systems for Digital Communication and Storage*. Prentice Hall, Inc., 1995.

[15] S. G. Wilson, *Digital Modulation and Coding*. Prentice Hall, Inc., 1996.

[16] L. Zhang, L. Vok, and Z. Cao, "Short BCH codes for wireless multimedia data," *Proc. IEEE Wireless Commun. and Networking Conf.*, pp. 220–222, Mar. 2002.

[17] R. Prasad, H. S. Misser, and A. Kegel, "Performance evaluation of direct-sequence spread spectrum multiple-access for indoor wireless communication in a Rician fading channel," *IEEE Trans. Commun.*, vol. 43, pp. 581–592, Feb.-Mar.-Apr. 1995.

[18] T. Kasmai and S. Lin, "Some results on the minimum weight of BCH codes," *IEEE Trans. Inform. Theory*, vol. 18, pp. 824–825, 1972.

[19] Z. Guo and K. B. Letaief, "Performance of multiuser detection in multirate DS-CDMA systems," *IEEE J. Select. Areas Commun.*, vol. 19, pp. 1019–1028, June 2001.

[20] M. Z. Win and R. A. Scholtz, "Ultra-wide bandwidth time-hopping spread-spectrum impulse radio for wireless multiple-access communications," *IEEE Trans. Commun.*, vol. 48, pp. 679–689, Apr. 2000.

[21] J. Wozencraft and I. Jacobs, *Principles of Communication Engineering*. Wiley, New York, 1965.

[22] G. C. Jr. and J. Cain, *Error-Correction Coding for Digital Communications*. Plenum Press, New York, 1981.

[23] D. Cassioli, M. Z. Win, and A. F. Molisch, "The ultra-wide bandwidth indoor channel:from statistical model to simulations," *IEEE J. Select. Areas Commun.*, vol. 20, pp. 1247–1257, Aug. 2002.

[24] J. W. C. Jakes, *Microwave Mobile Communications*. Wiley, New York, 1974.

[25] D. Cassioli, M. Z. Win, F. Vatalaro, and A. F. Molisch, "Performance of low-complexity rake reception in a realistic UWB channel," *Proc. IEEE Int. Conf. Commun.*, pp. 763–767, Apr.-May 2002.

[26] M. Win and R. Scholtz, "Impulse radio: How it works," *IEEE Commun. Letters*, vol. 2, pp. 36–38, Feb. 1998.

[27] ——, "Comparisons of analog and digital impulse radio for multiple-access communications," *Proc. IEEE Int. Conf. Commun.*, pp. 91–95, June 1997.

[28] ——, "Ultra-wide bandwidth time-hopping spread-spectrum impulse radio for wire-

less multiple-access communications," *IEEE Trans. Commun.*, vol. 48, pp. 679–691, Apr. 2000.

[29] M. Win, X. Qiu, R. Scholtz, and V. Li, "ATM-based TH-SSMA network for multimedia PCS," *IEEE J. Select. Areas Commun.*, vol. 17, pp. 824–836, May 1999.

[30] C. L. Martret and G. Giannakis, "All-digital PAM impulse radio for multiple-access through frequency-selective multipath," *Proc. IEEE Global Telecommun. Conf.*, vol. 1, pp. 77–81, Nov.-Dec. 2000.